23rd International Visual Field & Imaging Symposium

Date May 9(Wed.)-12(Sat.), 2018

Venue Ishikawa Ongakudo (Kanazawa, Japan)

Host Kazuhisa Sugiyama (Kanazawa University)
Aiko Iwase (Tajimi Iwase Eye Clinic)

Program & Abstract Book

IPS2018

23rd International Visual Field & Imaging Symposium

Kanazawa, Japan,
May 9th – 12th , 2018

Program & Abstract Book

Perimetry is the quantitative evaluation of the visual field. Ocular Imaging is the assessment and evaluation of the structual details of the eye. The aims of the IPS are

1) to promote the study of normal and abnormal visual function and of ocular imaging.
2) to ensure and facilitate the cooperation and friendship of scientists of different countries working and interested in these disciplines.

Previous Symposia

1974: Marseille, France
1976: Tübingen, Germany
1978: Tokyo, Japan
1980: Bristol, UK
1982: Sacramento, CA, USA
1984: Santa Margherita Ligure, Italy
1986: Amsterdam, The Netherlands
1988: Vancouver, Canada
1990: Malmö, Sweden
1992: Kyoto, Japan
1994: Washington, D.C. , USA
1996: Würzburg, Germany
1998: Gardone Riviera, Italy
2000: Halifax, Canada
2002: Stratford upon Avon, UK
2004: Barcelona, Spain
2006: Portland, OR, USA
2008: Nara, Japan
2010: Tenerife, Spain
2012: Melbourne, Australia
2014: New York, NY, USA
2016: Udine, Italy

Table of Contents

IPS2018 Host:

Kazuhisa Sugiyama, M.D., Ph.D.
Department of Ophthalmology,
Graduate School of Medical Sciences,
Kanazawa University, Kanazawa, Japan

Aiko Iwase, M.D., Ph.D.
Tajimi Iwase Eye Clinic, Tajimi, Japan

Dear Colleagues and Friends,

We are honored to be hosting the 23rd International Visual Field & Imaging Symposium (IPS2018) at the Ongakudo (in front of Kanazawa Station) in Kanazawa city, Japan, from May 9 to 12, 2018. The previous IPS meetings had been held in Japan 3 times; the 3rd IPS in Tokyo, 1978 (Prof. Harutake Matsuo), the 10th IPS in Kyoto, 1992 (Prof. Yoshiaki Kitazawa: boss of Aiko & Kazu), the 18th IPS in Nara, 2008 (Prof. Chota Matsumoto). It is our great pleasure to have the opportunity to organize such an influential academic conference and to welcome so many friends from all over the world to Kanazawa!

Kanazawa is unlike the populous metropolitan cities of Tokyo or Osaka; it is considered a popular tourist city where more than 8 million tourists visit each year to see and appreciate genuine Japanese culture. In the era of the Samurai (Edo period - 265 years), Kanazawa had a large population exceeded only by Tokyo, Osaka and Kyoto. This time period was prosperous and characterized by sophisticated foods, crafts, and art developed independently and known as the Hyakumangoku culture. Moreover, as Kanazawa has never been affected by war nor suffered any major natural disasters, the city has been able to maintain its historical districts, which include traditional Japanese dwellings, magnificent gardens, numerous shrines, and the remarkable Kanazawa Castle - all reflecting the culture of the Samurai. Welcome reception will be held in Kanazawa Castle in the evening of May 9 (Wednesday). The participants can enjoy the Congress Tour to the famous areas in Kanazawa City in the afternoon of May 11 (Friday). You will be able to immerse yourself in and experience authentic Japanese culture, including traditional Japanese dress, foods, and daily life, not easily appreciated in the larger metropolitan cities of Japan. Kanazawa is also blessed with beautiful natural surroundings and you can enjoy sophisticated Japanese cuisine such as sushi and tempura made from fresh local fish and shellfish caught and delivered directly from the Sea of Japan and sake (Japanese rice wine) produced from naturally clear local stream water.

The impact and influence of the previous IPS meetings as an international academic organization and the significant contributions made by the IPS members has resulted in a steady evolution in the understanding, technology, and diagnosis skill. However, it is also evident that many challenges still exist; our goals for this meeting are to identify and explore some of these challenges. We want to encourage the sharing of our knowledge and ideas, the discussing of experiences and successes, and the proposing of future directions of focus. We invited Prof. Michael Wall as a speaker of the IPS Lecture. We changed Aulhorn Lecture to Aulhorn Educational Lecture which is more educational contents including imaging and perimetry by 4 speakers. We also conducted the simultaneous meeting of Japan Perimetric Society (JPS2018) from May12 to 13, 2018 in Kanazawa.

We would be grateful if you would actively exchange your valuable knowledge and experience regarding the development of imaging and perimetry over the 3 days of the conference, enjoy the meeting with many friends and colleagues from all over the world, and form new and deepen old friendships at the same time.
Welcome to Kanazawa!

IPS Board Members:
President: Chota Matsumoto
Past President: Chris Johnson
Vice President: David (Ted) Garway-Heath
Vice President: Aiko Iwase
Secretary: Allison M. McKendrick
Treasurer: Mitchell Dul
Past-Secretary: David Henson

Members at Large:
Lyne Racette
Ryo Asaoka

Other Board Members:
Fritz Dannehim
Kazuhisa Sugiyama
Aiko Iwase

Group Chairs:

Awards Committee:	Fritz Dannehim
Education - Perimetry:	Chota Matsumoto
Education - Imaging:	David (Ted) Garway-Heath
Imaging Standards:	Linda Zangwill
Industry Liaison and PR Committee:	Paul Artes
Open Perimetry Interface:	Paul Artes; Andrew Turpin

Honorary Members of the IPS:
Stephen Drance
Jay Enoch
Franz Fankhauser
Lars Frisen
Erik Greve
Anders Heijl
Yoshiaki Kitazawa
Pam Sample

In Memoriam Honorary Members of the IPS:
Elfriede Aulhorn
Alan Friedmann
Hans Goldmann
Heinrich Harms
Haratuke Matsuo
Mario Zingirian

Local Organizing Committee
Host (Program Committee)
Kazuhisa Sugiyama
Aiko Iwase

Local Executive Committee (Local Organizing Committee)

Chota Matsumoto
Shinji Ohkubo
Tomomi Higashide
Tadashi Nakano
Makoto Nakamura
Sachiko Udagawa

Advisory Board

Keiji Yoshikawa
Hirotaka Suzumura
Satoshi Kashii
Goji Tomita
Yoshio Yamazaki
Takeshi Yoshitomi
Sachiko Okuyama

Advisory Steering Board

Kazutaka Kani
Makoto Araie
Shiroaki Shirato

JPS Board Members

Ryo Asaoka
Shiho Kunimatsu-Sanuki
Mineo Kondou
Kei Shinoda
Nobuyuki Shoji
Motohiro Shirakashi
Genichiro Takahashi
Satoshi Nakadomari
Takeo Fukuchi
Kyoko Fujita
Naoya Fujimoto
Akemi Wakayama

Honorary Members of the JPS

Haruki Abe
Nariyoshi Endou
Toshifumi Otori
Kazutaka Kani
Yoshiaki Kitazawa
Shiroaki Shirato
Shuji Maeda
Keiji Yoshikawa

Meeting Information

Venue

Ishikawa Ongakudo
Showa-machi20-1, Kanazawa-shi, Ishikawa, Japan 920-0856
FAX：+81-76-232-8101

Official Language

English

Registration Fee

Registration fee type	On-site Registration
IPS Members	65,000 JPY
IPS Non Members	75,000 JPY
*Residents/Fellows/Medical Staff	45,000 JPY
Accompanying Persons	45,000 JPY

*Residents/Fellows/Medical Staff must submit an official university/affiliation certificate or letter in English, in conjunction with on-site registration, which confirms their status. Documentation must be submitted on-site.

Registration Entitlements

[IPS Members, IPS Non Members, Residents/Fellows/Medical Staff]

- Congress Kit
- Access to all Scientific Programs
- Welcome Party on May 9 (Wed.)
- Conference Tour on May 11 (Fri.)
- Closing Banquet on May 12 (Sat.)
- Morning/Luncheon/Afternoon Seminars
- Coffee breaks

[Accompanying Persons]

- Welcome Party on May 9 (Wed.)
- Conference Tour on May 11 (Fri.)
- Closing Banquet on May 12 (Sat.)
- Coffee breaks

Accompanying Persons are NOT allowed to attend any scientific programs.

Meeting Information

Registration Desk

The registration desk is located in the lobby of ISHIKAWA ONGAKUDO on 1st floor. Registration Desk opening hours are:

Wednesday, May 9 16:00-17:45
Thursday, May10 7:30-18:00
Friday, May 11 7:30-13:00
Saturday, May 12 7:30-16:30

Cloakroom

Cloakroom is located in front of Koryu Hall on B1 floor. It opens as follows;

Thursday, May10 7:30-19:00
Friday, May 11 7:30-13:30
Saturday, May 12 7:30-17:30

Name Badge

All registered attendees will receive a name badge. Please wear the badge for the meeting activities.

General Information Desk

Inquiries concerning the meeting may be made at the general information desk located next to the registration desk.

Mobile Device Policy

Photography, filming, or recording is prohibited while presentations. Also, please respect presenters and other delegates by ensuring your mobile devices are switched off or on silent mode while you are in sessions.

Disclaimer

The organizing committee of IPS2018 will accept no liability for the safety of any participant, or for personal injury of loss, or damage to private property suffered during the meeting.

日本眼科学会専門医制度認定単位について

本会で取得可能な単位は以下の通りです。
受付場所：石川県立音楽堂 1F 正面ホワイエ
日時・単位数：5 月 10 日（木）9:00 ～ 18:30・3 単位
5 月 11 日（金）9:00 ～ 12:00・2 単位
5 月 12 日（土）9:00 ～ 16:35・3 単位※
※ 5 月 12 日（土）は IPS と JPS 合わせての単位となります。両学会に参加でも、どちらか 1 つに参加でも 3 単位となります。

For All Chairs

We ask that you strictly adhere to the time provided for presentations and Q&A to ensure smooth operation of the meeting. Please be prepared at the Chairperson's Seats in a session room no later than 15 minutes before the session, and notify staff nearby the Chairperson's Seats of your arrival.

For Oral Session Presenters

7minutes for presentation & 5minutes for Q&A

Please note that the session room will have a data projector and we will only accept computer-based presentations. Slide/Overhead/VCR projectors will NOT be available. To ensure your presentation runs smoothly, please bring your presentation data to PC Preview Desk located in the lobby on the first floor of the Ishikawa Ongakudo at least 60 minutes prior to your presentation. If you use Macintosh, please bring you own PC, and also stop by PC Preview Desk.

1. Our OS is Windows 10 and projector is XGA, or 1024 by 768 pixels.

2. If you bring your presentation data in a CD-R or USB flash memory stick, please follow the instructions below:

a) The computers provided for the sessions will be running the following operating systems with the following application software installed.
Windows: PowerPoint 2010, 2013, 2016

b) Use the above operating system's standard fonts
(e.g.) Windows: Century, Century Gothic, Times New Roman, etc

c) Name your presentation data as follows:
(e.g.) O1-1 John Smith.ppt

d) We use Windows Media Player for video software. Please ensure that your video is playable with the default codecs included in Windows Media Player.

3. If you bring your own laptop computer including Macintosh, please follow the instructions below:

a) Ensure that your computer is equipped with the monitor connector of mini D-sub 15 pins. If your computer does not have this connection, please bring an appropriate converter with you.

mini D-sub 15 pins

b) Be sure to bring an AC adaptor with you. The Japanese standard AC voltage is 100V.

c) Be sure to turn off screen saver or power saving mode of your laptop in advance.

4. A display monitor, keyboard, and remote mouse will be provided on a podium for presenters to operate. Sound speakers are not available.

5. Presentation data loaded on the computers provided will be completely deleted by the secretariat after your presentation.

6. The secretariat is not responsible for any projection troubles caused by computer technical difficulties. We recommend that all presenters bring back-up data.

7. Presenter view is available.

8. COI Disclosure on presentation
   When the authors disclose the conflict of interest in the presentation, the category and the names of the companies should be shown after the authors' names in the second slide or at the end of poster. If none of the authors has any conflict of interest to be disclosed, please write "there is no conflict of interest to be disclosed". For more details, please refer to “Call for Abstract” of IPS2018 website.

Sample of Slide

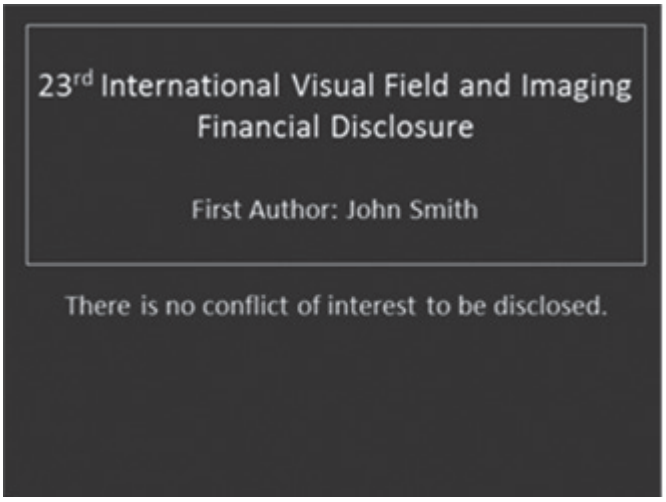

PC Preview Desk open hours:

Wednesday, May 9 16:00-17:45
Thursday, May 10 7:30-18:00
Friday, May 11 7:30-13:00
Saturday, May 12 7:30-17:00

Poster Presentation Guidelines

Posters are displayed through the duration of the meeting, May 10-12, 2018 and the time schedule for mounting and removing the posters is as follows.

Posters Mounting: 08:00-11:00, Thursday, May 10
Posters Removing: 17:00-18:00, Saturday, May 12

■ Poster Preparation and Mounting/Removing

1. The Poster board surfaces measure approximately W90cm × H180cm.
   Poster Presentation Number (20 cm × 20 cm) is displayed at the top left of the board.
2. A supply of pushpins will be available in the poster area for mounting your poster.
3. Each poster must have a label at the top that indicates the title of the paper, the name(s) of the author(s) and their affiliation(s). The presenting author should be marked with a circle.
4. Authors are required to mount and remove their materials scheduled as above.
5. We remind you that you should NOT leave poster tubes or cases in the poster areas. The organizers will not be held responsible for any losses which may be incurred.
6. Posters not removed by the removing time mentioned above will be removed and discarded by the secretariat.

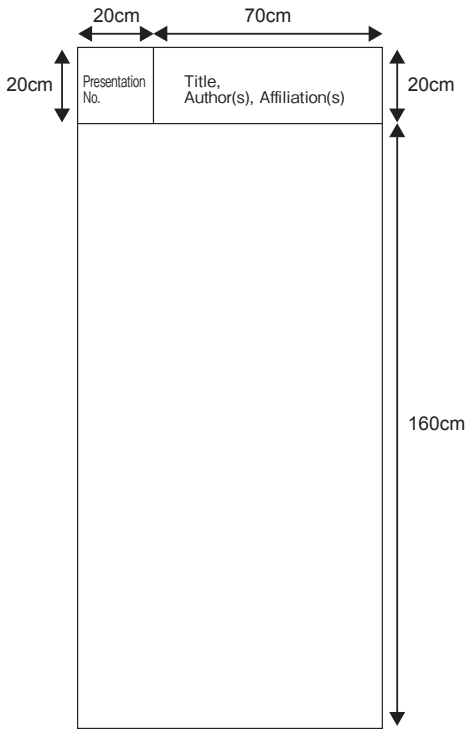

■ Oral Presentation

For All Chairs

We ask that you strictly adhere to the time provided for presentations and Q&A to ensure smooth operation of the meeting. Please be prepared at the Chairperson's Seats in a session room no later than 15 minutes before the session, and notify staff nearby the Chairperson's Seats of your arrival.

For All Poster Presenters

Poster presenters are required to deliver 8 minutes' presentation in an oral session room (3 minutes for presentation & 5 minutes for Q&A). This is designed for delegates to ask questions, the answers to which would be of interest to all delegates. Please note that the session room will have a data projector and we will only accept computer-based presentations. Slide/Overhead/VCR projectors will NOT be available. To ensure your presentation runs smoothly, please bring your presentation data to PC Preview Desk located in the lobby on the first floor of the Ishikawa Ongakudo at least 60 minutes prior to your presentation. If you use Macintosh, please bring you own PC, and also stop by PC Preview Desk.

Poster Presentation Guidelines

1. Our OS is Windows 10 and projector is XGA, or 1024 by 768 pixels.

2. If you bring your presentation data in a CD-R or USB flash memory stick, please follow the instructions below:

a) The computers provided for the sessions will be running the following operating systems with the following application software installed.
Windows: PowerPoint 2010, 2013, 2016

b) Use the above operating system's standard fonts
(e.g.) Windows: Century, Century Gothic, Times New Roman, etc

c) Name your presentation data as follows:
(e.g.) O1-1 John Smith.ppt

d) We use Windows Media Player for video software. Please ensure that your video is playable with the default codecs included in Windows Media Player.

3. If you bring your own laptop computer including Macintosh, please follow the instructions below:

a) Ensure that your computer is equipped with the monitor connector of mini D-sub 15 pins. If your computer does not have this connection, please bring an appropriate converter with you.

mini D-sub 15 pins

b) Be sure to bring an AC adaptor with you. The Japanese standard AC voltage is 100V.

c) Be sure to turn off screen saver or power saving mode of your laptop in advance.

4. A display monitor, keyboard, and remote mouse will be provided on a podium for presenters to operate. Sound speakers are not available.

5. Presentation data loaded on the computers provided will be completely deleted by the secretariat after your presentation.

6. The secretariat is not responsible for any projection troubles caused by computer technical difficulties. We recommend that all presenters bring back-up data.

7. Presenter view is available.

8. COI Disclosure on presentation

When the authors disclose the conflict of interest in the presentation, the category and the names of the companies should be shown after the authors' names in the second slide or at the end of poster. If none of the authors has any conflict of interest to be disclosed, please write "there is no conflict of interest to be disclosed". For more details, please refer to “Call for Abstract” of IPS2018 website.

Sample of Slide

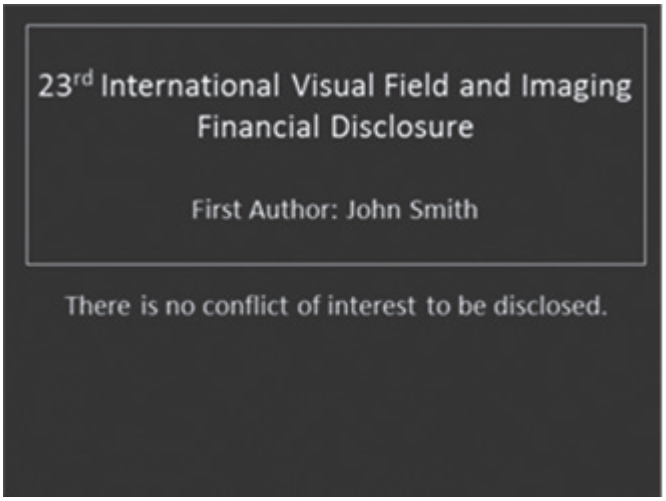

PC Preview Desk open hours:

Wednesday, May 9 16:00-17:45
Thursday, May 10 7:30-18:00
Friday, May 11 7:30-13:00
Saturday, May 12 7:30-17:00

Access to the Venue

Map of Ishikawa Prefecture

■ From Tokyo to Kanazawa

【Shinkansen - JR East】
・JR Hokuriku Sinkansen Kagayaki :
approx. 2 hours and 30 minutes
【Airplane】
・From Haneda Airport to Komatsu Airport :
approx. 60 minutes
・From Komatsu Airport to Kanazawa :
*<Bus (Super Express Non-stop)> :
approx. 45 minutes
*<Automobile>: approx. 40 minutes

■ From Osaka to Kanazawa

【JR West Japan】
・JR Special Express Thunderbird:
approx. 2 hours and 30 minutes

■ From Nagoya to Kanazawa

【JR Central and JR West】
*Shinkansen: approx. 2 hours and 30 minutes
*JR Special Express Shirasagi: approx. 3 hours

■ From Komatsu to Kanazawa

【JR】
・JR Special Express Thunderbird:
approx. 17 minutes

Downtown Kanazawa

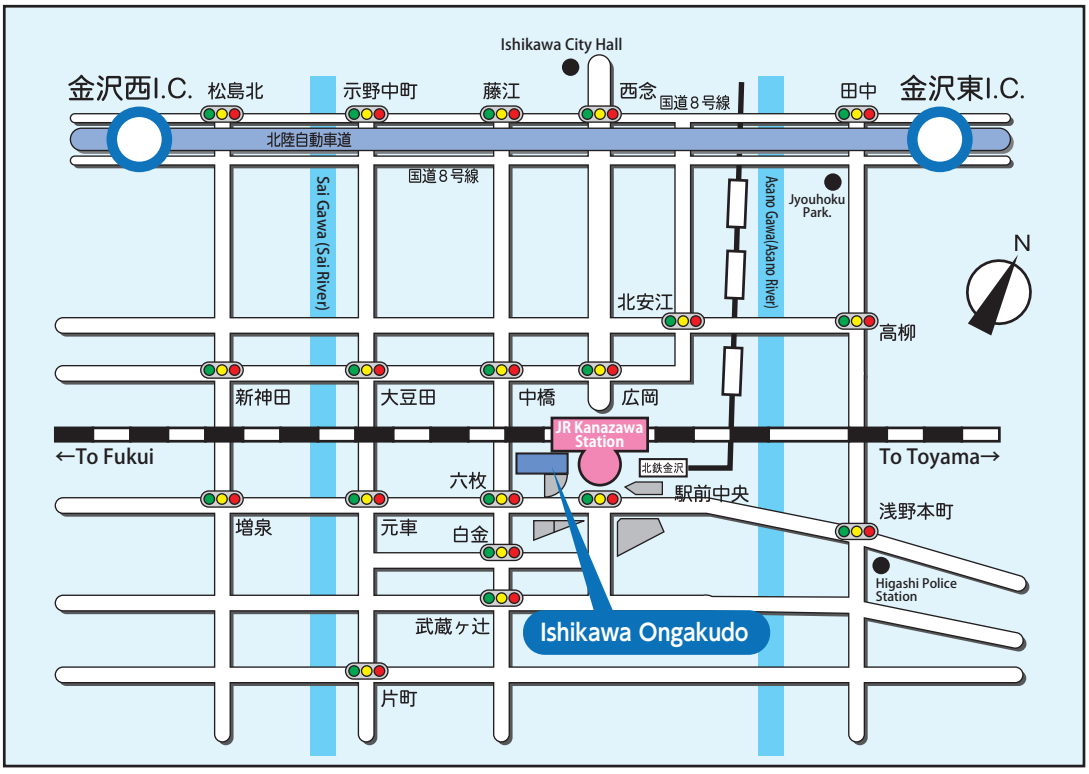

JR Kanazawa Station East Entrance (Kenrokuen Guchi)

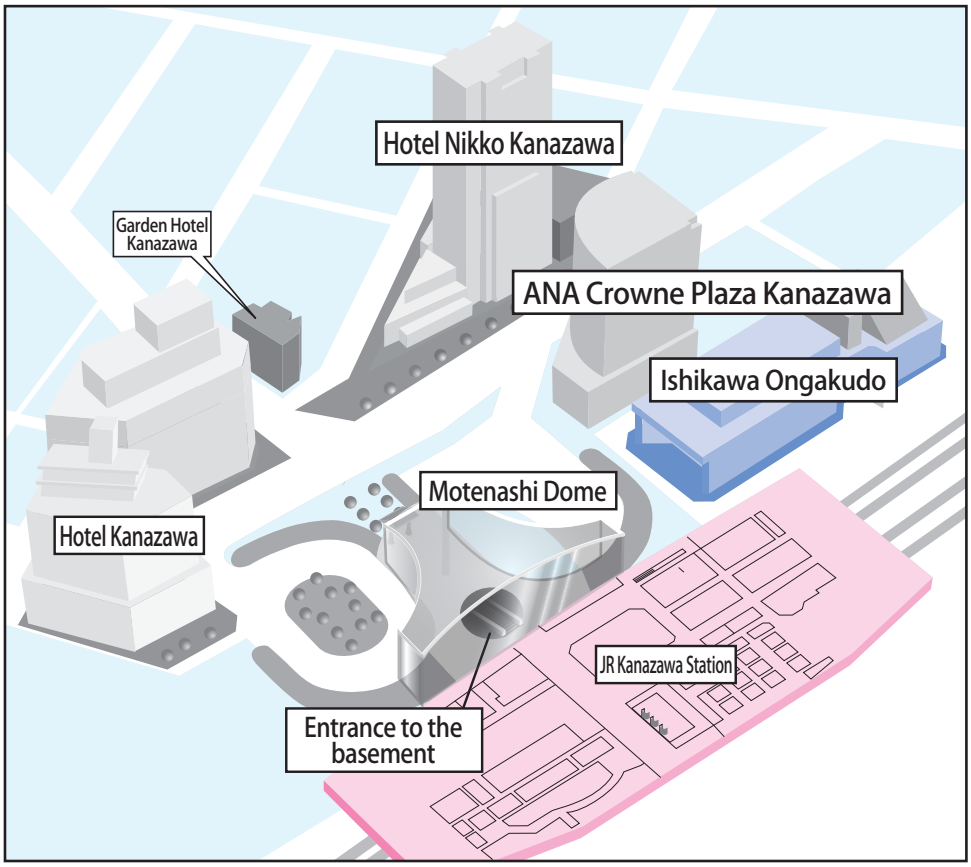

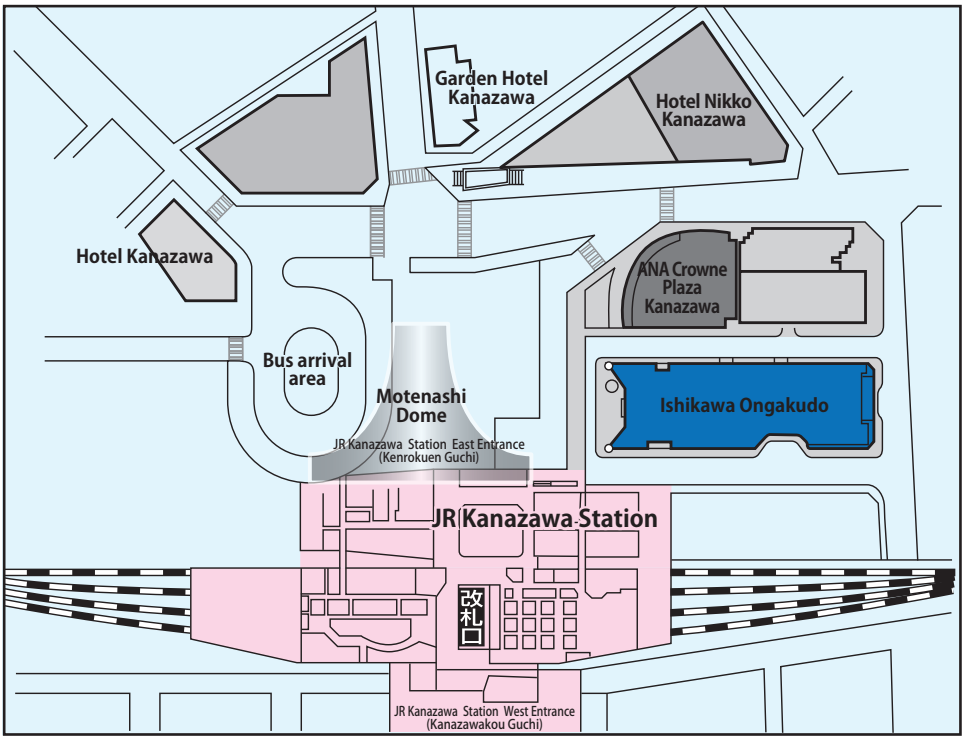

■ Ishikawa Ongakudo

B1 F

1 F

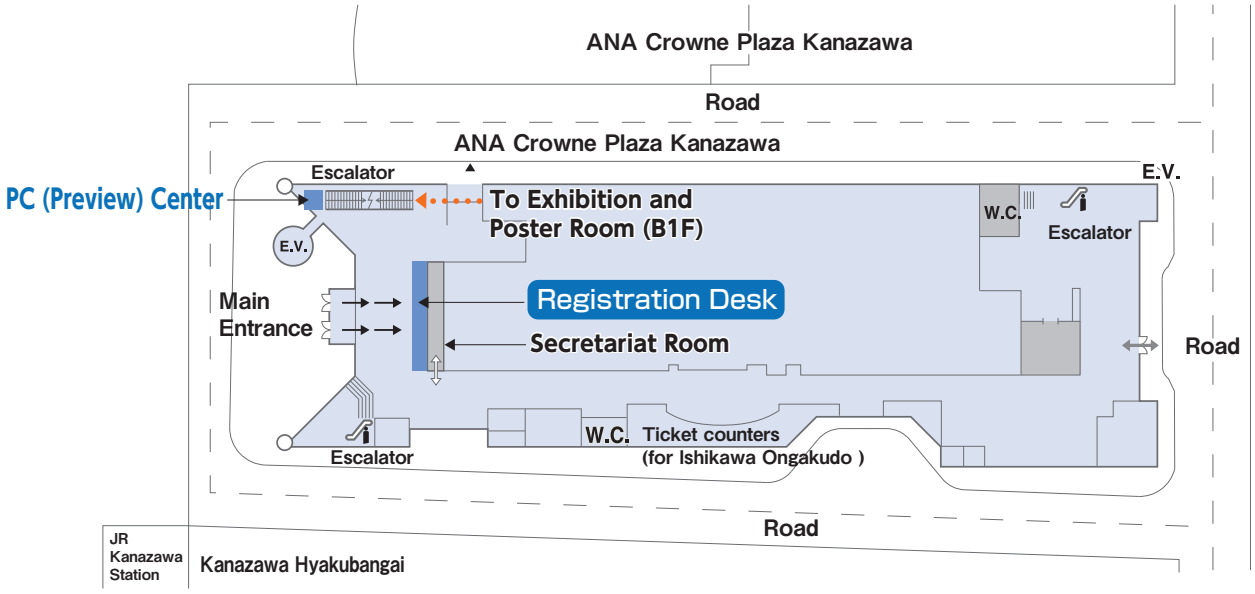

2 F

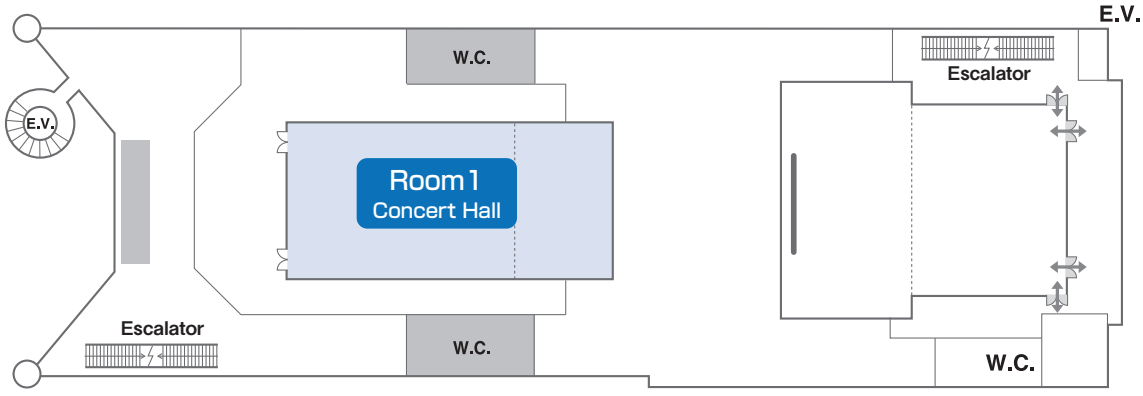

Sponsors and Endorsement

Seminars

Alcon Pharma K. K. / Novartis Pharma K. K.
Carl Zeiss Meditec Co., Ltd.
CREWT Medical Systems, Inc.
Heidelberg Engineering GmbH
Otsuka Pharmaceutical Co., Ltd.
Santen Pharmaceutical Co., Ltd.
Senju Pharmaceutical Co., Ltd.
TOPCON CORPORATION

Sponsors

Alcon Pharma K. K.
Bayer Yakuhin, Ltd.
Beeline Co., Ltd.
Carl Zeiss Meditec Co., Ltd.
CENTERVUE S.P.A.
CENTRAL MEDICAL Co., Ltd.
CREWT Medical Systems, Inc.
Gifu Ophthalmologists Association
Haag-Streit
HANDAYA CO., LTD
Heidelberg Engineering GmbH
HOYA CORPORATION
Inami & Co., Ltd.
Ishikawa Ophthalmologists Association
Kowa Company, Ltd.
Kowa Pharmaceutical Co. Ltd.
Maeda Book Store Ltd.
Medical Book Service
NIDEK CO., LTD.
OCULUS Optikgeräte GmbH
Ophthalmic Bookseller
Santen Pharmaceutical Co., Ltd.
SEED Co.,Ltd.
Senju Pharmaceutical Co., Ltd.
Tomey Corporation
TOMIKI MEDICAL INSTRUMENTS co., ltd
TOPCON CORPORATION

Endorsement

Japanese Association of Certified Orthoptists
Japanese Ophthalmological Society
Japan Ophthalmologists Association

*Alphebetical Order
as of April 2, 2018

Social Events

Wednesday, May 9

Welcome Party

Time: 18:30-20:30
Location: Gojukken Nagaya, Kanazawa Castle
Fee: Included in registration fee
Dress: Casual
Shuttle Bus: Depart at 17:45. Bus Stop is located between Ishikawa Ongakudo and ANA Crowne Plaza Kanazawa.

Welcome Party will be held in Gojukken Nagaya of Kanazawa-jo Castle, where weapons used to be stored. Let the networking begin while you enjoy food and drinks. Fee is included in registration fee, and the party is open to registered participants.

Thursday, May 10

Dinner party

Time: 19:30-22:00
Location: Japanese Restaurant "Tsubajin"
Fee: 25,000 JPY
Dress: Casual
Shuttle Bus: Depart at 18:45. Bus Stop is located between Ishikawa Ongakudo and ANA Crowne Plaza Kanazawa.

*Seats are available to the first 100 registrants

Tsubajin is the most traditional Japanese restaurant in Kanazawa, providing you with fresh local ingredients.

Friday, May 11

Conference Tour

Time: 13:15-17:15
Location: Kanazawa City
(Ishikawa Prefectual Museum of Art, Seisonkaku, Kenrokuen-Garden, Higashi chaya Districts)
Fee: Included in registration fee
Dress: Casual
Shuttle Bus: Depart at 13:10 (after Luncheon Seminar). Bus Stop is located between Ishikawa Ongakudo and ANA Crowne Plaza Kanazawa.

The local organizing committee offers a guided tour of Kanazawa City. The tour is included in registration fee and open to all registered participants.

Saturday, May 12

Closing Banquet

Time:18:30-21:30
Location: Room Tsuru on 4th floor in Hotel Nikko Kanazawa
Fee: Included in registration fee
Dress: Smart Casual

Closing Banquet will be held at Hotel Nikko Kanazawa as a final to IPS 2018.
Fee is included in registration fee and the banquet is open to all registered participants.

Banks/ATMs

Banks are open from Monday to Friday, 9:00-15:00(Closed on Saturdays, Saturdays, and national holidays). In 7-Eleven convenience stores have automatic teller machines (ATMs) that accept credit, debit and ATM cards issued outside Japan including Visa, Plus, MasterCard, Maestro, Cirrus, American Express and JCB cards with English user menu. Please note most Japanese banks' ATM do not accept foreign cards.

Currency Exchange

A money exchange counter, Travelex, in Kanazawa station is available from 10:00 - 20:00 every day. It is just a few minutes' walk from Ishikawa Ongakudo.

Climate

The temperature in Kanazawa in May typically ranges between 12-23 degrees centigrade (54-74F) during the day.

Electricity

100 volts alternating current at a frequency of 60 Hz. is used in Western Japan. The socket is type A, which has two flat plug holes.

Insurance

The Organizing Committee will assume no liability whatsoever for injury or damage to person or property during the congress. Please make your own arrangements for health insurance and any other necessary insurance.

Postal Service

Hotels often provide simple postage services. Post offices are open from Monday to Friday, 9:00 to 17:00.

Time

Japan Standard Time is 9 hours ahead of UTC (Coordinated Universal Time).

Tipping and Consumption Tax

Tipping is not customary in Japan. However, major restaurants or hotels may add a 10% to 15% service charge to your bill.

Map of Downtown Kanazawa


0 100 200 300m
Hondanomori Hall
本多の森ホール
Pref.Noh Theater
県立能楽堂
Kanko Bussankan
県観光物産館
Kenrokuen-shita
兼六園下
Conference Tour
Kenrokuen Garden
兼六園
Pref.History Museum
県立歴史博物館
Pref.Museum of Art 県立美術館
Conference Tour
石川門
Hirosaka
広坂
Kanazawa Castle Park
金沢城公園
広坂 Hirosaka
Pref. Library
県立図書館
Honda-machi 本多町
金沢歌劇座
Kanazawa Kagekiza
Shiinoki Cultural Complex
しいのき迎賓館
金沢21世紀美術館
21st Century Museum of Contemporary Art, Kanazawa
Central Park
中央公園
Kanazawa City Hall 金沢市役所
Daiwa Dept. Store / ATRIO
香林坊大和・アトリオ
百万石通り
Korinbo
香林坊
KOHRINBO 109
Kata-machi
片町
タテマチ商店街
Tate-machi Shopping Promenade
Saisei Bungakuhi-mae
犀星文学碑前
Sakura Bashi Bridge
桜橋
Saigawa River 犀川
Jusangen-machi
十三間町
木倉町通り
Kiguramachi-dori
Saigawa Ohashi Bridge
犀川大橋
長町武家屋敷跡
Naga-machi Buke Yashiki District
中央通り
Chuo Dori Ave.
寺町通り
Tera-machi Dori Ave.
Tera-machi Temples and Shrines
寺町寺院群
Hirokoji
広小路
Myoryuji Temple (Ninja Temple)
妙立寺（忍者寺）
Nishi Chaya Shiryokan Museum
にし茶屋資料館
にし茶屋街
Nishi Chaya District
Kutani Pottery Kosen Kiln
九谷光仙窯
Minami Odori Ave. 南大通り
御影大橋
Saigawa Odori Ave. 犀川大通り

Program at a Glance

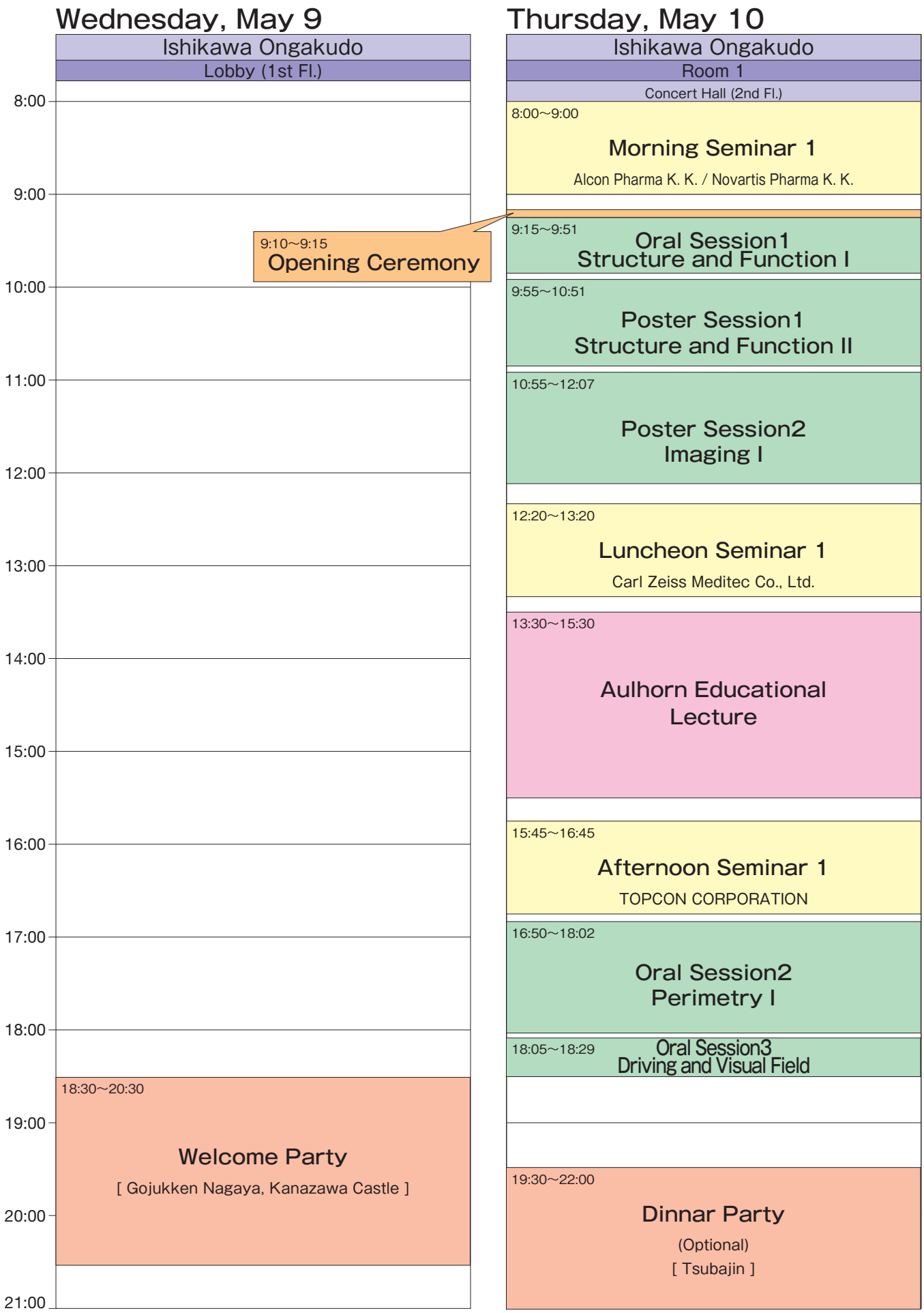

Friday, May 11

Ishikawa Ongakudo
Room 1
Concert Hall (2nd Fl.)

8:00～9:00
Morning Seminar 2
Santen Pharmaceutical Co., Ltd.

9:15～10:19
Poster Session3
Perimetry II

10:20～10:44
Oral Session4
Machine learning methods

10:45～11:45
IPS Lecture
Perimetry: Past, Present and Future

12:00～13:00
Luncheon Seminar 2
Heidelberg Engineering GmbH

13:15～17:15
Conference Tour
[Kanazawa City]

Saturday, May 12

Ishikawa Ongakudo
Room 1
Concert Hall (2nd Fl.)

8:20～9:20
Morning Seminar 3
CREWT Medical Systems, Inc.

9:30～10:42
Oral Session5
Imaging II

10:45～11:45
Poster 4 / Oral 6 Session
New Perimetry

12:00～13:00
Luncheon Seminar 3
Senju Pharmaceutical Co., Ltd.
Otsuka Pharmaceutical Co., Ltd.

13:10～13:58
Oral Session7
Structure and Function III

14:15～15:03
Oral Session8
Perimetry III

15:05～16:05
Oral Session9
Perimetry IV

16:15～17:00
Business Meeting

17:00～17:05
Closing Ceremony

18:30～21:30
Closing Banquet
[Hotel Nikko kanazawa]

Program

■ Thursday, May 10 Room 1 Ishikawa Ongakudo, Concert Hall (2nd Fl.)

8:00 ~ 9:00 Morning Seminar 1 HOW WE SHOULD MANAGE GLAUCOMA PATIENTS: ELDERLY AND MYOPIA

Chair: Tetsuya Yamamoto

Speaker : MANAGEMENT OF THE PERIMETRY IN ELDERLY GLAUCOMA PATIENTS

Megumi Honjo

MANAGING PATIENTS WITH MYOPIA AND GLAUCOMA -HOW AI CAN HELP

Robert T. Chang

Sponsor : Alcon Pharma K. K. / Novartis Pharma K. K.

9:10 Opening Ceremony

9:15-9:51 Oral Session 1 Structure and Function I

Chair: Ulrich Schiefer
Makoto Nakamura

Speaker :

O1-1 Structure-function correlation across the central visual field using pointwise comparisons and ganglion cell isocontours derived from pattern recognition

Michael - Kalloniatis

O1-2 Structure-function in ocular disease using different psychophysical procedures

Jack Phu

O1-3 Structure-function correlation consistent between normal and glaucomatous patients and improves with stimuli scaled to spatial summation area

Nayuta Yoshioka

9:55-10:51 Poster Session 1 Structure and Function II

Chair: Kazuhisa Sugiyama
Shinji Ohkubo

Speaker :

P1-1 Evaluating the usefulness of MP-3 microperimetry in glaucoma patients

Masato Matsuura

P1-2 Mapping the Central 10 Degrees Visual Field to the Optic Nerve Head using the Structure Function Relationship

Yuri Fujino

P1-3 The relationship among macular inner retinal layer, retinal nerve fiber layer, and visual field sensitivity in gemination period of glaucomatous optic nerve damage.

Yoshio Yamazaki

P1-4 Agreement of a nasal step border by a microperimeter with a temporal raphe by optical coherence tomography in glaucoma patients

Sotaro Mori

P1-5 The disc–fovea–temporal raphe angle is associated with the severity of glaucoma with a hemi-field defect

Takuji Kurimoto

P1-6 Relationship between rim width and nerve-fiber layer thickness in normal tension glaucoma.

Yoshinori Itoh

P1-7 Detection of early glaucomatous damage of the macula with OCT oriented perimetry in preperimetric glaucoma

Shinji Ohkubo

10:55-12:07 Poster Session 2 Imaging I

Chair: Balwantray C. Chauhan
Yoshio Yamazaki

Speaker :

P2-1 Retinal layer segmentation and clustering by spectral-domain optical coherent tomography in patient with open angle glaucoma

Shumpei Ogawa

P2-2 The effects of magnification correction or matching of axial length in normative database on early glaucoma detection by ganglion cell complex in eyes with long axial length

Tomomi Higashide

P2-3 Capability of asymmetry in macular ganglion cell layer/inner plexiform layer thickness by optical coherence tomography to detect preperimetric glaucoma.

Daisuke Takemoto

P2-4 Blood flow changes after trabeculectomy in and around the optic disc and the macula

Makoto Sasaki

P2-5 Correlation between optic disc vessel density and glaucoma severity : enhanced-depth imaging optical coherence tomography angiography study

Yuji Yoshikawa

P2-6 Relationship between Optical Coherence Tomography Angiography (OCTA) macular vessel density and visual field loss in glaucoma

Yusuke Nakatani

P2-7 The association between glaucomatous visual field defect, foveal avascular zone area and vessel density using swept-source optical coherence tomography angiography

Yosuke Miyasaka

P2-8 The association between change of radial peripapillary capillaries and disc hemorrhage occurrence in normal tension glaucoma

Koji Nitta

P2-9 Deep-layer microvasculature dropout in glaucoma

Kimikazu Sakaguchi

12:20 ~ 13:20 Luncheon Seminar 1　New Era in Perimetry

Chair: Aiko Iwase

Speaker : HFA central testing and the new 24-2C

Gary Lee

A new SITA test – SITA Faster

Anders Heijl

Sponsor : Carl Zeiss Meditec Co., Ltd.

13:30-15:30 Aulhorn Educational Lecture

Chair: Chris A. Johnson
Linda M. Zangwill

Speaker :

1 Visual function testing -new concepts in research and education

Ulrich Schiefer

2 Computerized perimetry　a catalyst for glaucoma science and management

Anders Heijl

3 Glaucoma Imaging Today and Tomorrow

Balwantray C.Chauhan

4 New technology of perimetry

Chota Matsumoto

15:45 ~ 16:45 Afternoon Seminar 1　An Update on the detection and management of Glaucoma with swept source OCT Triton

Chair: Linda Zangwill

Speaker : Clinical Application of Deep Optic Nerve Head and Peripapillary Imaging

Tae Woo Kim

Swept-source optical coherence tomography for retinal nerve fiber layer optical texture analysis (ROTA)

Christopher Leung

Sponsor : TOPCON CORPORATION

16:50-18:02 Oral Session 2　Perimetry I

Chair: Mitchell Dul
Sachiko Okuyama

Speaker :

O2-1 Visual Field Abnormality Classification in the Ocular Hypertension Treatment Study 20 Year Follow-up (OHTS-3)

John L Keltner

O2-2 Determination of the intra-subject variability of visual field examinations in glaucoma patients

Judith Ungewiss

O2-3 Agreement between multifocal pupillographic objective perimetry, Matrix and HFA in stroke

Ted Maddess

O2-4 A comparison between the Compass fundus perimeter and the Humphrey Field Analyzer

Susan Ruth Bryan

O2-5 Tablet derived Frequency-of-seeing curves for size-scaled spots in the central visual field

Algis J Vingrys

O2-6 Divergence Measures between Normal Subjects and Glaucoma Patients with Mild Visual Loss using Threshold Automated Perimetry of the Full Visual Field

Gideon KD Zamba

18:05-18:29 Oral Session 3 Driving and Visual Field

Chair: Ulrich Schiefer
Aiko Iwase

Speaker :

O3-1 Relationship between local binocular visual field sensitivity and location of undetected driving hazards. Gaze-movement corrected analysis in simulated driving.

Makoto Araie

O3-2 Effect of simulated superior and inferior visual field loss on vehicle control performance in a driving simulator

Makoto Inagami

■ Friday, May 11 Room 1 Ishikawa Ongakudo, Concert Hall (2nd Fl.)

8:00 ~ 9:00 Morning Seminar 2 Early detection and early treatment of PPG -Improvement of diagnostic skill and points of therapeutic intervention of PPG with using OCT-

Chair: Kazuhisa Sugiyama
Goji Tomita

Speaker : Utilization of OCT -Structural change detection of PPG

Ki Ho Park

Utilization of glaucoma inspection instrument -Diagnosis of PPG / Judgement of therapeutic intervention-

Toru Nakazawa

Sponsor : Santen Pharmaceutical Co., Ltd.

9:15-10:19 Poster Session 3 Perimetry II

Chair: Fritz Dannheim
Chota Matsumoto

Speaker :

P3-1 Visual field changes after vitrectomy for epiretinal membranes in glaucomatous eyes
Shunsuke Tsuchiya

P3-2 Usefulness of Clock Chart Driving Edition for self-checking the binocular visual field
Marika Yamashita

P3-3 Perimetry for Children or Mentally Handicapped
Fritz Dannheim

P3-4 Assessment of response reliability in visual field testing without using catch trials
Sachiko Okuyama

P3-5 Influence of Head tilted angle on Blind Spot location in Visual Field Test
Fumi Tanabe

P3-6 Contrast gain control in glaucoma under photopic and mesopic luminance conditions
Catarina A. R. Joao

P3-7 Dynamic color brightness adaptation abnormalities in early stages of glaucoma.
Muen Yang

P3-8 Estimating "True" Retinal Sensitivity from Time-series Visual Field Data Using Gaussian Process Regression
Eiji Murotani

10:20-10:44 Oral Session 4 Machine learning methods

Chair: Andrew Turpin
Hiroshi Murata

Speaker :

O4-1 Development of a deep learning algorithm to diagnose glaucoma from fundus photography
Naoto Shibata

O4-2 Deep Learning Approaches to Predict Standard Automated Perimetry Summary Metrics from SD-OCT Imaging
Mark Christopher

10:45-11:45 IPS Lecture Perimetry: Past, Present and Future

Chair: Chota Matsumoto

Speaker : Perimetry: Past, Present and Future
Michael Wall

12:00 ~ 13:00 Luncheon Seminar 2 OCT-Based Phenotyping of Eyes in Glaucoma Diagnostics

Chair: Makoto Araie

Speaker : The Importance of Aging Effects in the Assessment of Structural Changes in Glaucoma
Balwantray C. Chauhan

Detailed structural characteristics of the optic disc revealed by the Spectralis OCT
Tomomi Higashide

Sponsor : Heidelberg Engineering GmbH

■ Saturday, May 12 Room 1 Ishikawa Ongakudo, Concert Hall (2nd Fl.)

8:20 ~ 9:20 Morning Seminar 3 How should we evaluate the data provided by "imo"?

Chair: Chota Matsumoto

Speaker : What is imo?

Hiromasa Sawamura

Binocular visual field test with imo in clinical use.

Hiroki Nomoto

Sponsor : CREWT Medical Systems, Inc.

9:30-10:42 Oral Session 5 Imaging II

Chair: Christopher Leung
Kazuhisa Sugiyama

Speaker :

O5-1 Influence of Bruch ´ s membrane opening area on OCT diagnostic accuracy

Lucas A Torres

O5-2 Development of a large normative database to investigate physiological and pathological changes in the central retinal ganglion cell layer

Barbara Zangerl

O5-3 Relationship between peripapillary retinal arteries angle and Ocular Response Analyzer waveform parameters

Shotaro Asano

O5-4 Quantification of peripapillary nerve fibre elevation and its association with axial length in young healthy eyes

Masatoshi Tomita

O5-5 Relationship between peripapillary choroidal thickness and tessellation in young healthy eyes

Yusuke Matsushita

O5-6 Classification of macular shape of children on optical coherence tomography

Takehiro Yamashita

10:45-11:45 Poster 4 / Oral 6 Session New Perimetry

Chair: Chris A. Johnson
Nobuyuki Shoji

Speaker :

P4-1 Evaluation of pupil fields using a newly developed perimeter in glaucoma patients

Kazuko Totsuka

P4-2 Effect of non-measurement eyes on the result of measurement eyes by the monocular visual field tests under binocular open view

Hiroyasu Goukon

P4-3 The investigation of the difference of central visual field sensitivity between monocular and binocular measurement by head-mounted perimeter

Tomoyuki Kumagai

P4-4 Measurements of fixation eye movements during visual field test with head–mounted perimeter "imo".

Takuya Ishibashi

P4-5 Influence of a Binocular Viewing Condition on Monocular Sensitivites Measured by imo® in Patients with Glaucoma

Akemi Wakayama

P4-6 SMARTPHONE-BASED PERIMETRY FOR FAST AND LOW-COST VISUAL FIELD ACQUISITION

Jan Stapelfeldt

O6-7 Deploying virtual reality headgear and the foveation reflex to enhance the ergonomics of perimetry

Bertil Damato

12:00 ~ 13:00 Luncheon Seminar 3 Anterior Segment OCT and Glaucoma

Chair: Kazuhisa Sugiyama

Speaker : Anterior Segment OCT and Glaucoma

Tin Aung

sponsor : Senju Pharmaceutical Co., Ltd.
Otsuka Pharmaceutical Co., Ltd.

13:10-13:58 Oral Session 7 Structure and Function III

Chair: Linda M. Zangwill
Makoto Araie

Speaker :

O7-1 Focal lamina cribrosa defect in myopic eyes with non-progressive glaucomatous visual field defect

Yu Sawada

O7-2 Using structural information to improve perimetric examination of the macular visual field in glaucoma

Giovanni Montesano

O7-3 En face slab images of macula better accounts for visual functional outcomes compared with inner retinal thickness in eyes with optic neuritis

Mari Sakamoto

O7-4 Inner retinal structure-function relationship within the central 20 degrees in retinitis pigmentosa

Henrietta Wang

14:15-15:03 Oral Session 8 Perimetry III

Chair: Allison M. McKendrick
Ryo Asaoka

Speaker :

O8-1 EVALUATION OF THE NEW THRESHOLD STRATEGY USING A VARIATIONAL BAYES MODEL

Satoshi Shimada

O8-2 DENOISING VISUAL FIELDS USING AUTO-ENCODERS

Serife S. Kucur

O8-3 Cluster Identification Algorithm (CIA)

Anca D. Demea

O8-4 The usefulness of waveform parameters measured with the Ocular Response Analyzer to assess the progression of glaucoma

Shuichiro Aoki

15:05-16:05 Oral Session 9 Perimetry IV

Chair: Michael Wall
Takeshi Yoshitomi

Speaker :

O9-1 ARREST: A new visual field test algorithm designed to improve spatial resolution and test time for moderate-advanced visual field damage.

Allison M McKendrick

O9-2 Measuring Frequency of Seeing Curves On and Off Blood Vessels in Normal Eyes Using the Compass Perimeter Controlled by the OPI

Andrew Turpin

O9-3 Robustness of area-modulated perimetric stimuli to increased intraocular straylight

Lindsay Rountree

O9-4 The relationship between cortical receptive field size and eccentricity in V1, V2 and V3 of healthy individuals

Melissa E Wright

O9-5 Visual function and adaptation from star- to sunlight in glaucoma: a case-control study

Nomdo M. Jansonius

17:00 Closing Ceremony

Abstract

Perimetry: Past, Present and Future

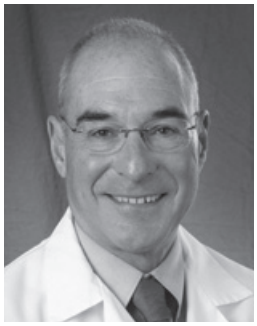

Michael Wall
University of Iowa, Iowa City, IA. USA

Perimetry was introduced into clinical medicine by von Graefe in 1856 by mapping central visual field defects with a piece of chalk on a chalk board. Aubert in 1857 extended perimetric examination to the far periphery. Emphasis returned to the central field in 1889 when Bjerrum introduced quantitive isopter perimetry. With the launch of the Goldmann bowl perimeter in 1945, stimulus and background were elegantly controlled and for the next three decades, the full limits of the visual field territory were examined. In the 1980s, threshold static automated perimetry became the clinical standard and emphasis eventually focused on the central 21 degrees of the visual field. By the late 1980s it was clear that major shortcomings of standard automated perimetry (SAP) were the 1) high retest variability, 2) long test time and 3) inability to efficiently test the far periphery. New Bayesian testing algorithms, dynamic timing routines and new strategies for catch trials helped shorten the test time. Investigations using stimulus size V for SAP showed it had lower retest variability, a greater useful dynamic range and could realistically be employed to test the far visual field periphery. Using the Open Perimetry Interface (OPI) our group has developed SAP with a size V Bayesian testing procedure using dynamic timing for the full visual field, along with a suprathreshold test to further shorten the testing time. Testing below 15 dB is not performed leading to a substantial improvement in retest variability without loss of the ability to detect visual field change. New patterns of visual field loss have surfaced with this new test. Future endeavors include virtual reality perimetry with eye movement position used as an outcome and automated kinetic testing. Metabolic and electrophysiologic testing all have promise for objective testing of the full visual field.

Biographical sketch

Michael Wall, M.D. is a professor of Neurology and Ophthalmology at the University of Iowa. His undergraduate and medical school education was at Tulane University; his neurology residency at Washington University in St. Louis and fellowship at Massachusetts Eye and Ear Infirmary. As a neuro-ophthalmologist he is involved in patient care, teaching and research. He is the author of 107 peer-reviewed journal articles and three books. He has been involved in idiopathic intracranial hypertension research for 30 years and is currently the Study Director of the NIH funded Surgical Idiopathic Intracranial Hypertension Treatment Trial. He has had continuous funding for perimetry research from the VA Merit Review system for over 25 years. His current perimetry grant is titled: "Testing of the far peripheral visual field – Obtaining the Full View." It employs the Open Perimetry Interface to develop new perimetric methods.

Visual function testing – new concepts in research and education

Ulrich Schiefer[1,2]

[1]Competence Center "Vision Research", Study Course Ophthalmic Optics, University of Applied Sciences Aalen, Germany
[2]University Eye Hospital and Research Institute of Ophthalmology, Eberhard-Karls-University Tübingen, Germany

On the 4th of March, 1991, Elfriede AULHORN, one of the most prominent German psychophysicists and ophthalmologists of the 20th century, passed away. She was born in 1923 and raised in Hannover. Having completed her high school diploma, she studied medicine in Freiburg and Göttingen. In 1947, she married the physiologist Otfried AULHORN, who died from the consequences of war injury, before their daughter was delivered. Elfriede AULHORN graduated (summa cum laude). The topic of her doctoral thesis (fixation width and fixation frequency during reading) aimed at a research area of her deceased husband. In 1961, she finalized her habilitation (i.e. the highest qualification in academics in Germany) in Tübingen, dealing with the interrelationship between luminance sensitivity and visual acuity. In 1966, she became the head of the Department of Pathophysiology of Vision at the Tübingen University Eye Hospital. Since 1970, she held a full professorship and the chair of Pathophysiology of Vision, which was extended by the sub-speciality "Neuro-Ophthalmology" in 1974. Elfriede AULHORN was the first woman in Germany to hold a departmental chair, which she held until her retirement in 1990. In 1985, she was elected a member of the Academic Society *Leopoldina.*

Elfriede AULHORN contributed to modern ophthalmology through an admirable variety of pioneering findings, ideas and inventions. Together with Heinrich Harms, who acted as her scientific and clinical mentor since 1954, she developed and refined a variety of perimetric techniques including kinetic and static procedures as well as "white noise field campimetry". She contributed to fundamental examination methods (among others: the phase difference haploscope and the haplophotometer). Together with Heinrich Harms, she was the founder of the profession of German "traffic ophthalmology", and contributed to almost all of the important investigations, regulations, and vision requirements in this area. She also developed novel examination tools for the evaluation of mesopic vision and glare sensitivity, such as the mesoptometer.

Elfriede AULHORN had already participated at the first IPS meeting in Marseille in 1974, and she hosted the second IPS meeting in Tübingen in 1976. AULHORN served as IPS president from 1976 through 1980 and as IPS vice president from 1980 through 1990. She is an honorary member of this society.

Elfriede AULHORN acted as an ingenious, extremely versatile personality of the highest integrity, who educated, mentored, and formed an entire generation of vision scientists and researchers.

This part of the IPS 2018 AULHORN Educational Lecture will deal with the following topics, that are all adressing Elfriede AULHORN´s legacy:

- Kinetic perimetry: Demands, obstacles, and challenges
- The future of conventional perimetric instruments
- "Traffic ophthalmology": More than just perimetry.

Prof. Dr. med. Elfriede Aulhorn

Curriculum vitae
Nationality: German
Family: married since 1983, three daughters
Medical Studies: 1976 – 1982, University of Düsseldorf
Medical Studies: April-28, 1983, Third (final) Medical State Examination
Military Service: 10/1983 – 11/1986, (rank: "Stabsarzt") Military Hospital Ulm,
Dept. of Ophthalmology (Head: Prof. Dr. med. E. Schütte)
Dissertation: March-26, 1984
Scientific employee 12/1986 – 03/1989, University Eye Hospital Tübingen
Board exam in ophthalmology: April-27, 1988
Senior physician ("Oberarzt"): since April-01, 1989, University Eye Hospital Tübingen
Habilitation: November-23, 1993
Executive senior physician,
Deputy of the director of Dept.: since March-15, 1994, University Eye Hospital Tübingen
Appointment as Ass. Professor: March-5, 1999
Visiting Professor: 04 – 05 / 2001 Washington University
Dept. of Ophthalmology and Visual Sciences, St. Louis, USA
Application for position as "Head of Neuroophthalmology" :
2003, University of Freiburg, Germany(successor of Prof. G. Kommerell): "secundo loco"
Application for position as "Head of Dept. of Ophthalmol." :
2007, University of Gießen, Germany (successor of Prof.G. Kaufmann): "tertio loco"
W3 Full Professorship "Vision Research" 12/2012, Course of Studies Ophthalmological Optics / Ophthalmological Optics – Audiology, Faculty of Optics & Mechatronics, University of Applied Sciences, Aalen, Germany

Awards:
1984 Award of the University of Düsseldorf: Best thesis of the year
1992 Award of the "Deutschen Ophthalmologischen Gesellschaft" (DOG, German Ophthalmologic Society) for an outstanding educational video film: *"About reading"*
1996 Elfriede-Aulhorn-Award of the DOG (German Ophthalmologic Society)
2002 Federal Teaching Award (Ministry of Science, Research and Arts, Baden-Württemberg)
2004 Baden-Württemberg Certification "Didactics in University Education"
2005 Video film-award of the DOG (German Ophthalmological Society) for an outstanding educational film: *„Subjective refraction using the Jackson cross cylinder "*
2006 Award of the Tübingen medical students: Best teachers of the medical faculty (rank 11 of 674 evaluated Medical University lecturers, Tuevalon)
2008 Award of the Tübingen medical students: Best teachers (rank 3 of 770 evaluated Medical University lecturers)
2010 Award of the Tübingen medical students: Best teachers (rank 1 of 1134 evaluated Medical University lecturers)
2010 "Ophthalmologist of the Year 2010" (Board of the Journal "Ophthalmologische Nachrichten")
2013 Joseph Ströbl Award of the Joseph & Sonja Ströbl Foundation for the advancement of excellent journalistic and scientific accomplishment with regard to traffic safety

Patents (German Patent office, Munich, Germany)
- Schiefer U, Witte A (1996) Patent: Perimetrisches Untersuchungsverfahren - Fundusgestützte Perimetrie II (Perimetric examination technique – fundus-oriented perimetry II)
- Schiefer U, Witte A (1996) Patent: Perimetrisches Untersuchungsverfahren - Autokinetische Perimetrie II (Perimetric examination technique – autokinetic perimetry II).
- Schiefer U, Witte A (1996) Patent: Perimetrisches Untersuchungsverfahren - Ja-/Nein-Patientenabfrage II (Perimetric examination technique – explicit yes-/no-response assessment II).
- Schiefer U, Witte A (2003) Patent: Perimetrisches Untersuchungsverfahren - Autokinetische Perimetrie unter Berücksichtigung und Korrektur der individuellen Reaktionszeit (Perimetric examination technique – Autokinetic perimetry with explicit consideration of and correction for the individual reaction time).

Membership on Academic Committees

Medical Department University Tübingen:
- Commission reviewing doctoral thesis proposed for a grade of "summa cum laude"
- several appeal committees of the Tuebingen Faculty of Medicine

Membership
- Studienstiftung des Deutschen Volkes
- Berufsverband der Augenärzte Deutschlands e.V. (BVA)
- German Ophthalmological Society (DOG)
- International Perimetric Society (IPS) – Board member since 09/2000 – Vice president 06/2002 to 06/2004 – Treasurer since 06/2004
- Bielschowsky Society for Strabismological Research and Neuro-Ophthalmology
- Arbeitsgruppe "Fahr-, Steuer- und Überwachungstätigkeiten" des Ausschusses Arbeitsmedizin der Berufsgenossenschaften
- DOG Commission for the Quality Assurance of Sensory Physiological Examination Methods and Instruments (Head since 2007)
- Association for Research in Vision and Ophthalmology (ARVO)
- Member of the Editorial Board of the Journal "Der Ophthalmologe"
- Board member of German Ophthalmological Society (DOG) since 10/2011

Regular activities in continuing education and further training
- Ophthalmology academy of Germany (AAD): 6 courses per year
- Course on Functional Diagnostics and Neuro-Ophthalmology (FUN): including organization
- Interactive Course on Advanced Functional Diagnostics and Neuro-Ophthalmology (FUN+)
- Course on Perimetry, Tübingen (TUP): including organization
- Glaucoma Workshop Tübingen: including organization
- Basic Science Courses (e.g. perimetry and neuro-ophthalmology)
- Interactive course on optics and refraction (RiTA) Tübingen, Aalen: including organization

Additonal Certification
- Course for principal investigators (Coordination Centres for Clinical Trials at University Hospitals Tübingen and Ulm)

further details: www.vision-research.de

Computerized perimetry- a catalyst for glaucoma science and management

Anders Harald Robert Heijl
Skåne University Hospital Malmö Lund University, Sweden

In this presentation I will give a report of the development of computerized perimetry and particularly how computerization of perimetry has faciliatated crucial clinical glaucoma studies. Together the development and the results of studies relying on computerized perimetry have shaped much of modern, indiviualized glaucoma management.

Anders Heijl M.D., Ph.D. - Biosketch

Anders Heijl is Professor at the Dept of Ophthalmology, Skåne University Hospital Malmö, Lund University, Sweden, where he served as chairman between 1990 and 2012.

Prof. Heijl is a graduate of the Lund University Medical School where he also completed his residency in ophthalmology. He received a Ph.D. from the University of Lund in 1977 for his early work on computerized perimetry, and later completed a post-doctoral fellowship under the mentorship of Professor Stephen Drance at the University of British Columbia.

Prof. Heijl and his research group have invented and developed the Statpac programs for the Humphrey perimeter, including the now widely used concepts of Probability Maps, Pattern Deviation, Change Probability Maps, the Glaucoma Hemifield Test. The Swedish Interactive Thresholding Algorithm (SITA) was also developed in his laboratory, as was the Glaucoma Progression Analysis (GPA) programmes and the VFI index. A new even faster SITA test (SITA Faster) has just been released after several years of testing.

Prof. Heijl initiated and has served as Study Director of the Early Manifest Glaucoma Trial (EMGT) and is medical director of the new Glaucoma Intensive Treatment Study (GITS).

Between 1980 and 1996 Anders Heijl served the International Perimetric Society first as Scientific Secretary and later as President. Between 2003 and 2008 he served as President of the Glaucoma Research Society. Dr Heijl is the past president of the Swedish Glaucoma Society and serves of the board of the European Glaucoma Society.

Prof. Heijl was the chief ophthalmological advisor to the Swedish National Board of Health and Welfare 2003-2012.

Prof. Heijl has published 200 scientific papers, chapters and books. He has served as Editor-in-Chief of Acta Ophthalmologica, and on the editorial boards of several ophthalmic journals.

Dr Heijl has received scientific awards, or delivered invited name lectures at about 25 instances. He is an Honorary Member of the International Perimetric Society, the Glaucoma Research Society, the Finnish Ophthalmological Society, The Swedish Ophthalmological Society and the South-African Glaucoma Society.

ANDERS HEIJL – SHORT CURRICULUM VITAE 2018

Senior Professor and Consultant at the Department of Ophthalmology, Skåne University Hospital in Malmö, University of Lund 2013-

Professor at the Department of Ophthalmology, Malmö University Hospital, later re-named Skåne University Hospital in Malmö, University of Lund 1990 –2012

President of the Internatioanl PeriemtricSociety 1988 – 1996,

President of the Glaucoma Research Society 2003 – 2008,

President of the Swedish Glaucoma Society 2010 –2016

Member of the Exective Committee of the European Glaucoma Society 2004 -;

Chairman of National Societies Liaison Committee 2009 -

Study Director and PI: The Early Manifest Glaucoma Trial (NIH, MFR) 1992 –2013

Chairman of the Department of Ophthalmology, Malmö University Hospital, University of Lund 1990 – 2012

Chief Advisor in Ophthalmology (Vetenskapligt Råd Oftalmologi) for the Swedish National Board of Health and Welfare 2003-2012

Chairman EBM project Open Angle Glaucoma, The Swedish Council on Technology Assessment in Health Care 2003-2009

Editor: Acta Ophthalmologica; Chief Editor Acta Ophthalmologica 2000-2005; Co-editor 2005-

Member of the editorial board:

Acta Ophthalmologica,, Journal of Glaucoma,

Honorary Memberships

2008 Honorary member of the International Perimetric Society

2011 Honorary member of the Finnish Ophthalmological Society

2012 Honorary member of the South African Glaucoma Society

2012 Honorary member of the Glaucoma Research Society.

2017 Honorary member of the Swedish Ophthalmological Society

Scientific Awards:

1984 The KKK Lundsgaard medal of the Nordic Ophthalmological Societies for best scientific paper in Acta Ophthalmologica 1982-1983.

1989 The Alcon Research Institute Award.

2003 The AIGS Award (Association of International Glaucoma Societies) for best glaucoma paper world wide 2002.

2003 The Ilmari Rendahl lecture and award of the Swedish Ophthalmological Society

2003 The Bjerrum lecture of the Danish Ophthalmological Society.

2004 The KKK Lundsgaard medal of the Nordic Ophthalmological Societies for best scientific paper in Acta Ophthalmologica 2002-2003.

2005 The Award of the Danish Synoptikfonden

2005 The Hjalmar Schiøtz medal of the Norwegian Ophthalmological Society

2005 Axel Hirsch' s prize of the Karolinska Institute for the paper "Reduction of intraocular pressure and glaucoma progression. Results from the Early Manifest Glaucoma Trial."

2006 The Award of the Swedish Association of the Visually Impaired

2008 The Trantas Medal of the Greek Glaucoma Society

2010 Acta Ophthalmologica Gold Medal

2012 EVER Acta Ophthalmologica lecture and Award

2016 The Bartisch lecture and Award

2016 The Goldmann lecture and medal of the Glaucoma Research Society

Other Name Lectures

2000 and 2002 The Allergan lecture of the Glaucoma Society of UK and Ireland, London, England

2003 The Barber lecture of the Royal Ophthalmological Society of Scotland, Glasgow. Scotland

2006 The Leopold lecture of the Annual Ocular Drug and Surgery Update Meeting, Laguna Beach, California

2008 The first Aulhorn Lecture of the International Perimetric Society, Nara, Japan

2008 The first Zingirian lecture of S.I.P.E. (The Italian Society for Perimetry and Imaging)

2012 The Leydhecker-Harms lecture of the Univ Dept of Ophthalmology, Würzburg

2017 The Roger Hitchings lecture of the Glaucomat Society of the United Kingdom and Eire

Glaucoma Imaging Today and Tomorrow

Balwantray C. Chauhan
Mathers Professor and Research Director
Dalhousie University, Halifax, Canada

Imaging techniques such as optical coherence tomography (OCT) has revolutionized ophthalmology. With advances in hardware, image quality and speed, ophthalmologists are able to visualize the optic nerve head and retina with unprecedented resolution. Visualizing this anatomy has highlighted the need to better understand our clinical examination and the significant interindividual variability among eyes. This presentation will review recent advances that are relevant to glaucoma, both in the clinical and basic sciences, and identify where there are needs for decision-making tools to help clinicians best exploit OCT advances.

Balwantray Chauhan is Mathers Professor and Research Director of Ophthalmology and Visual Sciences, and Professor of Physiology and Biophysics at Dalhousie University. He obtained his Ph.D. at the University of Wales, Cardiff, UK, and his postdoctoral training at the University of British Columbia, Vancouver, Canada, under Dr. Stephen Drance.

Dr. Chauhan's clinical research interests centre on changes in the visual field and optic nerve head in glaucoma. He has devised new strategies for detecting glaucomatous progression and conducted research leading to their translation to clinical practice. A key contribution in this area is the Topographical Change Analysis (TCA), used for identifying changes in optic nerve head topography with imaging techniques. His recent contributions have been on the acquisition and analysis of anatomically and geometrically accurate neuroretinal rim measurements. Dr. Chauhan is Principal Investigator of the Canadian Glaucoma Study, a multicentre study on the risk factors for the progression of open-angle glaucoma.

He also conducts research with experimental models of optic nerve damage. Areas of activity include studies of neuron-glia interaction in the retina and optic nerve, in vivo imaging of retinal ganglion cells and neuroprotection. This research is conducted in the Retina and Optic Nerve Research Laboratory, a multidisciplinary facility he was instrumental in establishing.

Dr. Chauhan has received numerous awards and recognitions including the Achievement Award of the American Academy of Ophthalmology, Gold Fellow of the Association for Research in Vision and Ophthalmology and the Alcon Research Institute Award. He is President of the Glaucoma Research Society. His research is funded by the Canadian Institutes of Health Research (CIHR), the Atlantic Innovation Fund and other public and private sector agencies.

New technology of perimetry

Chota Matsumoto
Department of Ophthalmology,
Kindai University, Faculty of Medicine, Japan

We developed a new portable head-mounted perimeter named imo which provides visual field testing without a dark room under flexible conditions. In imo, a test target is displayed using two sets of full HD transmissive liquid crystal displays and high intensity white LED backlights for each eye. The test target luminance of 0.1-10000 asb is generated with the background luminance of 31.4 asb using 10 bit resolutions. Test target sizes are Goldmann I to V, and any other optimal sizes and shapes are available. Both right and left pupils are illuminated by near infrared LED and these images are obtained using SXVGA (1280 X 960 pixel) resolution CMOS sensor and usable for eye tracking system. Using imo, not only the traditional perimetry in which right and left eyes are tested separately, but also a new testing approach which we call binocular random single eye test is available. In the binocular random single eye test, the test target is presented randomly to either eye under non-occlusion condition without the subject being aware of which eye is tested. In imo, we introduced a new thresholding algorithm 'Ambient Interactive ZEST' (AIZE) and its rapid version AIZE Rapid. In AIZE, during one point is tested by ZEST algorithm, likelihood function of neighboring test points in the same quadrant are weighted and applied depending on the distance and not depending on the disease characteristics. imo is a highly extensible device for many new perimetrical strategies. In this lecture these new characteristics of imo and its potential for future perimetry will be discussed.

Curriculum Vitae

1983 - 1985	Residency in Ophthalmology at Kindai University Hospital
1985 - 1989	Postgraduate Course for D.Sc. Kindai University Faculty of Medicine
1989 - 1990	Clinical fellow, Tane Memorial Eye Hospital
1990 – 1991	Clinical fellow, Department of Ophthalmology, Kindai University Faculty of Medicine
1991 - 1999	Assistant Professor, Department of Ophthalmology, Kindai University Faculty of Medicine
1998 - 1999	Visiting Assistant Professor, Johns Hopkins University School of Medicine, Wilmer Ophthalmological Institute, MD. U.S.A.
1999 - 2008	Associate Professor, Department of Ophthalmology, Kindai University Faculty of Medicine
2008 - present	Professor, Department of Ophthalmology, Kindai University Faculty of Medicine

Memberships for Scientific Societies
Imaging and Perimetry Society: President
Japan Perimetric Society: President
Japan Glaucoma Society: Board member
Japanese Ophthalmological Society: Councilor

O1-1

Structure-function correlation across the central visual field using pointwise comparisons and ganglion cell isocontours derived from pattern recognition

Michael - Kalloniatis[1], Janelle Tong[1], Nayuta Yoshioka[1], Sieu K Khuu[2], Jack Phu[1], Agnes Choi[1], Barbara Zangerl[1], Lisa Nivison-Smith[1], Bang V Bui[4], Bryan W Jones[3], Robert E Marc[3]

[1]School of Optometry and Vision Science, Centre for Eye Health, UNSW, Australia, [2]School of Optometry and Vision Science, UNSW, Australia, [3]Moran Eye Centre, University of Utah, Utah, USA, [4]Department of Optometry and Vision Science, Univ of Melbourne, Parkville, Australia

Purpose: To establish the correlation between visual field (VF) sensitivity and ganglion cell density (GCD) within the central 20°. We hypothesized that the use of a test stimulus within complete spatial summation (Goldmann II, GII) would display improved correlation compared to the standard GIII stimulus.

Methods: One eye of 40 normal subjects was tested. The Humphrey Field Analyzer was used in full threshold mode to test points within the 10-2 VF test grid and 12 points from the 30-2 grid matching the Spectralis optical coherence tomography (OCT) posterior pole scan. Ganglion cell layer (GCL) thicknesses were obtained for each of the 64 locations (~6880x6880 microns). VF sensitivity (dB) was plotted against GCD/mm^3 (calculated from GCL thickness and GCD from histological data, converted into dB). VF and OCT data were converted to a 50 year-old equivalent for analysis. Spatial correction was applied to VF data to allow comparison of structure and function (Fig 1). Linear regression analysis was conducted using pointwise comparison, and when grouped using 5, 6, 7 or 8 GC isodensity theme classes derived from pattern recognition (Fig 1, Yoshioka et al IOVS 2017). A non-parametric bootstrap was used to determine the 99% distribution limits of the slope and correlation.

Results: Table 1 shows the structure-function correlation slopes and coefficients of determination (R^2) for pointwise and grouped comparisons using GII and GIII. Using 7 or fewer theme classes resulted in a slope close to unity and high R^2 values (0.92) for GII. Slope and R^2 values found using grouped analysis (~1.00 and 0.92, respectively) were superior to pointwise analysis (0.84 and 0.73), confirmed using a non-parametric bootstrap. Correcting the data for test size difference (6 dB) did not result in data superimposition, confirming that GIII is not within complete spatial summation within the central 20°.

Conclusions: Using a test stimulus within complete spatial summation (GII) and grouping sensitivities according to GCD test grids derived using pattern recognition (7 or fewer GC theme classes), revealed correlations close to unity with R^2 greater than 0.90. The high correlations when using theme classes compared to pointwise data suggests that a grouped theme class approach would provide a useful method to predict alterations of VF sensitivity using OCT data.

Figure 1: *Left:* HFA 10-2 test grid (white) and points from the 30-2 grid (purple) superimposed upon the central Spectralis OCT scan following spatial correction (Drasdo et al VR 2007). Where more than one point fell on the Spectralis grid, the VF points were averaged. No data was provided for the 12 Spectralis points for which there was no corresponding VF location (blue cells). *Right:* Theme classes of GC isodensity plots (Yoshioka et al IOVS 2017).

Conflict of Interest: Yes, I have. **Ethics Committee Approval:** Yes, I have obtained **Informed Consent:** Yes, I have obtained

Figure 1:

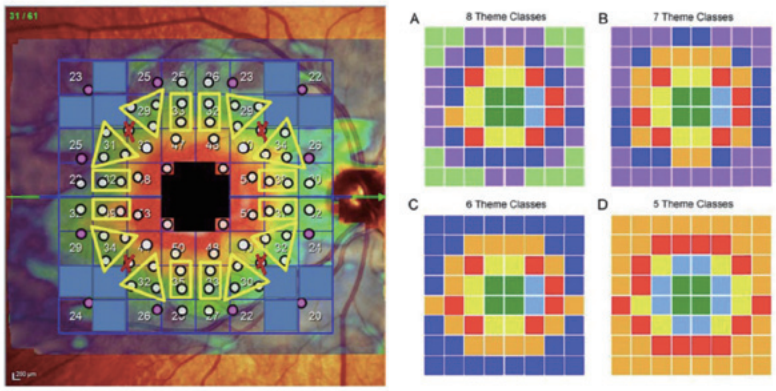

O1-2

Structure-function in ocular disease using different psychophysical procedures

Jack Phu[1,2], Michael Kalloniatis[1,2], Henrietta Wang[1,2], Sieu K Khuu[2]

[1]*Centre for Eye Health, University of New South Wales, Australia,* [2]*School of Optometry and Vision Science, University of New South Wales*

Purpose: Both structural and functional tests are used for the assessment of ocular diseases such as glaucoma and retinitis pigmentosa (RP). However, the structure-function relationship may be confounded by procedural variability, such as in visual field (VF) assessment. We compared the structure-function relationship in patients with retinal disease using two psychophysical procedures: one reflecting more subjective clinical protocols, and the other a more objective task.

Methods: We tested six glaucoma and four RP patients. Clinical perimetry (static and kinetic) was performed to identify a scotoma for further testing. Laboratory-based testing consisted of two phases. Firstly, a two-way Method of Limits (MoL) was performed at a scotoma border to determine the subjective limits of the border. The second phase was a two-interval forced choice (2IFC) procedure with three conditions: a static and a kinetic target (moving inward or outward at 4°/s). Stimuli were presented at ± 1° intervals (up to 4°) to obtain a psychometric function. Eccentricity thresholds were determined using a sigmoidal nonlinear regression function (Fig 1A). Then, patients underwent testing using optical coherence tomography (Spectralis OCT) along the same retinotopic meridian. Retinal thicknesses (RT) were compared with normal subjects to obtain a difference plot. Sigmoidal nonlinear regression was used to obtain the point of inflection (°) where there was a significant change in the RT compared to normal subjects (Fig 1B). The functional and structural thresholds were then compared.

Results: Scotomas identified by clinical perimetry were discordant with the position of RT change found on OCT (on average 3° discordant). Using the more objective 2IFC found better concordance between the location of functional change and the position of structural change, irrespective of whether the stimulus was static or moving (on average 0.7° discordant). Fig 1C shows the relative threshold eccentricity (°) as a function of measurement technique for a representative glaucoma patient. There was no significant difference between structural and 2IFC measurements, but >4° discordance when using MoL in this patient. No systematic discordance between MoL compared to 2IFC measurements across all subjects suggests that individual criterion bias and variability may play a role in structure-function discordance at the border of scotomata.

Conclusions: Using a more objective psychophysical procedure may provide a better structure-function relationship at the border of scotomata in patients with retinal disease, such as glaucoma and RP.

Conflict of Interest: No, I don't. **Ethics Committee Approval:** Yes, I have obtained **Informed Consent:** Yes, I have obtained

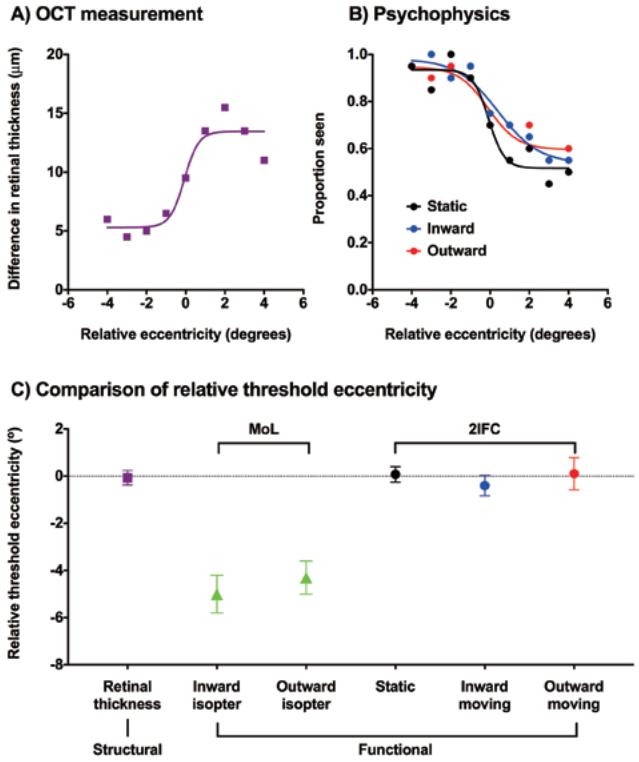

Fig 1: Results of psychophysical testing for a representative glaucoma patient

O1-3

Structure-function correlation consistent between normal and glaucomatous patients and improves with stimuli scaled to spatial summation area

Nayuta Yoshioka[1,2], Barbara Zangerl[1,2], Jack Phu[1,2], Agnes Choi[1,2], Sieu K Khuu[2], Katherine Masselos[1,3], Michael P Hennessy[1,3], Michael Kalloniatis[1,2]

[1]Centre for Eye Health, University of New South Wales Sydney, Australia, [2]University of New South Wales, School of Optometry and Vision Science, [3]Prince of Wales Hospital Ophthalmology Department

Purpose: To determine the effect of stimulus size and early glaucomatous damage on the structure–function relationship in the central retina. We firstly hypothesized the structure–function relationship between ganglion cell count per stimulus area (GCc) and visual field sensitivity approach a 1:1 positive correlation with stimulus sizes within the area of complete spatial summation (Ac), such as Goldmann stimulus sizes I and II (GI–II). Secondly, we hypothesized the underlying structure–function relationship remains consistent between normal and glaucomatous patient.

Methods: The normal and glaucomatous cohort each consisted of 25 subjects. Differential light sensitivity (DLS) data for GI–GV and a grid–wise ganglion cell layer thickness (GCLT) data were collected using Humphrey Field Analyzer across the 10–2 test grid and Spectralis OCT posterior pole scan respectively. To minimize data variability, DLS below the limit of reliable perimetric sensitivity (Gardiner, Ophthalmol 2014 and correction factors from Phu et al. IOVS abstract 2017) were excluded from analysis. The DLS and GCLT of each normal subject and glaucoma patient were age–corrected to the average age of the glaucoma cohort.(Choi et al. PLOS One 2016, Phu et al. IOVS 2017 and Yoshioka et al. IOVS 2017) The GCc was calculated *in vivo* from the GCLT and histological data using a previously described method (Yoshioka et al. IOVS 2017). The DLS and GCc data points were spatially matched (Drasdo, VR 2007) and correlated on a log–log plot both for individual stimulus size data and all data combined.

Results: Linear regression analysis for individual stimulus size demonstrated structure–function correlation improving and approaching 1:1 as the stimulus size is reduced. While the glaucomatous cohort demonstrated correlation closer to 1:1 compared to the normal cohort (ANCOVA $p<0.0001$ for each stimulus), when all stimulus size data were combined, the resulting quadratic regressions were comparable (Figure 1A–B).

Conclusions: The structure–function relationship is governed by the stimulus size and approaches a 1:1 correlation when using stimulus sizes near the size of Ac. The improved structure–function correlation may be clinically advantageous for early disease detection. The combined structure–function correlation curve was comparable between normal subjects and patients with early glaucoma, and therefore, a common structure–function model may be translated to both populations. The difference in structure–function relationship for individual stimulus size data between the normal and glaucomatous cohort may be attributed to a shift along the "structure–function continuum" as a result of glaucomatous damage.

Conflict of Interest: Yes, I have. **Ethics Committee Approval:** Yes, I have obtained **Informed Consent:** Yes, I have obtained

Figure & Legend:

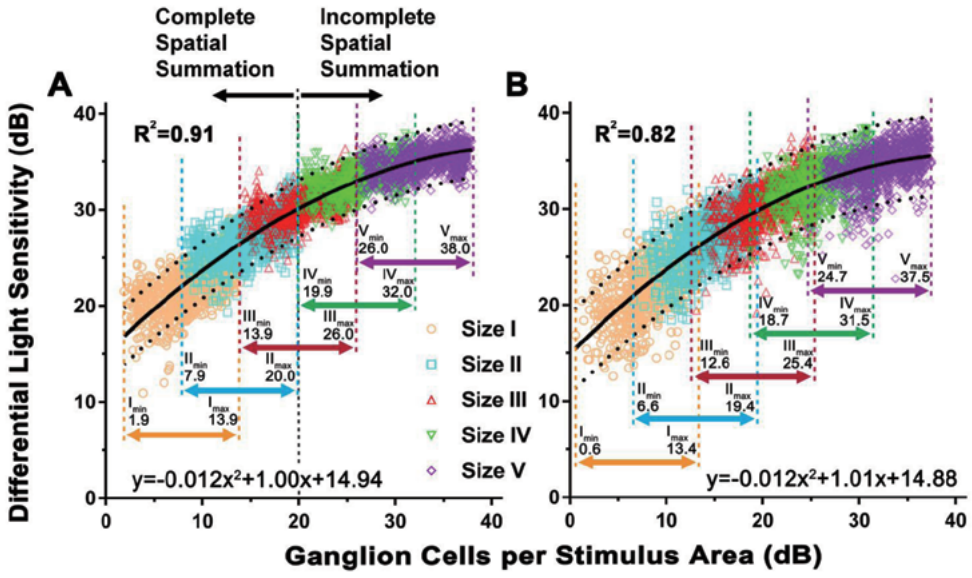

Figure 1: Structure-function relationship with combined stimulus size data for normal **(A)** and glaucomatous **(B)** cohort.

O2-1

Visual Field Abnormality Classification in the Ocular Hypertension Treatment Study 20 Year Follow-up (OHTS-3)

John L Keltner[1,2], Chris A Johnson[3], Kimberly E Plumb[1], Michael A Kass[4], Mae O Gordon[5]

[1]Department of Ophthalmology and Vision Science, University of California, Davis, United States, [2]Department of Neurology and Neurological Surgery, University of California, Davis, [3]Department of Ophthalmology and Visual Sciences, University of Iowa, [4]Department of Ophthalmology and Visual Science, Washington University School of Medicine, St. Louis, Missouri, [5]Department of Ophthalmology and Visual Science, Washington University School of Medicine, St. Louis, Missouri

Purpose:

To determine frequency and type of glaucomatous visual field (VF) loss and inter –reader agreement in the Ocular Hypertension Treatment Study 20 year follow –up (OHTS –3).

Materials and Methods:

OHTS –3 began in 2015 with 1,136 presumed survivors of 1,636 participants enrolled between 1994–96. In OHTS –1 and 2, VFs performed every 6 months were abnormal if the Glaucoma Hemifield Test was outside normal limits and/or the Corrected Pattern Standard Deviation was P < 5%. In OHTS –3, participants complete one VF and repeat VFs if unreliable or abnormal. We report the distribution of OHTS abnormality classifications for 300 abnormal VFs (600 hemifields) from 136 of 575 participants with at least one abnormal VF. Ninety of 136 participants (66%) had more than one abnormal VF, including 18 of 136 participants (13%) who converted to VF glaucoma in OHTS 1,2. Agreement among the 3 readers was reported as 0, 2 or 3 readers.[1]

Results:

VF were completed by 49.6% (594 of 1,136 participants) as of 1/8/18, and 70% (420/600) of the hemifield classifications indicated glaucomatous damage i.e., partial arcuate (26.2%) paracentral (22.2%), arcuate (12.7%) nasal step (4.7%), altitudinal (2.2%), temporal wedge (1.2%) and total loss (1.0%) defects. Approximately 16% (94/600) of the hemifields (arcuate 12.7%, altitudinal 2.2%, and total loss 1%) exhibited advanced loss, an increase as compared to the 7.6% reported in 2003.1 A total of 28.8% (173/600) of the hemifields exhibited non glaucomatous defects (normal 20.8%, widespread depression 7.7% and central 0.3%), and 1.2% (7/600) of the defects were attributed to testing artifacts (superior depression 0.5%, partial and peripheral rim 0.7%). 10 (2%) of the hemifields were required to be adjudicated in OHTS –3 with all 3 readers agreeing on 99.5% (597/600) of superior hemifields and on 98.8% (593/600) of inferior hemifields.

Conclusions:

OHTS –3 abnormal hemifields suggest glaucomatous damage among the selected participants with abnormal visual fields tested to date. Inter –reader agreement is excellent at 98%. However, as expected with an increase in participant age and advancing disease, there is a marked increase in advanced VF loss in OHTS –3 (16%) since our first report at the end of OHTS –2 in 2003 (7.6%).

Reference: 1. Keltner, Johnson Cello, et al, Arch Ophthalmol, 2003, 121: 643-650.

Conflict of Interest: No, I don't. **Ethics Committee Approval:** Not Applicable **Informed Consent:** Not Applicable

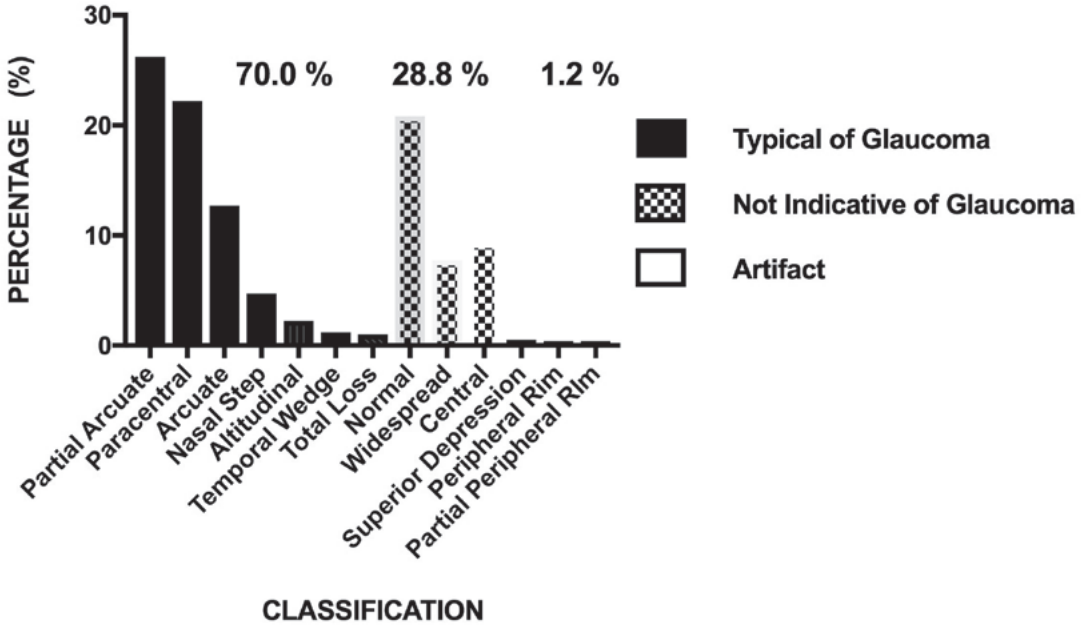

O2-2

Determination of the intra-subject variability of visual field examinations in glaucoma patients

Judith Ungewiss[1], Kilian Linden[1], Ulrich Schiefer[1,2,3]

[1]Competence Center Vision Reseach, Aalen University of Applied Sciences, Germany, [2]Dept. of Ophthalmology, University of Tuebingen, [3]Research Institute for Ophthalmology, University of Tuebingen

Purpose:

To determine the intra-subject variability of glaucomatous visual field defects (GVFD) by evaluating three repetitive baseline sessions within one month as a quality indicator of patients ability to participate in glaucoma progression studies.

Materials and Methods:

The fast thresholding strategy GATE (German adaptive threshold estimation) was used to assess visual fields in open angle glaucoma patients (with mild to moderate defects, Aulhorn stages I - III) with the OCTOPUS 101 perimeter (Haag-Streit AG, Koeniz, Switzerland). Scotoma were defined by local *p* values (probability pattern deviation plots) according to adapted criteria established by Katz et al. [1] and Martinez et al. [2]. Three baseline visits were planned for each patient of two glaucoma studies within the first month of the examination interval.

Intra-subject variability of scotoma position was determined by an agreement index, defined as the ratio between intersection and set union area. This was done for both, blind spot (BS) as a physiological reference scotoma and GVFD.Results were rated as pathological, if the agreement indices for both, BS and GVFD, fell below the lower quartile.

Results:

Sufficient data were obtained from 39 subjects (14 male, 25 female, age range 36 to 77 years, worse eye).Median of intra-subject agreement was 1.00 with IQR_{BS} = 0.45 (0.55 to 1.00) for BS and 0.37 with IQR_{GVFD} = 0.49 (0.13 to 0.62) for the GVFD with no significant correlation between the IQR_{BS} and IQR_{GVFD}. I.e. positional intra-subject agreement was better for BS than for GVFD.

The agreement index was pathological with regard to BS and GVFD in nine patients, each. In four subjects (10%), agreement index was pathological for both, BS and GVFD concordantly.

Conclusions:

Agreement indices for BS and for GVFD differ intra-individually. Therefore, only patients with consistently poor results can be excluded for glaucoma progression studies by now. Future prospective studies will have to show, which agreement index leads to a better prediction of actual variabilities in follow-up visual field examinations.

[1] Katz et al (1991) Arch Ophthalmol 109: 1684-1689
[2] Martinez and Sanchez (2008) Clin Ther. 30:1120-1134

Conflict of Interest: Yes, I have. **Ethics Committee Approval:** Yes, I have obtained **Informed Consent:** Yes, I have obtained

O2-3

Agreement between multifocal pupillographic objective perimetry, Matrix and HFA in stroke

Ted Maddess[1], Brendan Tonson-Older[1,3], Corinne F Carle[1], Josh P van Kleef[1], Emilie MF Rohan[1], Andrew C James[1], Jason Bell[4], Christian J Lueck[2,3]

[1]Neuroscience, John Curtin School of Medicial Research, Australian National University, Australia, [2]Dept Neurology, ACT Health, [3]ANU Medical School, [4]Dept Psychology, University of Western Australia

Purpose: To examine repeatability of two multifocal pupillographic objective perimetry (mfPOP) methods and to compare the results with Matrix and HFA perimetry.

Materials and Methods: We tested 27 patients with stroke affecting the occipital pole (11 females), age 69.0 +/- 11.8 years. The two dichoptic mfPOP methods presented yellow stimuli on a yellow background (YY), or green stimuli on a red background (RG). Evidence has been provided that both methods drive cortical inputs to the pupillary system (IOVS, 2013 54:467-475; Sci Reports, 2017 7:45847). The 88 mfPOP responses per eye were mapped onto a 24-2 format for comparison with Zeiss HFA and Matrix 24-2 tests completed on the same patients on the same days. Comparisons were made using principal curve analysis (PCurvA), Bland-Altman (BA) plots, and Intraclass Correlations (ICC). Analysis was by Matlab (2016b) and R.

Results: There was good agreement with visual field features like homonymous hemianopias across the perimetric tests. PCurvA showed that the relationship between mfPOP and Matrix sensitivities was more linear than either of those tests and HFA. HFA appeared to show sensitivity loss relatively late compared to Matrix, in agreement with previous PCurvA studies (Arch Opthalmol, 2010 128: 570-576; Optom Vis Sci, 2015 92:527-536). BA-plots comparing regional sensitivities for the repeated YY and RG tests showed lower inter-quartile ranges (IQRs) than BA plots comparing Matrix and HFA. This was especially true around 18 dB where mfPOP showed 8 dB lower IQRs for between-test repeatability. ICCs showed good agreement between all the perimetry tests ($r=0.90$, $p<0.0001$). For the mfPOP tests the best agreement was between repeats of the YY method ($r=0.97$, $p<0.0001$). Agreement between Matrix and HFA was similar ($r=0.96$, $p<0.0001$). While significant ($p<0.005$) agreement between mfPOP and Matrix or HFA was fair at 0.59 and 0.57. Examining individual fields showed that the lower correlation appeared to be due to the nonlinear relationship between mfPOP sensitivities and those of the other two. This was suggestive of the well-known nonlinear relationship between SAP decibel sensitivity and peripapillary RNFL thinning (e.g. IOVS, 2007 48: 3662-3668).

Conclusions: Our previous structure-function study suggested that mfPOP sensitivities are more linear with peripapillary thinning than HFA. The present study seems to support that conclusion. The observation of homonymous defects in patients with post-geniculate lesions tends to support a cortical drive to the irises for transient onset stimuli.

Conflict of Interest: Yes, I have. **Ethics Committee Approval:** Yes, I have obtained **Informed Consent:** Yes, I have obtained

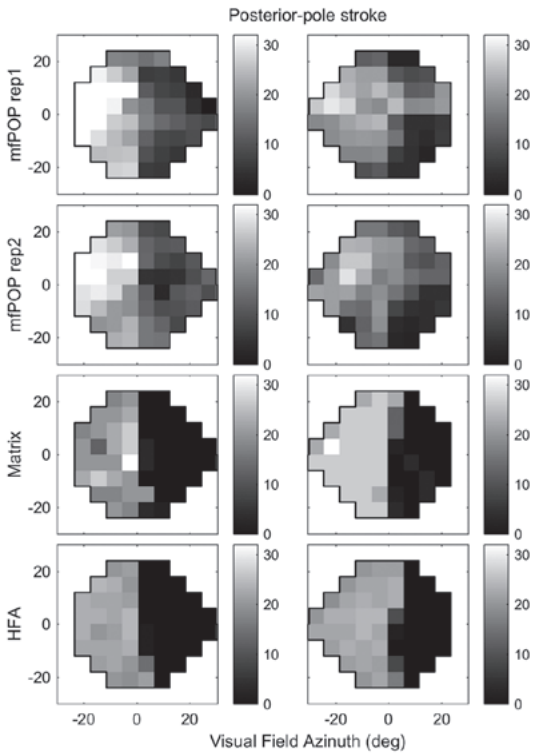

Sensitivities of a stroke patient as measured by two repeats of mfPOP, Matrix and HFA perimetry

O2-4

A comparison between the Compass fundus perimeter and the Humphrey Field Analyzer

Susan Ruth Bryan[1], Luca Mario Rossetti[2], Giovanni Montesano[1,2,3], Paolo Fogagnolo[2], Francesco Oddone[4], Allison M McKendrick[5], Andrew Turpin[6], Paolo Lanzetta[7], Chris A Johnson[8], David F Garway-Heath[3], David P Crabb[1]

[1]Optometry and Visual Sciences, City, University of London, London, United Kingdom, [2]Univeristy of Milan, ASST Santi Paolo e Carlo, Milan, Italy, [3]NIHR Biomedical Research Centre at Moorfields Eye Hospital NHS Foundation Trust and UCL Institute of Ophthalmology, London, UK, [4]G.B. Bietti Eye Foundation-IRCCS, Rome, Italy, [5]University of Melbourne , Department of Optometry and Vision Sciences, Melbourne, Australia, [6]University of Melbourne , Department of Computing and Information System, Melbourne, Australia, [7]Department of Medical and Biological Sciences, Ophthalmology Unit, University of Udine, Udine - Italy, [8]Department of Ophthalmology and Visual Sciences, University of Iowa Hospitals and Clinics, Iowa City, Iowa

Purpose: To compare clinical performance of the Compass (CMP, CenterVue, Italy) fundus perimeter with the Humphrey Field Analyzer (HFA, Zeiss, Dublin) in a multicentre cross-sectional study.

Materials and Methods: We recruited 498 patients with glaucoma and 436 age related normals . Patients had glaucomatous changes to the optic nerve head or nerve fibre layer as determined by a specialist from fundus photograph or OCT, independently of the visual field. Each participant (one eye) was examined with both HFA (SITA Standard strategy) and CMP (ZEST strategy) with a 24-2 grid. For both devices, linear regression was used to calculate the sensitivity decrease with age in the normal group to compute pointwise Total Deviation (TD) values and Mean Deviation (MD). We derived 5% and 1% pointwise age corrected normative limits. We used partial ROC curves and partial Area Under the Curve (pAUC) to compare the devices. MD and the total number of TD values below the 5% (TD5%) or the 1% (TD1%) limit per field were used as classifiers. Additionally, 44 glaucoma and 54 normal subjects were tested twice on both instruments. Pointwise Mean Absolute Deviation (MAD) and Bland Altman plots for the mean sensitivity (MS) were computed. Results are reported as mean difference ± standard error.

Results: Both devices showed similar discriminative power (Figure 1). Differences between pAUC were small (for MD -0.019, p = 0.03; for TD5% -0.012, p = 0.023; for TD1% (-0.003, p-value = 0.54). 95% limits of agreement of the MS were reduced by 14% in CMP compared to HFA in glaucoma subjects, and by 49% in normal subjects (Figure 2). MAD was smaller in CMP compared to HFA for glaucoma (0.03 ± 0.2 dB) and for normals (0.08 ± 0.16 dB), although not significantly. Average MS was lower with CMP than with HFA, both for glaucoma (-1.45 ± 0.01 dB) and normal subjects (-1.82 ± 0.11 dB).

Conclusions: Relative diagnostic precision of the two devices are equivalent. Test-retest variability of mean sensitivity for CMP was better than HFA. Fundus perimetry might be a promising multimodal tool for more accurate management of glaucoma patients.

Figure 1. pROC curves for MD, TD5% and TD1% for HFA (red) and CMP (blue). The shaded regions represent the 95% CIs.

Figure 2. Bland-Altman plots for HFA (in red) and CMP (in blue) with 95% limits of agreement (shaded region) and mean difference (solid line).

Conflict of Interest: Yes, I have. **Ethics Committee Approval:** Yes, I have obtained **Informed Consent:** Yes, I have obtained

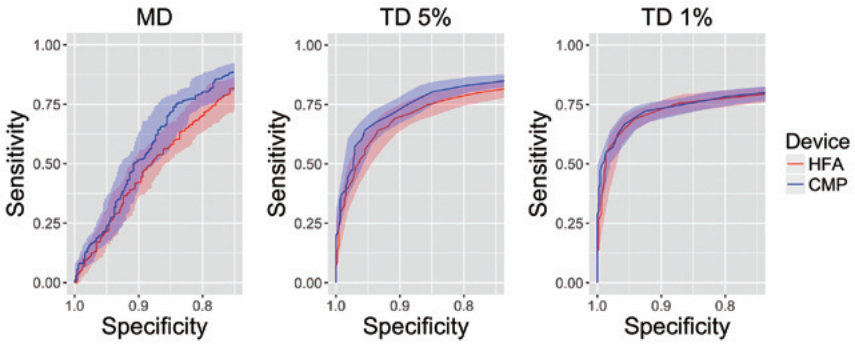

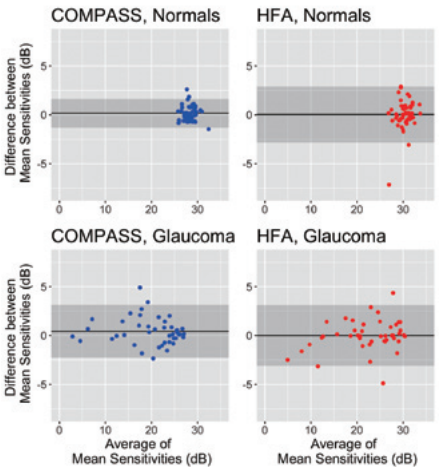

O2-5

Tablet derived Frequency-of-seeing curves for size-scaled spots in the central visual field

Algis J Vingrys[1], Selwyn M Prea[1], George YX Kong[2]

[1]Department of Optometry & Visions Sciences, The University of Melbourne, Australia, [2]The Royal Victorian Eye & Ear Hospital, East Melbourne

Purpose: It has been proposed that a fixed threshold can be returned across the visual field by having spot size scaled to stimulate a constant pool of retinal ganglion cells (Garway-Heath et al., 2000; Khuu & Kalloniatis, 2015). In this study we consider whether spot-size scaling will return constant Frequency-of-Seeing (FOS) slopes.

Materials and Methods: We measure FOS curves in a normal eye (RE VA=6/5) at foveal (1 degree) and peripheral (27 degrees) locations along the nasal meridian using spots scaled in size to yield similar thresholds (Sloan, 1961). FOS curves were established on a 5 $cd.m^{-2}$ background from 40 presentations at each of 9-10 luminance steps chosen to span threshold (total 360-400 presentations: 10-12 mins). The steps were created by implementing discrete digital driving levels (DDLs: +0 to +10, step ~0.5 dB or entire range at ~3 dB steps) above the background DDL on a gamma corrected iPad3 tablet. Response reliability was established by measuring false positive and false negative rates. Each DDL was converted into equipment specific decibels given the maximum light output of our tablet (360 $cd.m^{-2}$). FOS curves were parametrised by the mean and standard deviation of a cumulative normal distribution. The FOS for an eye with a macula scotoma (LE VA=6/36) was also determined at the same locations.

Results: Our observer gave reliable outcomes in both eyes with an average false positive rate 0.02 and a false negative rate of 0.03. We find that spot-size scaling for our background luminance returns similar thresholds at 1 and 27 degrees in a normal eye. The RE gave a T_{50} of 30.6 dB at 1 degree and 30.1 dB at 27 degrees. Despite the 0.5 dB difference in threshold (12% luminance increment), the standard deviation of the cumulative normal (FOS slope) was 44% flatter at the 27 degree location (slope 0.36) than at the central 1 degree location (slope 0.25). As expected, the LE with the macula scotoma, returned a normal FOS at 27 degrees (T_{50} 29.8 dB, slope 0.37) and a low threshold (T_{50} 14.8 dB) and very flat slope (5.71) at the 1 degree location.

Conclusions: Spots can be size-scaled to return constant thresholds across the visual field. Despite the threshold similarity after size-scaling, peripheral locations exhibit higher variability, which may arise from the increased noise of their larger receptive fields.

Conflict of Interest: Yes, I have. **Ethics Committee Approval:** Yes, I have obtained **Informed Consent:** Yes, I have obtained

O2-6

Divergence Measures between Normal Subjects and Glaucoma Patients with Mild Visual Loss using Threshold Automated Perimetry of the Full Visual Field

Gideon KD Zamba[1], Michael Wall[2]

[1]*Biostatistics, The University of Iowa, United States,* [2]*University of Iowa*

Purpose: To contrast test locations of visual field measurements of the full visual field between normal and glaucoma patients with mild visual loss (mean deviation > -4dB). The clinical significance of this work is to identify areas of dissimilarity so they can receive appropriate attention when testing for glaucoma detection or glaucoma progression.

Methods: We performed a cross-sectional clinical study to characterize the measures of divergence in the full visual field between glaucoma and control subjects. Twenty-eight glaucoma patients with mild visual loss and 61 healthy observers were used. Full visual field static threshold perimetry tests developed using an Octopus 900 perimeter, running the Open Perimetry Interface (OPI), were employed with stimulus size V on Bayesian testing strategy with dynamic timing[3]. At each location across the visual field, 3 statistical measures were used to explore the divergence characteristics between healthy control subjects and the mild glaucoma population. These statistical measures are **Total Variation** distance, **Kullback-Leibler** divergence and **Hellinger** distance[1,2]. The relative entropy of location-specific normal population measurements with respect to the glaucoma population was assessed on a heat-map to discriminate between similarly behaved fields and visual fields with strong contrasts.

Results: We found a systematic linear decrease in visual sensitivity with eccentricity. The effect was more pronounced in the glaucoma patients, $p < 0.001$. Since all three measures of discrepancy are somehow related and gave similar results, we only report the Hellinger findings. The Hellinger method of divergence (as well as others) has identified test locations in the mid-periphery of the visual field to be the areas of most discrepancy between mild glaucoma subjects and healthy observers (See Figure).

Conclusion: When testing the full visual field with static threshold automated perimetry using the OPI with a size V stimulus, test locations in the mid periphery appear to best discriminate healthy observers from glaucoma patients with mild visual loss.

References:

[1] Kullback, S., Liebler, R. A. (1951). On information and Sufficiency. Annals of Mathematical Statistics, 22(1), 79 − 86

[2] Hellinger, E. (1909) "Neue Begründung der Theorie quadratischer Formen von unendlich-vielen Veränderlichen", Journal für die reine und angewandte Mathematik 136: 210–271

[3] Turpin, A., McKendrick. A. M., Johnson, C. A., Vingrys, A. J. (2003). Properties of Perimetric Threshold Estimates from Full Threshold, ZEST, and SITA-like Strategies, as Determined by Computer Simulation. IOVS, 44(11), 4787 − 4795

Conflict of Interest: No. I haven't. **Ethics Committee Approval:** Not Applicable **Informed Consent:** Not Applicable

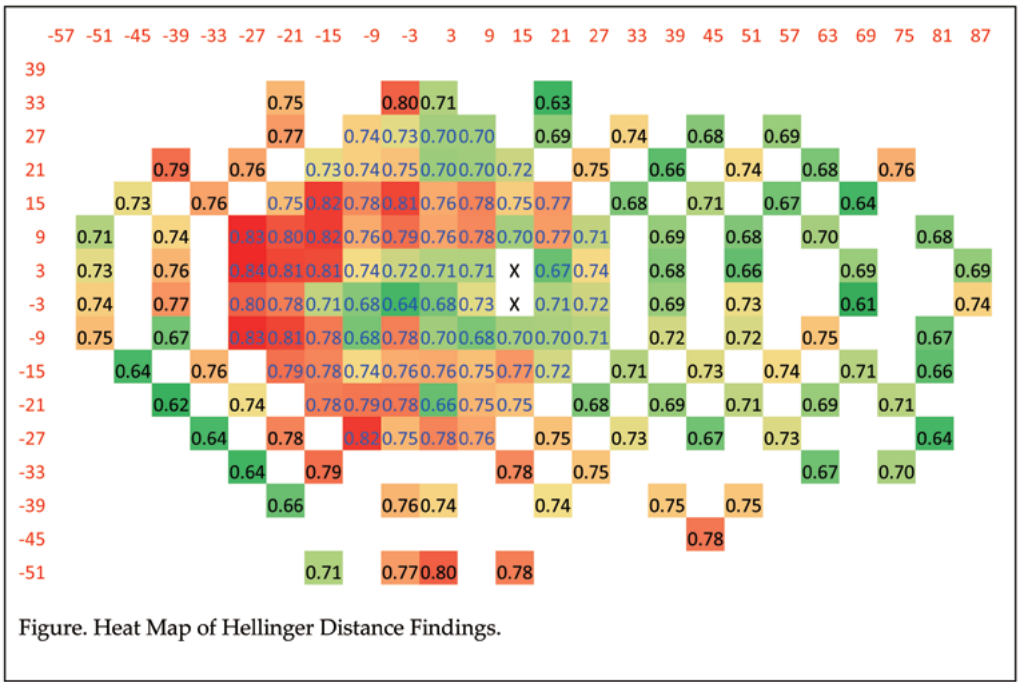

Figure. Heat Map of Hellinger Distance Findings.

O3-1

Relationship between local binocular visual field sensitivity and location of undetected driving hazards. Gaze-movement corrected analysis in simulated driving.

Makoto Araie[1,2], Aiko Iwase[3], Yuto Susuki[4], Shiho Kunimatsu-Sanuki[5], Hiroshi Ono[6], Yuko Ohno[4]

[1]Department of Ophthalmology, Kanto Central Hospital of the Mutual Aid Association of Public School Teachers, Japan, [2]The University of Tokyo, [3]Tajimi Iwase Eye Clinic, [4]Osaka University Graduate School of Medicine, [5]Tohoku University School of Medicine, [6]Honda Motor Co., Ltd.

Background: An increased risk of motor vehicle collisions (MVCs) in glaucoma suggested relationship of binocular visual field damage (VFD) to impaired hazard detection. Glen et al (Clin Exp Optom, 2016) simulated binocular VFD in healthy subjects and reported that simulated binocular VFD impaired hazard detection. Glaucoma subjects generally don ´ t perceive VFD, while healthy subjects perceive simulated VFD, and evidence is limited regarding whether glaucoma subjects were more likely involved in MVCs, because hazards happened to be located in an area of binocular VFD when MVC–avoidance reaction was needed.

Methods: 53 normal (mean age= 56.5 yrs.) and 55 glaucoma subjects (mean age=65.1 yrs, mean better eye MD=–8.7 dB) were involved. Binocular VF was integrated from monocular Humphrey Field Analyzer SITA–S 24–2 program test results in both eyes. A driving simulator, Honda Safety Navi (Honda Motor, Tokyo), was used, while gaze movement during simulated driving was monitored using an EMR–9 Eye Mark Recorder (nac Technology Inc., Tokyo).

Results: In 2 scenarios, A) Truck approaching from the left and B) Oncoming right–turning car, which were used for further analyses, the occurrence of MVCs was more frequent in the glaucoma than in normal subjects ($P<0.001$, $P=0.038$). The time when a subject noticed the hazard (notice time, NT) was determined by subtracting 0.2 sec from the time point when saccade toward the hazard was recorded. For the scenario A, the NT was delayed in the MVC–positive (MVCP) – than in MVC–negative (MVCN) – glaucoma subjects (0.87 ± 0.48 vs. 0.03 ± 0.97 sec, $P=0.008$) and in MVCP– than in MVCN–normal subjects (2.12 ± 0.17 vs. 0.06 ± 1.25 sec, $P=0.004$). Discriminant analysis yielded 0.57 sec as the time best discriminating the MVCP– from MVCN–subjects. Local binocular VF sensitivity corresponding to gaze–movement corrected location of the hazard at 0.57 sec was lower in the 24 MVCP– than in the 31 MVCN–glaucoma subjects (19.9 ± 2.0 dB vs. 23.7 ± 1.8 dB, $P=0.043$). A similar analysis for the scenario B yielded the corresponding VF sensitivities of 21.5 ± 2.4 dB and 24.2 ± 1.5 dB in the 16 MVCP– and 39 MVCN–glaucoma subjects, respectively ($P=0.034$).

Conclusion: Lower binocular VF sensitivity in a VF area corresponding to the gaze–movement corrected location of the hazard was thought to relate to delayed hazard recognition in glaucoma subjects.

Conflict of Interest: Yes, I have. **Ethics Committee Approval:** Yes, I have obtained **Informed Consent:** Yes, I have obtained

O3-2

Effect of simulated superior and inferior visual field loss on vehicle control performance in a driving simulator

Makoto Inagami[1], Hirofumi Aoki[1], Aiko Iwase[2], Yasuki Ito[1], Hiroko Terasaki[1], Motoyuki Akamatsu[3]

[1]Institutes of Innovation for Future Society, Nagoya University, Japan, [2]Tajimi Iwase Eye Clinic, [3]National Institute of Advanced Industrial Science and Technology

Purpose:
Drivers with glaucoma have been shown to have an increased risk of accidents, but evidence is limited on how driving performance is affected by different types of visual field loss (VFL). To investigate such effects systematically, we developed a novel system to simulate VFL in a driving simulator. This study used the system to examine the effects of superior and inferior VFL on vehicle control performance in a simple driving situation.

Materials and Methods:
We used a driving simulator where a vehicle body was surrounded by five screens: front, back, left, right, and floor. The cockpit was equipped with a gaze tracking system to measure the driver's eye and head movements. VFL was simulated by displaying an object to mask the virtual environment, and the object was moved according to the driver's gaze direction. For this experiment, we created a two-lane course that included curves different in curvature. The participants were 15 drivers aged 27-63 years, who had normal vision. They drove along the course under the following three VFL conditions: none, superior, and inferior. In the VFL conditions, we simulated the loss of each hemifield that did not include the central field within 5° . The velocity was automatically controlled at a constant rate, and the participants were instructed to keep the central position in the left lane. The instability of the lane position was assessed by calculating the standard deviation of the offset from the lane center. In addition, we quantified the roughness of steering control by using an index called steering entropy.

Results:
Analysis of variance showed significant main effects of the experimental conditions both for the instability of lane position ($p<0.001$) and the roughness of steering control ($p=0.02$). A multiple comparison showed that the instability of lane position was significantly higher in the inferior than superior VFL condition ($p<0.001$). For the roughness of steering control, a significant increase was observed in the inferior VFL condition compared to the no VFL condition ($p=0.03$).

Conclusions:
The results suggest that in this experimental setting, inferior VFL impaired vehicle control performance, whereas superior VFL enhanced the performance. The latter is likely due to attentional focusing on the information from the road surface, which may create other risks such as overlooking a traffic light.

Conflict of Interest: Yes, I have. **Ethics Committee Approval:** Yes, I have obtained **Informed Consent:** Yes, I have obtained

O4-1

Development of a deep learning algorithm to diagnose glaucoma from fundus photography

Naoto Shibata[1], Masaki Tanito[2], Keita Mitsuhashi[3], Yuri Fujino[4], Masato Matsuura[5], Hiroshi Murata[6], Ryo Asaoka[7]

[1]Queue.inc, Japan, [2]Division of Ophthalmology, Matsue Red Cross Hospital / Department of Ophthalmology, Shimane University Faculty of Medicine, Shimane, Japan, [3]Queue.inc, [4]Department of Ophthalmology, The University of Tokyo, [5]Department of Ophthalmology, The University of Tokyo / Department of Ophthalmology, Graduate School of Medical Science, Kitasato University, [6]Department of Ophthalmology, The University of Tokyo, [7]Department of Ophthalmology, The University of Tokyo

No method currently exists to automatically diagnose or screen for glaucoma from fundus photographs. We developed a deep learning algorithm to diagnose glaucoma from fundus photography. A training dataset consisted of 1,364 color fundus photographs with glaucomatous indications and 1,768 color fundus photographs without glaucomatous features. A testing dataset consisted of 60 eyes of 60 glaucoma patients and 50 eyes of 50 normal subjects. Using the training dataset, a deep learning algorithm known as Deep Residual Learning for Image Recognition (ResNet) was developed to diagnose glaucoma, and its diagnostic accuracy was validated in the testing dataset, using the area under the receiver operating characteristic curve (AROC). Fundus photographs were also classified by three Residents in Ophthalmology, and the AROC was calculated. The deep learning algorithm achieved significantly higher diagnostic performance compared to Residents in Ophthalmology; with ResNet, the AROC from all testing data was 96.5 (95% confidence interval [CI]: 93.5 to 99.6) % while the AROCs obtained by the three Residents were between 72.6% and 91.2%. The potential impact of the deep learning algorithm for the early detection of glaucoma and prevention of blindness cannot be overstated; fundus photography is commonly used at non-ophthalmological facilities, such as opticians, screening centers and internal medicine clinics.

Conflict of Interest: Yes, I have. **Ethics Committee Approval:** Yes, I have obtained **Informed Consent:** Yes, I have obtained

O4-2

Deep Learning Approaches to Predict Standard Automated Perimetry Summary Metrics from SD-OCT Imaging

Mark Christopher[1], Akram Belghith[1], Kyle Hasenstab[1], Christopher Bowd[1], Michael H Goldbaum[1], Christopher A Girkin[2], Jeffrey M Liebmann[3], Robert N Weinreb[1], Linda M Zangwill[1]

[1]Hamilton Glaucoma Center, Shiley Eye Institute, Dept. of Ophthalmology, University of California, San Diego, United States, [2]School of Medicine, University of Alabama-Birmingham, [3]Bernard and Shirlee Brown Glaucoma Research Laboratory, Edward S. Harkness Eye Institute, Dept. of Ophthalmology, Columbia University Medical Center

Purpose: To develop deep learning models that predict standard automated perimetry (SAP) mean deviation (MD), pattern standard deviation (PSD), and detect glaucomatous visual field damage from spectral domain optical coherence tomography (SD-OCT) imaging.

Methods: A cohort of 414 subjects (625 eyes) with glaucomatous visual field damage (GVF, mean MD=-4.6 dB) and 408 subjects (576 eyes) without visual field damage (non-GVF, mean MD=-0.7 dB) was followed longitudinally with visual field testing (24-2 SAP) and SD-OCT imaging (Spectralis optic nerve head cube and circle scans). From a total of 6089 SD-OCT cube scans, retinal nerve fiber layer thickness (RNFLt) maps were computed using our custom San Diego Automated Layer Segmentation Algorithm (SALSA). Scanning laser ophthalmoscopy (SLO) images were also extracted from each scan. Data was randomly partitioned by participant into independent training (90%) and testing (10%) sets. Deep learning models based on AlexNet architecture were trained on RNFLt maps and SLO images to predict MD and PSD from SAP testing within 90 days of imaging. A deep learning model was also trained on RNFLt maps and SLO images to identify eyes with repeatable glaucomatous visual field damage at the time of imaging. Transfer learning was used to initialize the models by training on ImageNet, a general image dataset. Models were refined by further training on the SD-OCT training set and evaluated on the test set. For comparison, predictions based on mean RNFL thickness from SD-OCT circle scans were also evaluated.

Results: The deep learning model explained roughly half of variance observed in MD (R^2=0.54, p<0.001) and nearly two-thirds in PSD (R^2=0.65, p<0.001), a greater proportion than mean circle scan RNFL thickness for MD (R^2=0.36, p<0.001) and PSD (R^2=0.34, p<0.001). In distinguishing GVF from non-GVF eyes, the deep learning model achieved an area under receiver operating characteristic (AUC) of 0.92 which outperformed the circle scan mean RNFL measurements (AUC=0.73, p<0.001).

Conclusions: Deep learning models can improve our ability to predict SAP summary measures and to identify functional loss in glaucoma based solely on SD-OCT imaging. The results suggest that applying deep learning models may provide guidance in interpreting images to identify patients with functional loss.

Conflict of Interest: Yes, I have. **Ethics Committee Approval:** Yes, I have obtained **Informed Consent:** Yes, I have obtained

O5-1

Influence of Bruch ´ s membrane opening area on OCT diagnostic accuracy

Lucas A Torres[1], Camila E Zangalli[3], Glen P Sharpe[1], Donna M Hutchison[1], Eduardo F Oda[2], Alexandre S Reis[3], Vital P Costa[3], Marcelo T Nicolela[1], Balwantray C Chauhan[1], Jayme R Vianna[1]

[1]Department of Ophthalmology, Dalhousie University, Canada, [2]University of São Paulo, [3]University of Campinas

Purpose: OCT measurements of minimum rim width (MRW) and retinal nerve fibre layer thickness (RNFLT) depend on Bruch ´ s membrane opening (BMO) area. Therefore, classifications ("within normal limits [WNL]", "borderline [BL], " and "outside normal limits [ONL]") are adjusted to account for BMO area. To determine the efficacy of this adjustment, we explored the diagnostic accuracy of MRW and RNFLT as a function of BMO area.

Materials and Methods:
One eye of 182 open-angle glaucoma patients and 146 healthy control subjects were imaged with OCT (Spectralis, Heidelberg Engineering) to obtain global MRW and RNFLT measurements. Patients and controls were divided into tertile groups of BMO area (small, medium and large) and the proportion of subjects classified as ONL, BL and WNL were analyzed with sensitivity and specificity analysis. BMO area correlations with MRW and RNFLT measurements were also determined.

Results: The median (interquartile range) age of the patients and controls was 71.2 (64.8 to 77.7) and 61.8 (47.0 to 68.0) years, while BMO areas were 1.8 (1.5 to 2.1) and 1.7 (1.5 to 2.0) mm2, respectively. Visual field mean deviations for patients were -4.7 (-9.2 to -1.9), -3.6 (-7.3 to -1.7) and -3.7 (-8.6 to -1.5) dB for small, medium and large BMO areas, respectively (p=0.12). MRW ONL sensitivity did not change with increasing BMO area (59.0% to 52.5%, p=0.76, Fig. 1), but RNFLT ONL sensitivity increased significantly (59.0% to 80.3%, p=0.04, Fig. 1). RNFLT ONL sensitivity was higher than MRW for the medium (p=0.04) and large BMO area groups (p<0.01). MRW and RNFLT WNL specificities were not significantly different for either BMO area subgroups (p>0.12) and did not vary with BMO area (p>0.28). The effect of BMO area on MRW measurements was 1.8 times higher in controls (-59.7 μm/mm2) than in patients (-31.8 μm/mm2), while this effect on RNFLT measurements was 11.4 times higher in controls (9.7 μm/mm2) than in patients (0.8 μm/mm2, Fig. 2).

Conclusion: Unlike MRW, RNFLT ONL classification had a higher sensitivity to detect glaucoma in larger BMO areas. This higher sensitivity could be explained by the smaller effect of BMO area on the RNFLT in glaucoma patients, compared to controls (Fig. 2).

Conflict of Interest: Yes, I have. **Ethics Committee Approval:** Not Applicable **Informed Consent:** Not Applicable

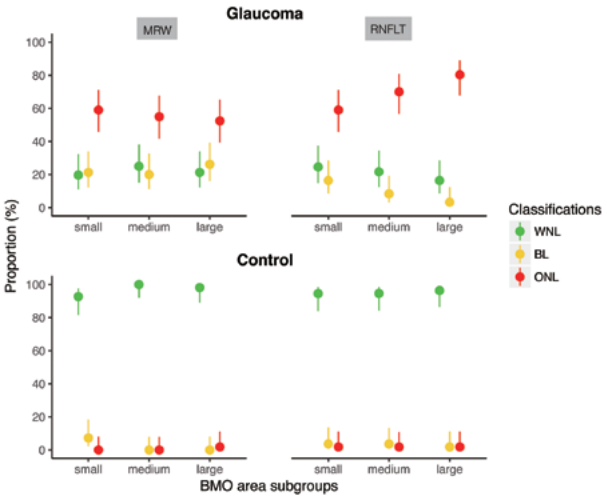

Figure 1. Proportion of subjects flagged with each classification (WNL = "within normal limits", BL = "borderline", ONL = "outside normal limits) among the BMO area tertile groups. Vertical line ranges represent 95% confidence interval.

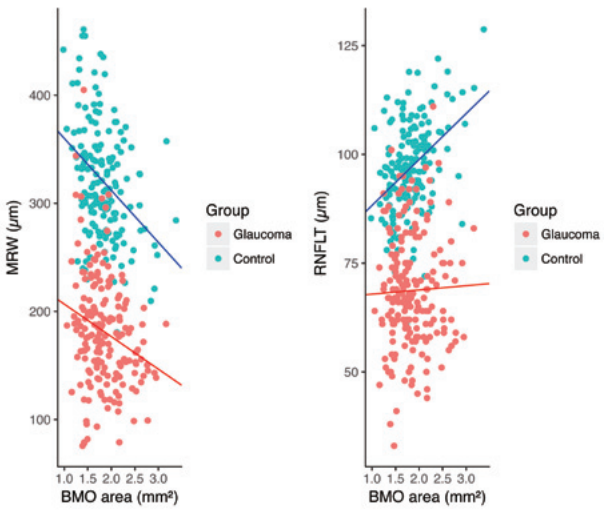

Figure 2. Scatterplots of BMO area with MRW and RNFLT measurements. Lines represent linear regression models.

O5-2

Development of a large normative database to investigate physiological and pathological changes in the central retinal ganglion cell layer

Barbara Zangerl[1,2], Nayuta Yoshioka[1,2], Michael Kalloniatis[1,2]

[1]Centre for Eye Health, University of New South Wales Sydney, Australia, [2]School for Opometry and Vision Science, University of New South Wales Sydney

Purpose:
The retinal ganglion cell layer (GCL) is commonly assumed to reduce in thickness with age and disease, most prominently glaucoma. This study utilised the integration of a previously established pattern recognition method with regression models to robustly describe physiological age-related changes of the GCL and develop models for discrimination of age-related changes from disease processes.

Materials and Methods:
Spectralis optical coherence tomography of the central macular 30x25° field was obtained from 254 patients with intraocular pressures below 22 mmHg and no evidence of optic neuropathy or posterior pole disease. Grid-wise GCL thickness was extracted for the 8x8 posterior pole grid resulting in 64 approximately 860x860 µm area measurements, with adjustments for the foveal pit. Dependence of measurements on patient characteristics were examined applying χ *-square* statistics or Pearson's correlation for nominal and interval data respectively. Regression models were applied to obtain best fit predicting age related loss of GCL thickness.

Results:
Data were collected from one eye each, including 132 (52.0%) right eyes, of 109 (42.9%) male and 145 (57.1%) female aged 20.2 to 84.9 years (50.3 ± 14.4) of Caucasian (n=157; 61.8%), Asian (n=93; 36.6%) and other (n=2; 0.8%) ethnic background. Spherical equivalent ranged from -6 to +3 D (-0.47 ± 1.74). GCL thickness measurements were not impacted by gender, ethnicity, eye laterality or spherical equivalent.
Non-linear models described change over time with substantial fit indicated by R^2 values ranging between 0.86 and 0.97 compared to moderate fit with linear models (R^2 between 0.58 and 0.80). Using a second order polynomial curve, the vertex points predicted onset of GCL thinning at 35 to 42 years of age. Within the examined macular area, central locations were preserved until an older age, but subsequently lost at higher absolute rates (Figure 1, green) than those in more peripheral locations (Figure 1, purple).

Conclusions:
A combination of pattern recognition and regression analysis allows the development of robust models describing changes in central GCL with age. Similar to previously established models and concordant with visual function loss, identified changes in the GCL are age and location dependent. Optimised models are now being employed to develop a large age-corrected normative database and investigate its utility in the earlier prediction of disease related GCL changes.

Figure 1: Change in central ganglion thickness over time based on location

Conflict of Interest: No, I don't. **Ethics Committee Approval:** Yes, I have obtained **Informed Consent:** Yes, I have obtained

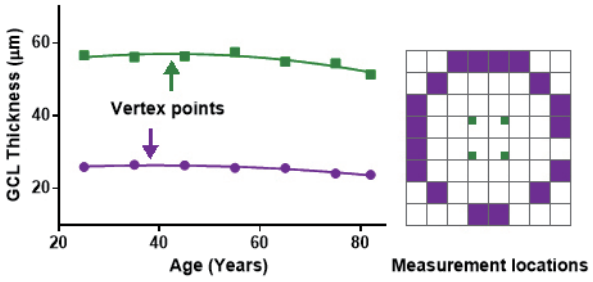

O5-3

Relationship between peripapillary retinal arteries angle and Ocular Response Analyzer waveform parameters

Shotaro Asano[1,2], Takehiro Yamashita[2], Shuichiro Aoki[1], Masato Matsuura[1], Hiroshi Murata[1], Ryo Asaoka[1]

[1]Department of Ophthalmology, University of Tokyo, Japan, [2]Kagoshima University Graduate School of Medical and Dental Sciences

Purpose: We have recently reported that the magnitude of retinal stretch due to the elongation of an eyeball is reflected by the peripapillary retinal arteries angle (PRAA): Yamashita T et al. IOVS 2013. The purpose of the current study was to evaluate the relationship between PRAA and Ocular Response Analyzer (ORA) parameters, including the waveform parameters, in healthy subjects.

Methods: Fourty-nine eyes of 51 healthy subjects (51.6 ± 21: mean ± standard deviation, years old) were enrolled in the current study. ORA measurements were carried out three times and average values of these parameters were calculated. Fundus photographs were obtained using either of OCT-2000® and TRC-50DX® (Topcon, Japan) and the PRAA was calculated as the positions of major retinal arteries in the superotemporal and inferotemporal areas decided by identifying the points where the retinal artery and the 3.4-mm-diameter peripapillary scan circle (adjusted for axial length using the Bennett ´ s formula) overlapped, using the ImageJ program. Then, first, the relationship between PRAA and 43 variables of age, corneal curvature, axial length, central corneal thickness, ORA corneal hysteresis (CH), ORA corneal resistant factor, and 37 ORA waveform parameters was analyzed using the linear mixed model. Then the optimal model for PRAA was identified using the generalized least absolute shrinkage and selection operator (LASSO) regression to decide ten candidate variables, followed by the model selection with the corrected Akaike information criterion (AICc) using the ten variables.

Result: PRAA was 135 ± 14 degrees. PRAA was significantly related to axial length, but not to age ($p = 0.044$, $p = 0.43$, respectively, linear mixed model). The model explaining PRAA only with CH or axial length had the AICc value of 420.1 or 419.5. The optimal model for PRAA was PRAA = 126.2+0.021 × p2area-0.042 × p2area1 (AICc = 412.3), where P2area and P2area1 represents the area of applanation peak 2 from 25% base to peak and that from 50% base to peak, respectively.

Conclusion: ORA waveform parameters were associated with peripapillary retinal arteries angle.

Conflict of Interest: No, I don't. **Ethics Committee Approval:** Yes, I have obtained **Informed Consent:** Yes, I have obtained

O5-4

Quantification of peripapillary nerve fibre elevation and its association with axial length in young healthy eyes

Masatoshi Tomita, Takehiro Yamashita, Minoru Tanaka, Yuya Kii, Kumiko Nakao, Taiji Sakamoto

Department of Ophthalmology, Kagoshima University, Japan

Purpose: The eyes with peripapillary nerve fiber elevation (NFE) have discrepancy between optic disc margin in color fundus photograph and Bruch membrane opening in optical coherence tomography (OCT) cross-sectional image. The purpose of this study was to quantify the height of the NFE in young healthy eyes and to investigate the relationship between the NFE height and axial length.

Materials and Methods: A prospective observational cross-sectional study comprised 117 right eyes. All participants (mean age 25.8 years) underwent comprehensive ophthalmologic examination, including axial length, fundus photograph, peripapillary and optic disc imaging. The NFE height was defined as the distance between retinal surface plane and the top of the NFE in optic disc OCT cross-sectional image. Optic disc tilt was assessed using sine curve approach of the RNFL B-scan image. Conus area in color fundus photograph was measured by ImageJ and the magnification effect was corrected by the Bennett formula. The relationship between the NFE height and the axial length, optic disc tilt, conus area were determined by Spearman's correlation analysis.

Results: Sixty five eyes had the NFE, and mean NFE height was 84.7 micrometer. The NFE height was significantly positively associated with the axial length ($r=0.32$, $p<0.001$), optic disc tilt ($r=0.25$, $p=0.008$) and conus area ($r=0.27$, $p=0.004$).

Conclusion: The NFE was not rare in young healthy eyes. The eyes with NFE have longer axial length, larger optic disc tilt and conus area.

Conflict of Interest: Yes, I have. **Ethics Committee Approval:** Yes, I have obtained **Informed Consent:** Yes, I have obtained

O5-5

Relationship between peripapillary choroidal thickness and tessellation in young healthy eyes

Yusuke Matsushita, Takehiro Yamashita, Yukimi Kumahara, Naoya Yoshihara, Minoru Tanaka, Yuya Kii, Kumiko Nakao, Taiji Sakamoto

Department of Ophthalmology, Kagoshima University, Japan

Purpose: Degree of the tessellation was correlated with choroidal thickness in macular area (Yamashita et al. PlosONE 2014;9:e103586). However, there are few reports about peripapillary tessellation. Therefore, the purpose of this study was to see the relationship between peripapillary choroidal thickness (PPCT) and degree of the tessellation in young healthy eyes.

Materials and Methods: A prospective observational cross-sectional study was performed in 119 right eyes of young healthy volunteers. PPCT was manually measured at eight locations (nasal, supra-nasal superior, supra-temporal, temporal, infra-temporal, inferior, infero-nasal) around the optic disc using the B-scan image of the Topcon 3D OCT-1000 MARK II RNFL 3.4 mm circle scan. Using the color fundus photograph, degree of the tessellation were classified into three categories; non-tessellated (NT), weakly tessellated (WT), and strongly tessellated (ST) in same eight locations by three experienced retina specialists. The inter-rater agreement of the subjective classifications was assessed with the Fleiss kappa method. The Steel-Dwass multiple comparison test was used to analyze the significant differences of PPCT among the three groups.

Results: Mean age was 25.8 years and mean axial length was 25.5 mm. The interrater agreement of the subjective classifications was high with Fleiss kappa =0.71. The PPCT became significantly thinner as the degree of tessellation became stronger ($p<0.05$) at all eight locations.

Conclusion: Strong tessellation is associated with thinner PPCT in young healthy eyes.

Conflict of Interest: Yes, I have. **Ethics Committee Approval:** Yes, I have obtained **Informed Consent:** Yes, I have obtained

O5-6

Classification of macular shape of children on optical coherence tomography

Takehiro Yamashita, Yoshiki Namiki, Naoya Yoshihara, Naoko Kakiuchi, Taiji Sakamoto

Department of Ophthalmology, Kagoshima University, Japan

Purpose: Irregular configuration of posterior eye, such as staphyloma, dome-shaped macular, affects visual field sensitivity. Vertical cross-sectional image of the macular in optical coherence tomography (OCT) can detect mild posterior staphyloma, which is undetectable by fundus examination. However, there is no report about the chronological change of posterior eye along with growth. Therefore, the purpose of this study was to investigate the irregularity of posterior eye in elementary school student.

Methods: A prospective cross-sectional observational study of 122 right eyes in healthy elementary school students (age 8 or 9 years) was performed. Axial length was measured with OA-2000 (TOMEY, Japan). Vertical cross-sectional image of macular was obtained with OCT machine 3D OCT-1 Maestro (Topcon, Japan). First, they were classified based upon its vertical symmetry, and then sub-classified them into convex, flat, concave and dome type according to retinal pigment epithelium curvature. The axial length difference between symmetry and asymmetry group was analyzed using Mann-Whitney U test.

Results: Mean axial length was 23.41 mm. One hundred and two eyes were categorized to symmetric group, of which 78 eyes were place in convex, 2 eyes in flat, 0 eyes in concave, and 22 eyes in dome type. Twenty eyes were categorized to asymmetric group, of which 7 eyes in convex, 4 eyes in flat, 2 eyes in concave, and 7 eyes in dome type in upper part, 5 eyes in convex, 2 eyes in flat, 8 eyes in concave, and 5 eyes in dome type in lower part. There was no significant difference in axial length between symmetry and asymmetry groups. (p=0.52).

Conclusions: There was already irregularity of the posterior pole of the eyes in elementary school students.

Conflict of Interest: Yes, I have. **Ethics Committee Approval:** Yes, I have obtained **Informed Consent:** Yes, I have obtained

O6-7

Deploying virtual reality headgear and the foveation reflex to enhance the ergonomics of perimetry

Bertil Damato[1], Benjamin T. Backus[2], James B. Blaha [2], Michael Deiner[1], Manish Gupta[2], Mitchell S. Dul[3]

[1]Ophthalmology, University of California at San Francisco, USA, [2]Vivid Vision Inc, San Francisco, CA, USA, [3]SUNY College of Optometry, New York, NY, USA

Purpose: We developed a form of perimetry, deploying virtual-reality headgear using an interactive target to avoid fixation loss, exploit the orienting reflex to signal stimulus awareness, and reduce the size and expense of the testing device. The resulting test was evaluated and compared with commercially available static automated perimetry in patients with glaucoma and controls.

Materials and Methods: Subjects were tested while seated in a comfortable chair, wearing a head-mounted display. After a brief training program, the subjects saw the interactive fixation target, consisting of an orange spot (i.e., 'gaze point'), moved by tilting the head so that it was superimposed on a tiny black spot. A test stimulus was then presented for 200 msec in the visual field area of interest, whereupon the patient tilted their head to move the gaze point into that area. A new fixation target appeared and the test resumed. Sixty-nine points in the central 24° field were examined. Missed points were tested a second time. Results were compared with the Humphrey Visual Field Analyzer (HVFA) SITA 24-2. In controls, results were evaluated according to blind-spot detection. Ergonomics of the head-mounted system and the HVFA were documented with a questionnaire.

Results: The head mounted system demonstrated the presence of decreased sensitivity in all cases of glaucoma and correctly identified the physiologic blind spot in all subjects. To address false negatives that occurred as a consequence of lapses of attention and blinking, we modified our test strategy to re-examine missed points, with only consistently missed points considered abnormal. Studies are in progress to determine which of the two perimeters provides the most repeatable results. Patients and controls found the head mounted system to be more user-friendly, but some reported that the head-mounted display was heavy.

Conclusions: Head mounted perimetry can be user-friendly and its results appear to correlate with the HVFA. We are incorporating artificial intelligence to enhance sensitivity while shortening the test duration. This technology may facilitate perimetry at home and in a wide variety of non-specialist clinics.

Conflict of Interest: Yes I have. **Ethics Committee Approval:** Not Applicable **Informed Consent:** Yes I have obtained.

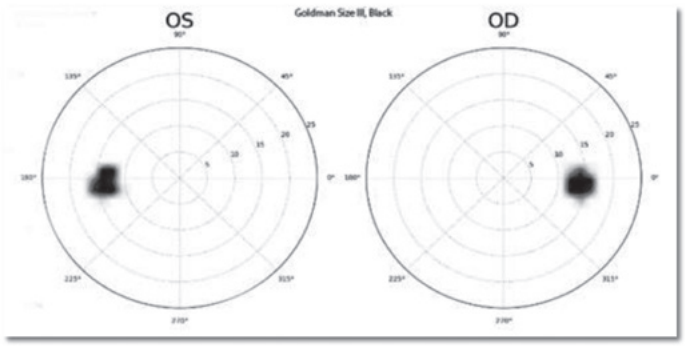

Figure 1. VVP results in a normally-sighted 28-year-old.

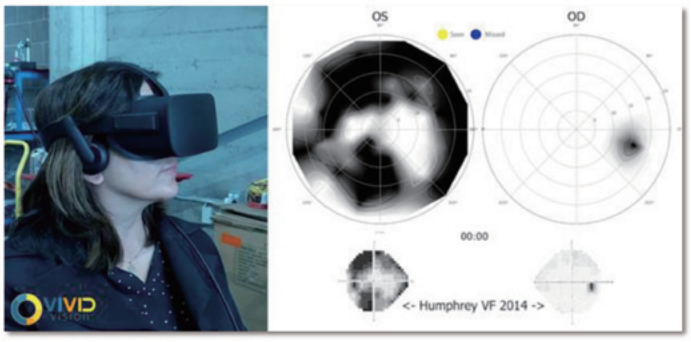

Figure 2. Asymmetric glaucomatous visual field loss in a 48-year old woman, measured for the first time in 2017 (top) and with the HVFA 24-2, performed three years previously (bottom). The two methods show good concordance. The test duration was xxx seconds with VVP and xxx seconds with the HVFA.

O7-1

Focal lamina cribrosa defect in myopic eyes with non-progressive glaucomatous visual field defect

Yu Sawada[1], Takako Matsui[1], Takeshi Yoshitomi[1], Makoto Araie[2]

[1]Department of Ophthalmology, Akita University, Japan, [2]Kanto Central Hospital of the Mutual Aid Association of Public School Teachers

Purpose: To investigate factors discriminating between progressive and non-progressive eyes with myopic glaucoma and to describe unique pattern of focal lamina cribrosa (LC) defect that correspond spatially to the plausibly non-progressive glaucomatous visual field defect (VFD).

Subjects and Methods: In this retrospective study, we included 188 eyes of 132 myopic subjects (axial length equal to or more than 24mm) who exhibited VFD which was considered glaucomatous and followed up for 7 years.Serial enhanced depth imaging spectral domain-optical coherence tomography (EDI OCT) B-scans of the optic discs were reviewed for the LC defect. Non-progressive VFD was defined as having more than 1 progressing test point of Humphrey VF with a slope calculated using pointwise linear regression worse than -1.0dB/year at P less than 0.01, and mean deviation (MD) change rate of more than -0.2dB/year. Eyes were classified as having either progressive or non-progressive VFD, and associating factors were compared between groups.

Results: Mean age at the time of EDI OCT was 53.4years and mean axial length was 26.10mm. Seventy-seven eyes (41.0%) exhibited non-progressive VFD with mean MD slope of -0.03dB/year. LC defect was more common in eyes with non-progressive VFD than in those with progressive VFD (39.0% vs. 18.9%, P = 0.0004). Multivariate logistic regression analysis revealed that presence of LC defect was significantly associated with non-progressive VFD (odds ratio, 5.73; P = 0.002). The location of LC defect corresponded spatially to the location of VFD. Non-progressive eyes with LC defect exhibited greater myopic optic disc deformation (9.6 degrees vs. 1.3 degrees, P = 0.0001 in torsion angle), lower baseline intraocular pressure (IOP) (16.5 mmHg vs. 21.1mmHg, P = 0.0001), and smaller IOP reduction rate (12.9% vs. 30.8%, P = 0.0001) than those without LCD.

Conclusions: In myopic eyes, presence of focal LC defect was significantly associated with non-progressive VFD. The non-progressive eyes exhibited great myopic deformation of the optic disc, but small IOP reduction rate from the middle-teen baseline IOP.

Conflict of Interest: No, I don't. **Ethics Committee Approval:** Yes, I have obtained **Informed Consent:** Yes, I have obtained

O7-2

Using structural information to improve perimetric examination of the macular visual field in glaucoma

Giovanni Montesano[1,2,3], Antonio Modarelli[2], Luca Mario Rossetti[2], David P Crabb[1]

[1]Optometry and Visual Sciences, City, University of London, London, United Kingdom, United Kingdom, [2]Univeristy of Milan, ASST Santi Paolo e Carlo, Milan, Italy, [3]Moorfields Eye Hospital, London, United Kingdom

Purpose: To improve the testing strategy of the macular visual field in glaucoma with prior structural information.

Materials and Methods: We analysed one eye of 17 healthy and 31 glaucoma subjects. Macular OCT scan (Spectralis, Heidelberg Engineering) and 10-2 perimetric test with the Compass fundus perimeter (CenterVue) were performed. We matched fundus images to precisely place tested locations on the OCT maps (Fig 1). Probability-of-seen curves, at different levels of local structural damage, were estimated from yes/no responses to stimuli and used to build priors for a macular structural ZEST (MacS-ZEST) strategy (Fig 1).
We compared MacS-ZEST to ZEST simulating reliable (false positive rate = 0.03) and unreliable subjects (false positive rate = 0.13). For simulations, to accurately estimate true input thresholds in glaucoma subjects, we tested 12 patients with 8 points at 1 and 3 degrees from fixation with 4-2 strategy, three times, taking the average. Data from fellow eye were used for healthy subjects. Mean absolute deviation (MAD) from input thresholds was calculated. Mean difference ± standard error is reported.

Results: MacS-ZEST reduced the number of presentations in normals (reduction per 68-locations; reliable: 145 ± 0.27, 31%; unreliable: 167 ± 0.27, 33%) and glaucomas (reduction per 8-location; reliable: 6 ± 0.10, 13%; unreliable: 7 ± 0.10, 14%).
Error was reduced in MacS-ZEST in glaucomas (MAD reduction per test; reliable: 0.13 ± 0.01 dB; unreliable: 0.33 ± 0.01 dB, Fig 2) and normals (reliable: 0.07 ± 0.002 dB; unreliable: 0.33 ± 0.002 dB). All $p < 0.001$.

Conclusions: We used fundus perimetry to accurately model mean and variance of structural priors. MacS-ZEST efficiently allocates more presentations for diseased locations, increasing precision and reducing overall test time.

Fig 1. Compass fundus image (left) and overlaid Spectralis fundus image after matching (middle). Red dots indicate tested locations. On the right, an example of the starting priors for MacS-ZEST of two locations with different ganglion cell damage. Tested locations were moved on the ganglion cell map to account for Henle fibre displacement.

Fig 2. Error (vertical axis) at different input thresholds (horizontal axis) for unreliable glaucoma subjects. Boxes enclose the interquartile range, the green and red lines enclose the 95% and 99% quantiles respectively.

Conflict of Interest: Yes, I have. **Ethics Committee Approval:** Yes, I have obtained **Informed Consent:** Yes, I have obtained

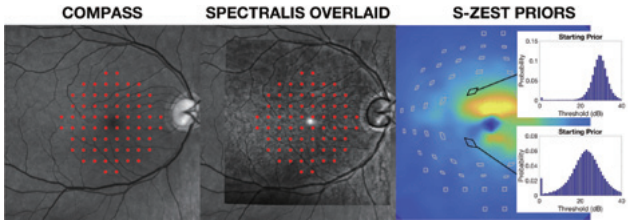

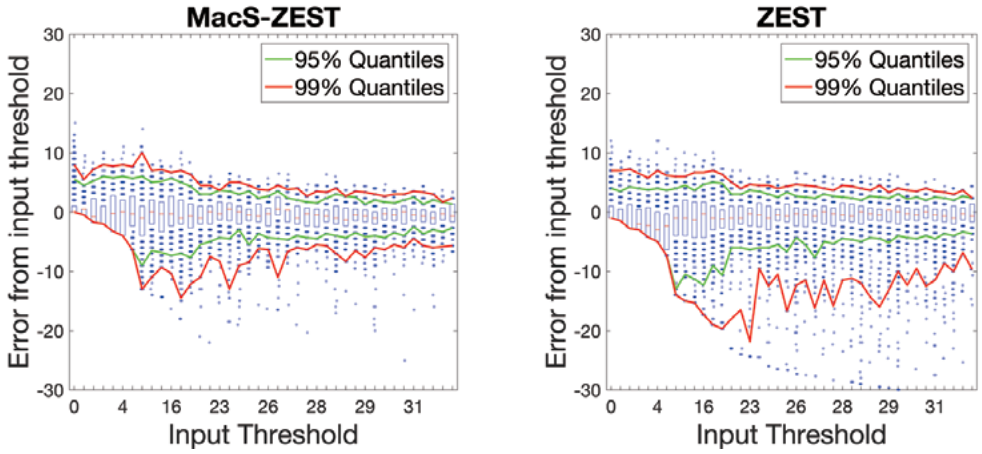

O7-3

En face slab images of macula better accounts for visual functional outcomes compared with inner retinal thickness in eyes with optic neuritis

Mari Sakamoto, Sotaro Mori, Kaori Ueda, Yukako Inoue, Takuji Kurimoto, Yuko Yamada, Makoto Nakamura

Department of Ophthalmology, Kobe University, Japan

Purpose: Recently we reported that there was a clear relationship between function and thickness–based structure detected using optical coherence tomography (OCT) in eyes with neuromyelitis optica (NMO), whereas there was not such a relationship in eyes with idiopathic optic neuritis (Matsumoto et al., PlosOne 2017). The aim of this study is to assess whether the en face OCT slab images of macula could account for the visual functional outcome in eyes with a past history of optic neuritis.

Material and methods: Medical records of 28 eyes of 28 patients (39.4 ± 14.5 years, male: female=6:22) who underwent both Cirrus SD OCT and the Humphrey VF tests 30–2 SITA standard program at 6 months or later after the onset of diseases and exhibited thickness of GCL+IPL less than 70μm on Ganglion Cell Analysis. Twelve patients had NMO, whereas sixteen patients had other etiologies. The pseudo–colored en face slab images of macula were reconstructed from the 6 × 6 macular cube using advanced visualization analysis and then converted to binary images. Eyes were divided into high and low reflective based on the presence and absence, respectively, of high reflective signals in the papilla–macular bundle (PMB) region. Multiple regression analysis was conducted to which among GCL+IPL thickness, slab reflectivity (high or low reflective group), and disease (NMO or non–NMO) could account for logMAR converted best–corrected visual acuity (VA) or mean deviation (MD).

Results: There were 20 eyes with high reflective areas in the PMB region, whereas 8 eyes had no high reflective areas. The mean (SD) thickness of GCL+IPL was 57.60 (6.07) μm and 51.63 (2.56) μm in the high and low, respectively, reflective group (p=0.0011).Likewise, logMAR VA was -0.078 (0.101) and 1.27 (0.81), respectively, (p=0.0023). MD was -2.95 (1.62) dB and -26.71 (4.09) dB, respectively (p<0.0001). The multiple regression analyses demonstrated that only the slab reflectivity could account for either logMAR VA or MD with adjusted coefficient of determination of 0.672 (p<0.0001) and 0.949 (p<0.0001). The NMO group had a significantly higher proportion of low reflective eyes (Fisher's exact test, p=0.0042).

Conclusion: The presence of high reflective areas in the PMB region is better correlated with visual functional outcome compared with the GCL+IPL thickness in eyes that underwent optic neuritis.

Conflict of Interest: No, I don't. **Ethics Committee Approval:** Yes, I have obtained **Informed Consent:** Yes, I have obtained

O7-4

Inner retinal structure-function relationship within the central 20 degrees in retinitis pigmentosa

Henrietta Wang[1,2], Jack Phu[1,2], Lisa Nivison-Smith[1,2], Nayuta Yoshioka[1,2], Janelle Tong[1], Michael Kalloniatis[1,2]

[1]Centre for Eye Health, University of New South Wales, Australia, [2]School of Optometry and Vision Science, UNSW

Purpose: Retinitis pigmentosa (RP) is a progressive outer retinal degeneration associated with loss of vision. Outer retinal (OR) thickness is a predictive of visual field (VF) sensitivity however its ease of discrimination and dynamic range reduces with disease progression. Inner retinal structures such as the ganglion cell complex (GCC) may provide a wider dynamic range as it is often less affected until later disease stages. We aimed to establish the relationship of retinal thickness: outer versus inner and visual function.

Materials and Methods: This study included seven RP subjects with disease progression within the central 20° with visible ellipsoid zones, and seven age-matched normals. GCC (the anterior border of the inner plexiform layer to retinal nerve fiber layer) and outer retina (from the basement membrane to the external limiting membrane (ELM), or to the inner border of the RPE in the absence of the ELM) thicknesses was determined from the Spectralis OCT 8x8 macular cube grid (61 B-scans over 30x25°). Visual function was determined using the Humphrey Field Analyzer (10-2 test grid) using standard protocols (Goldmann size III and 200 ms stimulus duration). Sensitivities were plotted as a function of retinal thickness values, as well as calculated ganglion cell count (GC_{Count}) per stimulus area, at corresponding retinotopic locations.

Results: Linear regression showed significant correlations between OR thickness and sensitivity in normal (slope = 5.56 ± 0.82, R^2 = 0.16, $p<0.01$) and RP (slope = 5.42 ± 0.24, R^2 = 0.69, $p<0.01$) subjects with no significant difference in slope value ($p = 0.94$). There were significant correlations between GCC thickness and sensitivity in normal (slope = 1.01 ± 0.12, R^2 = 0.22, $p<0.01$) and RP (slope = 4.21 ± 0.39, R^2 = 0.31, $p<0.01$). GCC regression slopes in normal versus RP differed significantly suggesting the inner retinal structure-function relationship changes in RP. Comparison of GCC and OR correlations in RP showed a slight, but significant difference between the slope values. A similar difference in slope value between normal and RP patients was found when using GC_{Count} ($p<0.05$).

Conclusions: GCC thickness and GC_{Count} are alternative measurements to OR thickness predictive of visual function in RP. Although its structure-function relationship is similar to OR thickness in RP patients with visible ellipsoid zones, it has potential as an alternative structural measurement in advanced disease. Further studies could examine the structure-function relationship along the disease spectrum to determine optimal structural and functional techniques for measuring progression.

Conflict of Interest: No, I don't. **Ethics Committee Approval:** Yes, I have obtained **Informed Consent:** Yes, I have obtained

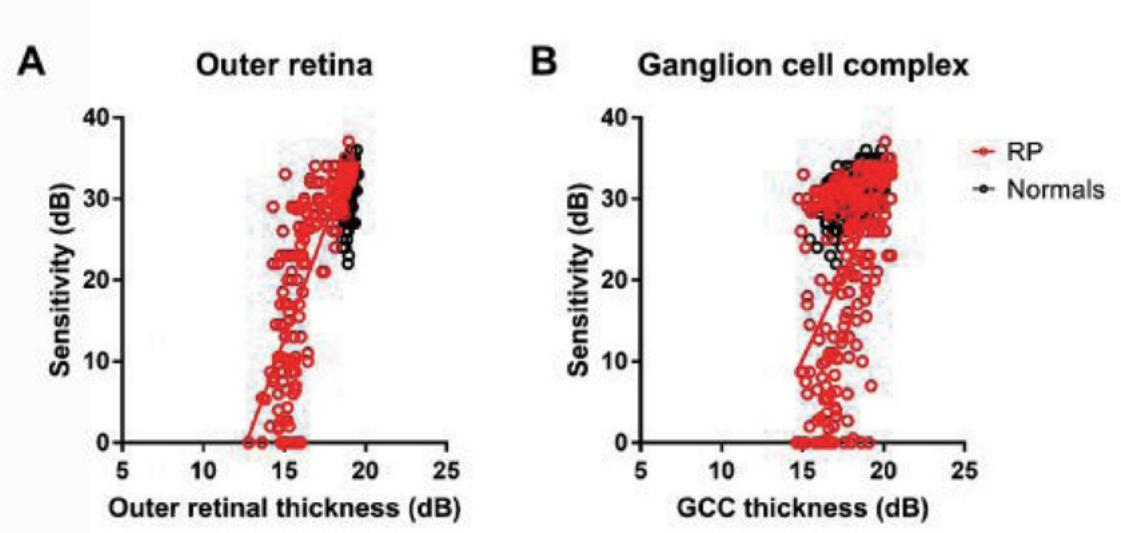

Figure 1: Sensitivity (dB) plotted as a function of thickness (dB) for **(A)** outer retina and **(B)** GCC in RP (red) and normal subjects (black).

O8-1

EVALUATION OF THE NEW THRESHOLD STRATEGY USING A VARIATIONAL BAYES MODEL

Satoshi Shimada[1], Hiroshi Murata[2], Ryo Asaoka[2]

[1]Research & Development Department, Medical Device Devision, Kowa Company, Ltd., Japan, [2]Department of Ophthalmology, University of Tokyo, Tokyo, Japan

Purpose: The variational Bayes (VARB) model is an algorithm to predict future visual fields (VFs) from the patients&acute previous VF records, developed using VF records of 5,049 eyes of 2,858 glaucoma patients (Murata et al, IOVS 2014). The purpose of the current study was to investigate the accuracy and the examination time of a new threshold strategy using the VARB (VARB-T) by a computer simulation.

Materials and Methods: A computerized VF simulation model (full-threshold) was developed that determines the response by setting the frequency of seeing curves for each point. This simulation model was applied to 24-2 VF from 911 eyes of 547 glaucoma patients (mean deviations: MD were -7.8 ± 6.2 dB, mean ± Standard deviation: SD). This simulation was carried out adding i) no measurement noise (ideal response) and ii) measurement noise of SD = 2.1dB. During the simulated threshold examination with VARB-T, the initial values for each point were decided using the VARB predicted VF sensitivity, and also the termination of the thresholding was decided. As VF sensitivities are determined, the prediction for the VF sensitivities of remaining test points were updated using VARB. The accuracy of the VF sensitivity with the VARB-T, with/without update of initial values and also terminating values, was evaluated through the root mean squared error (RMSE). The examination time was also calculated.

Results: i) Simulation with ideal response; without updating initial and termination values, the RMSE and the examination time were 0.9 ± 0.3 dB and 408 ± 78 sec, whereas these were 0.9 ± 0.3 dB and 343 ± 26 sec with update of initial values but not termination values. These values were 1.9 ± 1.0 dB and 199 ± 71 sec, when both of initial and terminating values were updated.
ii) Simulation with measurement noise; without updating initial and termination values, the RMSE and the examination time were 2.2 ± 0.2 dB and 489 ± 77 sec, whereas these were 2.2 ± 0.2 dB and 417 ± 29 sec., with update of initial values. These values were 2.6 ± 0.7 dB and 261 ± 65 sec, when both of initial and terminating values were updated.

Conclusions: Our simulation experiments suggested that the VF examination time can be shortened with a marginal decrease of measurement accuracy, using the new threshold strategy of VARB-T.

Conflict of Interest: Yes, I have. **Ethics Committee Approval:** Yes, I have obtained **Informed Consent:** Not Applicable

O8-2

DENOISING VISUAL FIELDS USING AUTO-ENCODERS

Serife S. Kucur, Raphael Sznitman

ARTORG Center, University of Bern, Switzerland

Purpose: Perimetry testing is one of the most widely used methods to estimate visual fields (VF) and highly effective to quantify visual function for diagnostics and follow up purposes. While the test relies on a query-feedback process to accurately estimate differential light sensitivities at given VF locations, a longstanding problem is in reducing the overall number of stimuli presentations to acquire accurate VFs. To this end, many strategies have been proposed to shorten the testing time. Along this line of research, we propose in this study a post-processing method, used in combination with a fast testing strategy, to keep the number of presentations low while vastly increasing the accuracy of VF estimation.

Materials & Methods: We use the Tendency-Oriented Perimetry (TOP) strategy to acquire fast but inaccurate VFs and propose a denoising approach to further increase the quality of these in a post-processing step. To do this, we designed a novel deep learning method based on auto-encoders (AE). Our AE is a neural network containing 3 fully connected layers that take the TOP-acquired VF as input and outputs a denoised version of the input VF. The AE starts by encoding the input using two layers, having 512 and 1024 hidden units each, in order to map the noisy input to a high dimensional space (*i.e.* 1024 dimensions). The decoding part contains one hidden layer with 512 hidden units. The parameters of the AE were learned during a training phase with the back-propagation algorithm and a training set of pairs of TOP-simulated and true VFs. Our AE was implemented in Python using the Keras deep learning framework. VF simulations were performed using the Open Perimetry Interface.

Results: In this study, we used 5108 (4863 glaucomatous, 245 healthy) 24-2 pattern VFs from the Longitudinal Glaucomatous Visual Field Dataset (collected by Rotterdam Ophthalmic Institute using Humphrey Field Analyzer II, Carl Zeiss Meditec AG, Germany). We trained our AE in a 10-fold cross-validation manner, leaving test subjects out of corresponding training sets. On its own, TOP provides Root Mean Square Error (RMSE) of 5.163 ± 1.37 for a total of 54 presentations. Our approach yields RMSE of 3.955 ± 1.45 using the same 54 presentations whereas Dynamic Strategy (DS) provides RMSE of 3.604 ± 1.07 with 144.22 ± 11.93 stimuli presentations (See Fig.1-2). Besides, running the AE for a single VF takes less than a second on a standard PC.

Conclusion: In this work, we proposed a new post-processing step that increases the accuracy of VFs acquired with fast but noisy strategies. These results indicate that strategies such as TOP could be refined without impacting the testing time. The proposed model has a comparable performance with a standard clinical approach (i.e. DS), which highlights its potential for broad use in clinical settings.

Conflict of Interest: No, I don't. **Ethics Committee Approval:** Not Applicable **Informed Consent:** Not Applicable

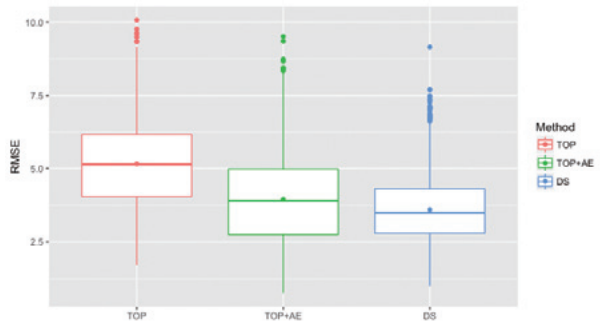

Fig.1: RMSE for different strategies. Middle line and dot show median and mean values respectively. Note that all the 10-fold results are accumulated.

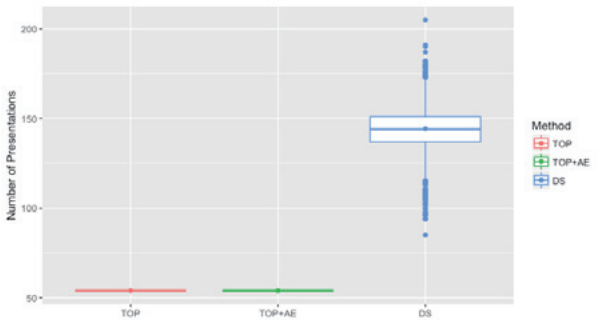

Fig.2: Number of stimuli presented by different strategies. Middle line and dot show median and mean values respectively. Note that all the 10-fold results are accumulated.

O8-3

Cluster Identification Algorithm (CIA)

Anca D. Demea, Horea T. Demea

University of Medicine and Pharmacy Cluj-Napoca, Romania, Romania

Purpose: The Cluster Identification Algorithm is a method of quantifying the severity of defects in each cluster of the vision field.It generates the Cluster Identification Number (CIN), a code that allows ranking the severity of the cluster defects.

Materials and Methods: We used the Octopus 900 perimeter, G-Top program. The results were analysed on a custom print with four maps: Gray Scale, Defect Curve, Cluster Analysis and Comparison.On the Cluster Analysis map, the ten clusters were named according to their position towards the horizontal meridian, macula and papilla as following:a. Central: CS - Upper Central, CI - Lower Centralb. Peripheral: UT - Upper Temporal, TS - Temporal Superior, UN - Upper Nasal, NS - Nasal Superior, TI - Temporal Inferior, LT - Lower Temporal, LN - Lower Nasal, NI - Nasal Inferior.We introduce the Cluster Severity Score protocol to assess the severity of scotomas at each cluster level. It divides the visual field defects into alarm ranges (in dB), each score being associated with a qualitative severity score and a symbol.Thus, based on the severity scores, we obtained five alarm intervals:0 - 4 dB: OK, one green circle symbol5 - 9 dB: Low, one red circle symbol10 - 14 dB: Medium, two red circles symbol15 - 19 dB: High, three red circles symbol> 20 dB: Very high, one black circle symbole.g. if in TS cluster the visual field defect is 18 dB, the severity score is HighThe results with severity symbols are organised in the Location and Score table, separately for peripheral and central clusters.The Number of defects table counts the number of clusters that have the same severity indicator separately for the peripheral and central ones and generates the Cluster Identity Number (CIN). CIN is a 5 digits code which displays the defects as follows, the last position of the unit is reserved for undefective clusters, the 2nd for low, the 3rd for medium, the 4th for high and the 5th for very high.e.g. the CIN code of Outer Clusters is 22310 which means that the severity of defects in peripheral clusters map is: 2 Very High, 2 High, 3 Medium and 1 Low, without regular clusters.ResultsCluster Identification Number is a unique method which quantifies the severity of visual field defects, individualised for peripheral and central clusters.

Conclusions: Cluster Identification Algorithm (CIA) is a fast, easy and accurate method of identifying the severity of visual field defects. Since most of the visual fields have a non-parametric distribution, the measurement of MD and LV is less accurate in terms of global appreciation of visual field defects.The Cluster Identification Number (CIN) has no limitations imposed by the non-parametric distribution so it is safer to use.

Conflict of Interest: No, I don't. **Ethics Committee Approval:** Not Applicable **Informed Consent:** Not Applicable

Tabel 1

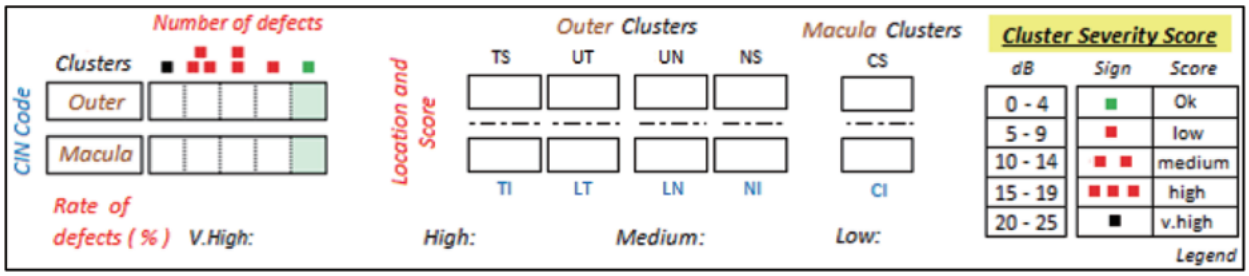

O8-4

The usefulness of waveform parameters measured with the Ocular Response Analyzer to assess the progression of glaucoma

Shuichiro Aoki[1], Hiroshi Murata[1], Masato Matsuura[2], Kazunori Hirasawa[2,3], Shunsuke Nakakura[4], Yoshiaki Kiuchi[5], Ryo Asaoka[1]

[1]Department of Ophthalmology, The University of Tokyo, Japan, [2]Kitasato University, [3]Moorfields Eye Hospital NHS Foundation Trust and University College London, [4]Tsukazaki Hospital, [5]Hiroshima University

Purpose: Corneal hysteresis (CH) measured with Ocular Response Analyzer (Reichert: ORA) is closely related to glaucomatous visual field (VF) progression. In ORA measurement, ORA measures the intensity of the reflected infrared light from the deforming corneal surface which is the waveform record with two peaks, represented by 38 waveform parameters. The purpose of this study was to investigate the relationship between the ORA waveform parameters and glaucomatous visual field progression, in comparison with CH.

Materials and Methods: Subjects comprised of 101 eyes with primary open angle-glaucoma in 68 patients with eight reliable (fixation loss < 20% and false positive < 15%) VFs with the Humphrey Field Analyzer (24-2 or 30-2). The mean of total deviation (mTD) value of the 52 test points in the 24-2 HFA VF test pattern was calculated. Intraocular pressure (IOP) was measured using the Goldmann applanation tonometer (GAT-IOP) during the eight VF measurements. The progression rate of mTD was determined using the eight VFs from each eye. ORA measurement was performed three times with a sufficient quality index (waveform score < 6.5) in a same day within 180 days from the eighth VF measurement, and average values of three measurements were used in the analysis. From the 38 waveform parameters, first, 16 parameters associate with mTD progression rate were selected using least absolute shrinkage and selection operator (LASSO) regression. Then, the variables related to the mTD progression rate were identified from the 23 variables of these selected 16 waveform parameters and seven other parameters (age, mean GAT-IOP, standard deviation (SD) of GAT-IOP, central corneal thickness, axial length, mTD in the initial VF, CH), using a linear mixed model, followed by the model selection with the second order bias corrected Akaike Information Criterion (AICc) index (optimal linear mixed model).

Results: The mTD progression rate was -0.25 ± 0.31 (mean ± SD) dB/year. The optimal linear mixed model for the mTD progression rate was: mTD progression rate = 1.57 - 0.031 × path21 - 0.011 × dslope2 - 0.048 × w21 (AICc=44.19). This model was 8.12 times better than the optimal model compared to the model only with CH (AICc=48.38).

Conclusions: ORA waveform parameters were significantly correlated with glaucomatous VF progression. The association was stronger than a simple CH model.

Conflict of Interest: No, I don't. **Ethics Committee Approval:** Yes, I have obtained **Informed Consent:** Yes, I have obtained

O9-1

ARREST: A new visual field test algorithm designed to improve spatial resolution and test time for moderate-advanced visual field damage.

Allison M McKendrick[1], Vasanth Muthusamy[1], William H Morgan[2], Andrew Turpin[3]

[1]Department of Optometry & Vision Sciences, The University of Melbourne, Australia, [2]Center for Ophthalmology and Visual Science, Lions Eye Institute, The University of Western Australia, Perth, Australia, [3]School of Computing & Information Systems, The University of Melbourne, Parkville, Australia

Purpose: Visual field assessment lacks precision in moderate to advanced glaucoma. We assessed a new test algorithm that doesn't attempt to threshold accurately in highly variable areas, but instead expends presentations increasing spatial fidelity. We studied algorithm performance using two methods: 1) computer simulation and 2) human testing with artificially progressing scotomata.

Materials and Methods: Our procedure ARREST, a variant of ZEST, applies the following: once a location has estimated sensitivity less than 17dB (a defect), we check that it is not an absolute defect (<0dB, blind). Saved presentations are used to test extra locations spatially near the defect. Visual field change events are: a) decreasing in the range 40 to 17dB; b) decreasing from above 17dB to defect; or c) defect to blind. The computer simulation input was derived from an empirical database of 121 eyes with progressing moderate-advanced 24–2 visual fields. We ran both ARREST and ZEST on these fields, with typical rates of modelled observer false responses and psychometric function slopes. For the human experiment, we measured fields using ARREST implemented using the OPI on an O900 perimeter (Haag–Streit AG) in 5 people with normal vision. Progressing artificial scotoma generation was added to a series of 16 visual field tests by modifying dB levels presented to the participants to simulate both reduced sensitivity and altered psychometric function slope.

Results: For the computer simulation, with matched specificity for detecting progression (95%), ZEST and ARREST showed similar sensitivity to detect progression. ARREST used 25-40% fewer presentations in advanced damage. In humans, outcomes were consistent with the simulation. For the most advanced field defect, compared to ZEST, ARREST averaged 30 presentations faster (range 18 to 40), and had more seen stimuli (63% versus 44%), resulting in 17 to 25% shorter test time (reduction of 1 min 40 secs to 2 min 37 secs). For the final field, ARREST averaged 85 test locations (range 79 to 89) significantly increasing the spatial description of the visual field compared to the 24–2 pattern.

Conclusions: Our simulations indicate that giving up attempting to quantify size III white–on–white thresholds below 17dB and using the presentations saved to test extra locations should better describe spatial progression in moderate to advanced glaucoma, and also save some test time.

Conflict of Interest: Yes, I have. **Ethics Committee Approval:** Yes, I have obtained **Informed Consent:** Yes, I have obtained

O9-2

Measuring Frequency of Seeing Curves On and Off Blood Vessels in Normal Eyes Using the Compass Perimeter Controlled by the OPI

Andrew Turpin[1], Allison M McKendrick[2]

[1]*School of Computing and Information Systems, The University of Melbourne, Australia,* [2]*Department of Optometry and Vision Sciences*

Purpose: To use angioscotoma to investigate the difference in perimetric thresholds and variability both with and without fundus tracking on the Compass Perimeter controlled by the Open Perimetry Interface (OPI).

Methods: Frequency of Seeing (FoS) curves using a Size III white-on-white stimuli were measured in 5 subjects with normal vision at three locations: one directly on a major retinal vein, one close to the vein, and in a retinal area free of major blood vessels in the quadrant opposite the other two at similar eccentricity. Locations were chosen manually based on the infrared retinal image returned by the Compass for the first run, and then algorithmically aligned with subsequent photos on subsequent runs using custom software written using Open CV in Python. The FoS curves were collected using a yes-no procedure comprised of a total of 20 presentations at each of 14 dB levels (19...32 dB), a total of 280 presentations, for each location. Data collection was divided into groups of 84 presentations which contained all dB levels at each location presented twice in random order. After 2 runs, the subject was instructed to rest and lights were turned on to avoid dark adaption. FoS curves were collected both with and without retinal tracking enabled. Curves were fitted with a Cumulative Gaussian function with asymptotes fixed at 100% and 0% seeing, (except for subject 5) with threshold taken as the mean.

Results: With retinal tracking on, thresholds on the vein were lower than the normal location and FoS slopes flatter for the 5 subjects: threshold differences (dB) 5.5, 2.4, 2.0, 2.5, 2.2; standard deviation (spread, dB) differences 0.64, -0.05, 0.61, 0.82, 0.28. There was no significant difference between thresholds with tracking turned on and off (ANOVA, $p=0.77$). Slopes of the FoS curves were shallower without tracking on ($p=0.03$), with a mean difference in standard deviation of the FoS curves of 0.461 dB. Examining fixation data returned from the Compass for 3 subjects when tracking was turned off showed that between 10% to 15% of presentations occurred when fixation was more than $\pm$ 0.5 degrees from (0,0).

Conclusions: The Compass can be successfully controlled using the OPI. When measuring FoS curves in an area of the retina with a small dB gradient, retinal tracking does not affect threshold measurements, but does effect slope measurements.

Conflict of Interest: Yes, I have. **Ethics Committee Approval:** Yes, I have obtained **Informed Consent:** Yes, I have obtained

Figure: Retinal images around the 3 stimuli locations for 5 subjects.

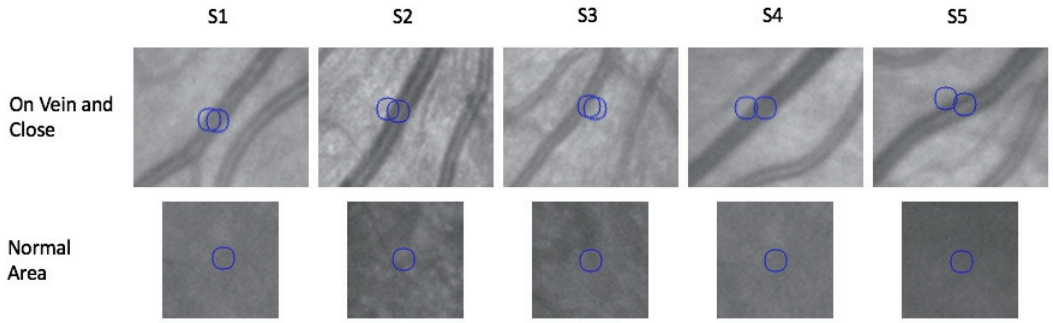

Table: FoS fits for 5 subjects S1-S5 both with ("On") and without ("Off") retinal tracking.

	On Vein				Close to Vein				Vessel free area			
	Threshold		Slope		Threshold		Slope		Threshold		Slope	
	Off	On	Off	On	Off	On	Off	On	Off	On	Off	On
S1	25.45	2.83	24.76	2.00	26.25	3.12	24.80	2.09	30.37	1.82	30.29	1.36
S2	28.10	3.11	28.82	1.41	26.96	3.13	26.85	3.01	31.31	1.52	31.23	1.46
S3	27.17	2.88	27.02	2.64	26.79	2.75	27.27	2.07	29.10	2.11	29.01	2.02
S4	28.39	1.95	28.11	2.24	27.29	2.30	28.00	2.27	30.84	1.07	30.56	1.42
S5	27.47	2.09	28.88	1.56	26.55	2.93	28.31	1.04	30.69	1.17	31.12	1.28
Mean	27.32	2.57	27.52	1.97	26.77	2.85	27.05	2.10	30.46	1.54	30.44	1.51

O9-3

Robustness of area-modulated perimetric stimuli to increased intraocular straylight

Lindsay Rountree[1], Padraig J. Mulholland[2,3], Roger S. Anderson[2,3], Tony Redmond[1]

[1]School of Optometry and Vision Science, Cardiff University, United Kingdom, [2]Ulster University, [3]National Institute for Health Research (NIHR) Biomedical Research Centre at Moorfields Eye Hospital NHS Foundation Trust and UCL Institute of Ophthalmology

Purpose:

To investigate the effect of simulated intraocular straylight (IOS) on threshold for stimuli optimised to map to the altered spatial summation curve in glaucoma.

Materials and Methods:

Energy (luminance × area × duration) thresholds were measured at 18 visual field locations in one eye of five young, healthy participants (median [IQR] age: 29.6 [26.1, 28.7] years) with four stimuli that modulated in differing dimensions, under six levels of IOS (simulated using white opacity-containing filters; LEE filters, Andover, UK). The order of experiments with different stimulus forms and straylight levels was randomised for each participant. Stimuli were: A – fixed contrast (log Δ I/I: -0.3, starting within Ricco's area), varying in area; CR – fixed area (-1.93 log deg^2, within Ricco's area), varying in contrast; AC – varying in area and contrast simultaneously (starting within Ricco's area); GIII – fixed area (-0.95 log deg^2), Goldmann III equivalent, varying in contrast. Log energy step sizes were approximately equal, from an equivalent reference, for all stimuli. Threshold energy was measured with a 1:1 staircase, which terminated after four reversals. Threshold was determined as the mean of the final two reversals. IOS was measured for each participant at baseline (no filter) and with each of the five filters (Fog 1-5), in random order, with an Oculus C-Quant (Ocular, Wetzlar, Germany). Mean threshold was compared between stimulus forms for all 18 locations, and within five eccentricity zones. Linear mixed effects analysis was used to investigate differences in the effect of IOS on threshold between stimulus forms.

Results:

Mean IOS ranged from 1.2 log(straylight, s) at baseline (no filter), to 2.0 log(s) with Fog 5. Overall, the AC stimulus demonstrated the greatest resilience to increased IOS, with little increase in threshold with Fog 1-3 (consistent with normal lenticular aging changes). In addition, threshold increase from baseline with this stimulus was generally the lowest of the four stimuli at each IOS level. This was true when all test locations were considered together (figure 1), and separately within each of the five eccentricity zones.

Conclusions:

Stimuli modulating in area and contrast simultaneously show modestly increased resilience to increased IOS, compared with conventional perimetric stimuli (GIII).

Conflict of Interest: Yes, I have. **Ethics Committee Approval:** Yes, I have obtained **Informed Consent:** Yes, I have obtained

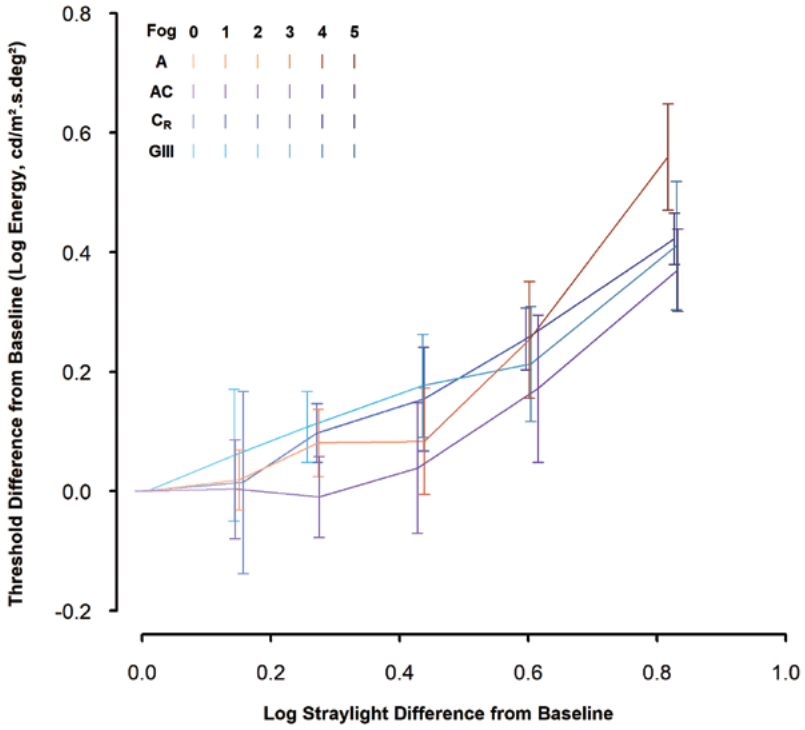

O9-4

The relationship between cortical receptive field size and eccentricity in V1, V2 and V3 of healthy individuals

Melissa E Wright[1,2,3], Krishna D Singh[2,3], Simon K Rushton[3], D Samuel Schwarzkopf[4], Tony Redmond[1]

[1]School of Optometry and Vision Sciences, Cardiff University, United Kingdom, [2]Cardiff University Brain Research Imaging Centre, Cardiff University, Cardiff, UK, CF24 4HQ, [3]School of Psychology, Cardiff University, Cardiff, UK, CF10, [4]School of Optometry and Vision Science, University of Aukland, New Zealand

Purpose: Ricco's area of complete spatial summation was previously found to be enlarged in glaucoma, and early perimetric sensitivity loss in those patients could be mapped to the shifted spatial summation curve (Redmond et al, IOVS, 2010;51:6540–8). Pan & Swanson (J Vis, 2006;6:1159–71) demonstrated that spatial summation of perimetric stimuli could not be explained by probability summation across retinal ganglion cells, but rather cortical pooling by multiple spatial mechanisms. Cortical receptive field size therefore plays a critical role in determining visual field sensitivity. Receptive fields of cortical cells increase in size with eccentricity, at least up to 9° eccentricity. Little is known, however, about the size of cortical receptive fields, in vivo, at eccentricities commonly affected in conditions like glaucoma. Here, we use functional Magnetic Resonance Imaging (fMRI) to investigate the association between cortical receptive field size and eccentricity in mid–peripheral regions in healthy individuals.

Materials and Methods: Population receptive field size (pRF; estimate of the size of receptive fields of all functional neurones within a voxel or 3D pixel) was measured in 12 healthy individuals (median (IQR) age: 19.9 (19.5, 20.2) yrs; median (IQR) VFI: 99 (99, 100)) with high–field 7T fMRI, allowing fine spatial resolution (1mm3). Here, pRFs were measured in central (0–6° eccentricity) and peripheral regions (14–18° eccentricity) relating to the inferior temporal visual field. Visual areas V1–V3 were manually delineated per participant using retinotopic maps, owing to between–subject variation, and used as masks to extract cortical pRF size. The association between pRF size and eccentricity was investigated.

Results: As previously reported, there is a positive association between pRF size and eccentricity in the central visual field in visual area V1–V3 (slope: 0.17, $p<0.0001$). Here, we find that the association continues into mid–peripheral regions, with a small increase in slope (0.22, $p<0.0001$). Slopes for V2 and V3 were similar (0.17 and 0.26, respectively, $p<0.0001$). Greater within–subject variance is observed in data for peripheral region, compared to that in data from the central regions. Between–subject differences in the association were modest. A typical example of data from one participant is shown in Figure 1.

Conclusions: This is the first study to report the effect of eccentricity on pRF size beyond the central visual field in multiple cortical hierarchies. Population receptive field size is increased in the mid–periphery, but notable variance in the data is apparent. Establishing normal values for cortical receptive field size is important for a better understanding of spatial summation of perimetric stimuli.

Conflict of Interest: No, I don't. **Ethics Committee Approval:** Yes, I have obtained **Informed Consent:** Yes, I have obtained

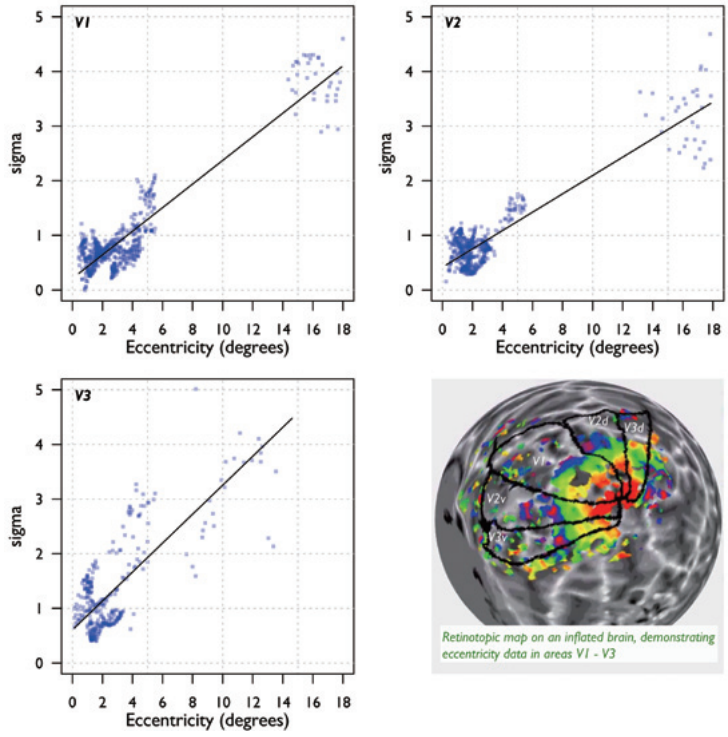

O9-5

Visual function and adaptation from star- to sunlight in glaucoma: a case-control study

Nomdo M. Jansonius, Ronald A.J.M. Bierings

Department of Ophthalmology, University of Groningen, University Medical Center Groningen, Netherlands

Purpose: In a recent questionnaire study, we found that the concept of (early-stage) glaucoma as an asymptomatic disease is only valid with optimal luminance. Compared to optimal luminance (outdoor on a cloudy day), differences in visual complaints between glaucoma patients and controls were greater in the dark, and also with a high luminance, or a sudden decrease or increase. The aim of this study was to compare light and dark adaptation and visual function under extreme luminance conditions between glaucoma patients and healthy subjects.

Materials and Methods: Case-control study with 23 glaucoma patients and 51 controls. Cases were selected to have moderate or advanced visual field loss in combination with a normal visual acuity. Psychophysics was performed monocularly using a high-luminance monitor (EIZO radiforce G21) and a projector-based stimulus, and neutral-density filters. Standard automated perimetry and an assessment of the critical fusion frequency (CFF) were performed for a background luminance between 0.02 to 200 cd/m^2. The contrast sensitivity function (CSF) was measured between 0.01 and 10,000 cd/m^2. Light and dark adaptation were measured foveally going from 0.0032 to 10,000 cd/m^2 (LA), and back (DA).

Results: Foveally, perimetric logCS was proportional to log luminance at lower luminances (de Vries-Rose) and saturated at higher luminances (Weber); glaucoma patients had a 0.4 log unit lower logCS than controls ($P<0.001$), independent of luminance. Peripherally, the difference was more pronounced at lower luminances ($P=0.007$). CFF was linearly related to log luminance (Ferry-Porter). Glaucoma patients had a lower CFF compared to controls ($P<0.001$), with a smaller slope of the CFF versus log luminance curve, for both the fovea (6.8 versus 8.7 Hz/log unit; $P<0.001$) and the periphery (2.5 versus 3.4 Hz/log unit; $P=0.012$). Regarding the CSF, the logCS versus log luminance curve of glaucoma patients was similar to that of healthy subjects for 1 and 10 cpd. For 3 cpd, patients had a lower CS than controls (approximately 0.2 log unit; $P=0.031$); the difference seemed more pronounced at lower luminances ($P<0.001$). After LA, glaucoma patients had a 0.13 log unit lower CS plateau than controls ($P=0.010$); after DA, this difference was 0.30 log unit ($P<0.001$). DA time (time to reach 50% of plateau sensitivity) of glaucoma patients and controls were similar (18.2 versus 16.6 minutes; $P=0.14$).

Conclusions: The general trend is a lower sensitivity in glaucoma, without a strong dependency on luminance. Our results could explain complaints of glaucoma patients in the dark and during a decrease in luminance; they do not uncover why glaucoma patients also complain about high luminances.

Conflict of Interest: No, I don't. **Ethics Committee Approval:** Yes, I have obtained **Informed Consent:** Yes, I have obtained

P1-1

Evaluating the usefulness of MP-3 microperimetry in glaucoma patients

Masato Matsuura[1,2], Hiroshi Murata[1], Yuri Fujino[1], Kazunori Hirasawa[3], Mieko Yanagisawa[1], Nobuyuki Shoji[2], Ryo Asaoka[1]

[1]Department of Ophthalmology, Tokyo University, Japan, [2]Kitasato University, [3]Moorfields Eye Hospital NHS Fundation Trust

Purpose: The purpose of the current study was to evaluate the test-retest reproducibility and structure-function relationship of MP-3 microperimeter visual fields (VFs), compared to Humphrey Visual Analyzer (HFA).

Material and methods: Thirty eyes of 30 open angle glaucoma patients (POAG) were enrolled. VFs were measured twice with MP-3 and HFA, using the 10-2 test grid pattern in both perimeters. Ganglion cell complex (GCC) thickness was measured using 3D optical coherence tomography (OCT)-2000. Test-retest reproducibility was assessed using the mean absolute deviation (MAD) measure at all 68 points, and also the intraclass correlation coefficient (ICC) of the repeated VF sensitivities. The structure-function relationship between VF sensitivities measured with MP-3 and HFA and the GCC thickness adjusted for the GCC displacement (Sjostrand J, Graefes Arch Clin Exp Ophthalmol, 1999) was analyzed using the linear mixed modelling.

Results: There was no significant difference in MAD and ICC values between HFA (MAD: 0.83 ± 0.69 dB and ICC: 0.89 ± 0.69, mean ± standard deviation) and MP-3 (MAD: 0.65 ± 0.67 dB and ICC: 0.89 ± 0.69). MP-3 (AICc were 13451.1 and 13474.5, in the first and second measurements, respectively) had the stronger structure-function relationships with GCC thickness, compared to HFA (AICc were 13491.4 and 13500.8, in the first and second measurements, respectively).

Conclusions: MP-3 has similar test-retest reproducibility and better structure-function relationship compared to HFA.

Conflict of Interest: No, I don't. **Ethics Committee Approval:** Yes, I have obtained. **Informed Consent:** Yes, I have obtained.

P1-2

Mapping the Central 10 Degrees Visual Field to the Optic Nerve Head using the Structure Function Relationship

Yuri Fujino[1], Hiroshi Murata[1], Masato Matsuura[1,2], Mieko Yanagisawa[1], Nobuyuki Shoji[2], Kenji Inoue[3], Junkichi Yamagami[4], Ryo Asaoka[1]

[1]Department of Ophthalmology, Tokyo University, Japan, [2]Department of Ophthalmology, Kitasato University School of Medicine, Kanagawa, Japan, [3]Inoue Eye Hospital Tokyo, Japan, [4]JR Tokyo General Hospital, Tokyo, Japan

Purpose: Hood et al. generated a comprehensive mapping between test points in 10 degree visual field (VF) and optic disc, using retinal nerve fiber layer bundle (Prog Retin Eye Res 2013). The purpose of the current study is to confirm the mapping using the strength of structure function relationship between the Humphrey field analyzer (HFA) 10-2 VF (Carl Zeiss Meditec, Dublin, California, USA) and circumpapillary retinal nerve fiber layer (cpRNFL) thickness measurements from Spectral-domain Optical coherence tomography (SD-OCT).

Methods: cpRNFL thickness measurements were obtained using SD-OCT and the 10-2 VF was measured with the HFA. The relationship between visual sensitivity and cpRNL thickness values in the temporal 180 degrees was analyzed using least absolute shrinkage and selection operator (LASSO) regression. Optic disc angle corresponding to each VF test point was then derived using the coefficients from the optimal LASSO regression.

Results: The structure-function map obtained was largely consistent with the mapping reported by Hood et al; superior central VF test points correspond to a vulnerable area of optic disc, more distant toward the inferior pole from the center of the temporal quadrant (9:00 o'clock for the right eye) while inferior VF test points correspond to the superior pole of optic disc.

Conclusions: The structure-function map obtained largely confirms the map reported by Hood et al., however, some important differences were observed.

Conflict of Interest: No, I don't. **Ethics Committee Approval:** Yes, I have obtained **Informed Consent:** Yes, I have obtained

P1-3

The relationship among macular inner retinal layer, retinal nerve fiber layer, and visual field sensitivity in gemination period of glaucomatous optic nerve damage.

Yoshio Yamazaki, Hajime Kondo

Department of Ophthalmology, Tokai University Tokyo Hospital, Japan

Purpose: To clarify the onset of glaucomatous optic nerve damage, we analyzed the relationship among visual field (VF) sensitivity, macular ganglion cell complex (GCC) thickness and circumpapillary retinal nerve fiber layer (cpRNFL) thickness in primary open-angle glaucoma (POAG) patients confined to hemifield defect.

Methods: One eye of 40 healthy subjects and 50 POAG with a reproducible classic localized VF defect confined to superior hemifield was enrolled. All participants had no history of intraocular surgery and spherical equivalent above than -6.0 diopters. The thickness of superior sectoral GCC and superior cpRNFL were measured by RS 3000 (NIDEK, Japan). The mean total deviation (TD) in inferior hemifield was recorded with the HFA 24-2 program (Carl-Zeiss Meditec, USA). The relationships between structure and function in the spared inferior hemifield were investigated.

Results: There were statistically significant differences between healthy and POAG groups for GCC in superior macular region (p=0.001) and cpRNFL thickness at 11 o'clock sector (p=0.001). The mean TDs in the inferior nasal Bjerrum area showed significantly related to the GCC in the superior temporal macular region (p=0.03).

Conclusion: The structural change of inner retinal layer associated with the functional change at corresponded locations of the VF will occur prior to the onset of a reproducible classic localized VF defect.

Conflict of Interest: No, I don't. **Ethics Committee Approval:** Not Applicable **Informed Consent:** Not Applicable

P1-4

Agreement of a nasal step border by a microperimeter with a temporal raphe by optical coherence tomography in glaucoma patients

Sotaro Mori, Mari Sakamoto, Kaori Ueda, Yukako Inoue, Takuji Kurimoto, Yuko Yamada, Makoto Nakamura

Division of Ophthalmology, Kobe University, Japan

Purpose: To evaluate agreement of a nasal step border detected using a microperimeter <MP–3> with a temporal raphe detected using optical coherence tomography <OCT> in patients with a glaucomatous hemifield defect.

Materials and Methods: Enrolled were 25 eyes of 25 glaucomatous patients who showed either an upper or lower hemifield defect detected on the Humphrey visual field <HVF> 30–2 SITA standard program. Visual field sensitivity along the nasal step border was evaluated by using twenty-five test points located from eight to eighteen degrees <2–degree apart each> from the fovea on the MP–3. Data were superimposed on fundus photographs, from which the nasal step border for each patient was determined by the least square method using Image J. The temporal raphe was delineated by visualizing the nerve fibers on the transverse section analysis mode of Spectralis OCT. An angle between a line connecting the fovea and the disc center and the nasal step border was defined as DFN <disc–fovea–nasal step border> angle, while that between the fovea–disc center line and the temporal raphe as DFR<disc–fovea–raphe> angle. The Bland–Altman analysis was conducted to evaluate the agreement between the DFN and DFR angle.

Results: The mean <standard deviation> of age, axial length, mean deviation was 61.6 <13.5> years, 24.5 <1.5> mm, –7.86 <3.76> dB, respectively. The DFN angle determined by the MP–3 was 168.7 <3.9>°, while the DFR angle determined by Spectralis was 168.1 <3.7>°. There was no systematic bias of the two measurements <the mean difference=0.53°; SD of the difference=5.44° >

Conclusions: The DFN angle extrapolated from the nasal step border detected using the MP–3 was comparable with the DFR angle extrapolated from the temporal raphe detected using Spectralis OCT.

Conflict of Interest: No, I don't. **Ethics Committee Approval:** Yes, I have obtained **Informed Consent:** Yes, I have obtained

P1-5

The disc–fovea–temporal raphe angle is associated with the severity of glaucoma with a hemi-field defect

Takuji Kurimoto, Sotaro Mori, Mari Sakamoto, Kaori Ueda, Yukako Inoue, Yuko Yamada, Makoto Nakamura

Division of Ophthalmology, Department of Surgery, Kobe University Graduate School of Medicine, Japan

Purpose: To evaluate the relationship between the disc–fovea–temporal raphe angle (DFRA) determined by the images of optical coherence tomography (OCT) and the severity of hemifield visual field (VF) defect in glaucoma patients.

Materials and Methods: Enrolled were 25 eyes of 25 patients with an either upper or lower VF defect detected on the Humphrey visual field test with a 30–2 SITA standard program. The nerve fiber layers were visualized by Spectralis® OCT with transverse section analysis that constructs *en face* reflectance images by retinal layer segmentation. The delineated nerve fiber end points in undamaged hemi–retinal region were manually plotted on the OCT images superimposed on infrared fundus photographs. Temporal raphe (TR) was calculated as an approximate curve by the least-square method based on the plotted points. The DFRA was defined as the angle between the optic disc–fovea and TR lines. The patients were divided into upper hemifield defect (UFD/14 eyes) group and lower hemifield defect (LFD/11 eyes) group. The correlation between age, axis length, refractive values, mean deviation (MD) and DFRA were analyzed using Pearson ´ s correlation, and coefficients of determination (r) were calculated. To determine the effect of various factors on DFRA, multiple linear regression analyses were performed with stepwise variable selection ($p<0.05$). The dependent variable was UFD or LFD. The independent variables were age, axial length and MD.

Results: The ages of UFD and LFD (mean ± SD) were 64.1 ± 13.9 and 58.4 ± 12.7, refractive values (D) were -2.3 ± 3.3 and -2.8 ± 2.8, axial length (mm) were 24.4 ± 1.4 and 24.5 ± 1.8, and MD (dB) was -8.1 ± 4.0 and -7.5 ± 3.6, respectively, (n.s. for all, unpaired t–test). The DFRA of UFD and LFD (°) were 166.5 ± 3.2 and 170.5 ± 3.2 ($p<0.01$, unpaired t–test). The DFRA was not significantly related to age, axis length and refractive values in either group. The DFRA was negatively correlated with the MD values in the LFD group($r=-0.74$, $p<0.01$), whereas it was positively correlated with the MD values in the UFD group ($r=0.64$, $p<0.05$). Multiple linear regression analysis confirmed these correlations ($\beta=-0.74$, $p<0.001$ for the LFD group and $\beta=0.70$, $p<0.01$ for the UFD group) and showed the age was another independent variable associated with the DFRA in the UFD group ($\beta=-0.58$, $P<0.05$).

Conclusions: The variations of DFRA are related to the severity of localized glaucomatous hemifield visual field defect.

Conflict of Interest: No, I don't. **Ethics Committee Approval:** Yes, I have obtained **Informed Consent:** Yes, I have obtained

P1-6

Relationship between rim width and nerve-fiber layer thickness in normal tension glaucoma.

Yoshinori Itoh[1], Keiji Yoshikawa[2], Shumpei Ogawa[3], Tomoyuki Watanabe[1], Sachiyo Okude[1], Tadashi Nakano[1]

[1]Department of Ophthalmology, Jikei university school of medicine, Japan, [2]Yoshikawa Ophthalmic Clinic, [3]Atsugi City Hospital

Purpose:
Glaucomatous optic disk is characterized by a thinning of the rim and impairment of the retinal nerve fiber layer(NFL). Both features provide a highly accurate evaluation and definition of the boundary of the Bruch membrane opening(BMO) of the optic disk.This study aimed to analyze the relationship between spectral domain optical coherence tomography(SD OCT) derived minimum rim width(MRW) and nerve fiber layer thickness(NFLT), in normal tension glaucoma(NTG).

METHODS:
The study included 94 eyes in 94 patients with NTG that satisfied the following criteria, intraocular pressure, 10–20 mmHg during the follow up period, corrected visual acuity ≥ 0.7; refraction ≥ -6D, glaucomatous visual field defect judged by Anderson ´ s criteria "Humphrey field analyzer, SITA standard, C 24–2 program " mean deviation (MD), 0– -12 dB. The patients underwent optic nerve head(ONH) and NFL imaging with SD OCT (Spectralis 2, Heidelbrg). The minimum rim width at Bruch ´ s membrane opening (BMO–MRW) and NFLT were calculated in each of the 6 areas according to ONH classification chart system applying GMPE software. The correlation between MRW and NFLT was examined in the 6 areas of the classification chart. We also stratified the groups based on the MD value as, MD ≥ -3dB, -3dB > MD ≥ -6dB, -6dB > MD, the difference of MRW-NFLT was compared and examined in the 6 regions.

RESULTS:
The correlation coefficients between MRW and NFLT were r:0.570, r:0.723, r:0.817, r:0.234, r:0.380, r:0.500 in the temporal(T), temporal upper(TS), temporal lower(TI), nasal(N), nasal upper(NS) and nasal lower(NI) areas, respectively (Spearman ´ s correlation coefficient). Correlation was better on the temporal area than on the nasal area.In the analysis of MRW-NFLT, significant differences were observed only in the T, TS, and TI of the two groups MD ≤ -3dB and -6dB > MD, and the value of MRW-NFLT was lower in the -6dB > MD group than in the MD >-3dB group.

Conclusions:
In this study, thinning of optic disc rim width was apparent as compared to the degree of impairment of NFL, in particular , in the early stage NTG eyes. SD OCT derived MRW thought to be useful in quantitative assessment of the optic disc damage in NTG eyes.

Conflict of Interest: No, I don't. **Ethics Committee Approval:** Yes, I have obtained **Informed Consent:** Yes, I have obtained

P1-7

Detection of early glaucomatous damage of the macula with OCT oriented perimetry in preperimetric glaucoma

Shinji Ohkubo[1], Sachiko Udagawa[1], Tomomi Higashide[1], Aiko Iwase[2], Kazutaka Kani[3], Satoshi Shimada[4], Kazuhisa Sugiyama[1]

[1]Department of Ophthalmology and Visual Science, Kanazawa University Graduate School of Medical Science, Japan, [2]Tajimi Iwase Eye Clinic, [3]Kyushu University of Health and Welfare, [4]Kowa Company, Ltd

Purpose: To evaluate the optical coherent tomography (OCT) oriented perimetry with adjusting for retinal ganglion cell (RGC) displacement (Kowa AP –7700), for the ability of the detection of glaucomatous visual field abnormalities in eyes with macula damage and with normal standard automated perimetry(preperimetric glaucoma (PPG) with macula damage).

Methods: Fourteen eyes of 13 PPG subjects who had glaucomatous optic disc abnormalities with localized retinal nerve fiber layer defect (RNFLD) in lower hemi–retina were included in this study (59.1 ± 8.6 years). None of reliable SAP results showed glaucomatous visual field (VF) defects, which were determined according to Anderson ´s criteria. All subjects had complete ophthalmic examinations including 10–2 VF and OCT. The 10–2 VFs were classified as abnormal if there was a cluster of 3 contiguous points (5%, 5%, 1% or 5%, 2%, 2%) within a hemifield on pattern deviation (PD) plots. The macular damage were confirmed by OCT macula scans (9 × 9mm, RS–3000 advanced). The ganglion cell complex (GCC) map was superimposed to fundus photograph and the perimetry was conducted using the superimposed GCC map presented upside–down automatically corresponding to visual field. The examiner should arrange the image by pointing to the fovea and the center of the optic disc. The test points of 10 –2 was superimposed the integrated GCC map and the location of test points were adjusted for RGC displacement. We selected 34 test points from approximately upper hemifield of 10–2. The 2°grid pattern outside 10°(28 test points) and the grid pattern with double density of 10 –2 (10 test points) were added corresponding to GCC thinning. We selected in total fixed 72 test points. We evaluated focal PD (FPD) and diagnosed according to the following criteria: having a cluster of three or more points with p<5% and at least one point with p<1% corresponding to GCC thinning area. We also evaluate percentage of test points of FPD probability plots of P<5%, p<1%, p<0.5% at each test point location.

Results: Three among 14 (21.4%) eyes on 10 –2 VF revealed abnormal. The sensitivity of FPD of OCT oriented perimetry was 100% (14/14). The number of test point locations of over 50% of eyes that had FPD probability plots of P<5%, p<1% and p<0.5% were 9, 4 and 2, respectively.

Conclusions: The OCT oriented perimetry with adjusting for RGC displacement and FPD were useful for evaluation of PPG with GCC thinning. This study shows vulnerable points of VF for PPG.

Conflict of Interest: Yes, I have. **Ethics Committee Approval:** Yes, I have obtained **Informed Consent:** Yes, I have obtained

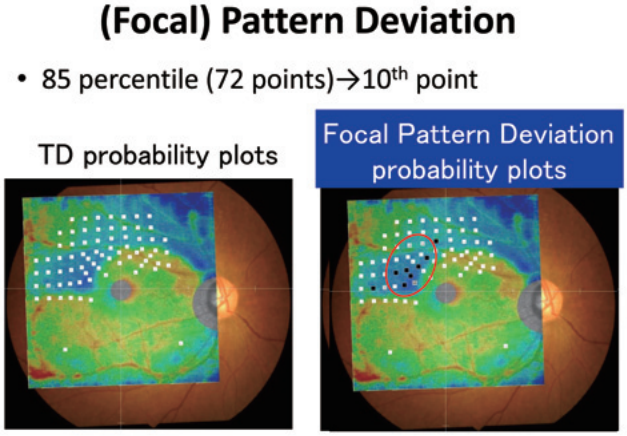

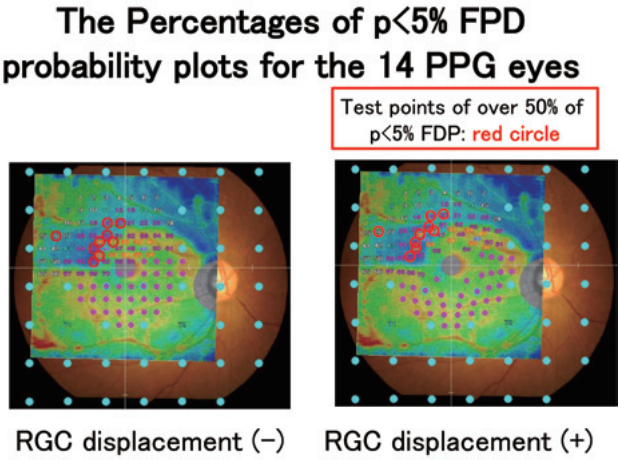

P2-1

Retinal layer segmentation and clustering by spectral-domain optical coherent tomography in patient with open angle glaucoma

Shumpei Ogawa[1,2], Keiji Yoshikawa[2,3], Yoshinori Itoh[2], Yoshimasa Tanabe[2], Tadashi Nakano[2]

[1]Department of Ophthalmology, Atsugi city hospital, Japan, [2]The Jikei University School of Medicine, [3]Yoshikawa eye clinic

Purpose: The purpose of this study was to segment retina into six intra-retinal layers in patient with open angle glaucoma (OAG; normal tension glaucoma and primary open angle glaucoma) and to cluster the macular areas in each intra-retinal layer.

Methods: The study included 86 eyes of 86 OAG patients. Macular retinal nerve fiber layer (mRNFL), ganglion cell layer (GCL), inner plexiform layer (IPL), inner nuclear layer (INL), outer plexiform layer (OPL) and outer nuclear layer (ONL) were automatically segmented with spectral-domain OCT (Posterior pole retinal thickness; Spectralis 2, Heidelberg). The region of interest was centered on the fovea and layer thickness was measured at each point on 8 by 8 grids (a grid has 3 by 3 degrees square). Explanatory factor analysis (EVA) was performed to cluster grids in each layer into a smaller number of clusters. The correlations between the grids in each layer and the 24 cpRNFLT sectors were evaluated by Pearson correlation analysis.

Results: At least 3 areas including upper and lower hemisphere and papillomacular nerve fiber bundle (PNFB) were identified and number of grids highly correlated with specific cpRNFLT sectors in mRNFL and GCL, whereas in IPL EVA identified no horizontal boundary and PNFB correlated with several temporal cpRNFLT sectors ($p < 0.01$).

Conclusion: Glaucomatous retinal damage in mRNFL, GCL and IPL could be clustered by posterior pole retinal thickness, but not in INL, OPL, and ONL. Topological IPL damage by glaucoma was different from mRNFL and GCL.

Conflict of Interest: No, I don't. **Ethics Committee Approval:** Yes, I have obtained **Informed Consent:** Yes, I have obtained

P2-2

The effects of magnification correction or matching of axial length in normative database on early glaucoma detection by ganglion cell complex in eyes with long axial length

Tomomi Higashide, Sachiko Udagawa, Shinji Ohkubo, Kazuhisa Sugiyama

Department of Ophthalmology and Visual Science, Kanazawa University, Japan

Purpose: To investigate the effects of using normative databases (NDBs) with magnification correction (MC) or those with matching the axial length on diagnostic ability of macular ganglion cell complex (GCC) for identifying early glaucoma in eyes with a long axial length.

Materials and Methods: The study involved 56 eyes from 56 patients with primary open angle glaucoma and 46 healthy eyes from 46 subjects. All eyes had an axial length ≥ 26 mm. The glaucomatous eyes including those in the preperimetric status had structural abnormalities compatible with glaucoma in the optic disc and a MD > -6 dB in Humphrey 24-2 visual fields. The GCC in the macular area (6-mm nominal diameter) was measured with a spectral-domain optical coherence tomography (RS-3000, NIDEK) and compared with an ordinary normative database (ONDB, spherical equivalen ≥ -6D) or a normative database for long axial length (LANDB,≥ 26 mm). Both NDBs were constructed with or without MC using the Bennett formula and the study eyes were tested against NDBs in the matched condition regarding MC. The eyes having GCC thickness below the lower 95th percentile in at least one of 10 regions of GCC measurement area were diagnosed as glaucoma.

Results: Using ONDB without MC, sensitivity and specificity were 92.9% and 60.9%, respectively. Using ONDB with MC, sensitivity and specificity were 83.9% and 76.1%, respectively. Using LANDB without MC, sensitivity and specificity were 82.1% and 87.0%, respectively. Using LANDB with MC, sensitivity and specificity were 82.1% and 82.6%, respectively.

Conclusion: MC and LANDB were both effective for increasing specificity for detecting early glaucoma in eyes with a long axial length. However, MC for LANDB did not further improve the specificity.

Conflict of Interest: No, I don't. **Ethics Committee Approval:** Yes, I have obtained **Informed Consent:** Yes, I have obtained

P2-3

Capability of asymmetry in macular ganglion cell layer/inner plexiform layer thickness by optical coherence tomography to detect preperimetric glaucoma.

Daisuke Takemoto[1], Shinji Ohkubo[1,2], Sachiko Udagawa[1], Tomomi Higashide[1], Kazuhisa Sugiyama[1]

[1]Department of Ophthalmology, Kanazawa University Graduate School of Medical Science, Japan, [2]Ohkubo Eye Clinic

Purpose: We assessed the ability of asymmetry in macular ganglion cell layer/inner plexiform layer (GCL/IPL) thickness by spectral-domain optical coherence tomography (SD-OCT), to detect preperimetric glaucoma (PPG).

Materials and Methods: We enrolled 20 normal eyes and 50 PPG eyes who were imaged using SD-OCT (3D OCT-2000, Topcon, Tokyo, Japan). PPG was defines by the existence of glaucomatous optic neuropathy (using fundus photograph) and no visual field defect (using Humphrey Field Analyzer 24-2 program) during the course. Three-dimensional OCT scans were acquired from each eye, then the thickness of the GCL/IPL were obtained within a 6.0 × 6.0 mm macular area divided into 10 × 10 grids of 600 × 600 μm superpixels. We calculated the thickness differences between the upper and lower macula halves of the subject eyes for each of the corresponding superpixels in 6 × 8 girds centered on the foveal pit, then evaluated the mean absolute value of the thickness differences and the number of superpixels in which the thickness difference was greater than or equal to 7μm (Lee, et al. 2016 PLoS One). These two parameters (= asymmetry parameters) were compared to the average GCL/IPL thickness measurement of total and hemiretinal sectors or cluster criteria (Kanamori et al. 2013 IOVS) with the area under receiver operating characteristic (ROC) curves and specificity/sensitivity values.

Result: The mean absolute value of the asymmetry thickness differences of GCL/IPL of PPG eyes was significantly larger than that of normal eyes (8.12 ± 4.03 μm and 3.17 ± 0.72 μm, $P < 0.001$). The number of superpixels in which the thickness difference ≥ 7 μm of PPG patients was significantly larger than that of normal eyes (10.0 ± 4.8 and 2.6 ± 1.9, $P < 0.001$). The area under ROC curves (AUC) for the absolute value of the asymmetry thickness differences was 0.950 (95% confidence interval (CI): 0.877-0.981), and the AUC for the number of superpixels in which the thickness difference ≥ 7 μm was 0.922 (95% CI: 0.837-0.964). The abilities to detect PPG of these asymmetry parameters were higher than of total or hemiretinal GCL/IPL measurements. Using ROC-based cut-off criterion of these two asymmetry parameters, if the specificity values were both 90%, sensitivity values were 90% and 84%, respectively. On the other hand, the specificity and sensitivity values of cluster criteria were 90% and 64%, respectively.

Conclusion: Evaluation of asymmetry in macular GCL/IPL thickness may be useful in the early detection of glaucoma.

Conflict of Interest: No, I don't. **Ethics Committee Approval:** Yes, I have obtained **Informed Consent:** Yes, I have obtained

P2-4

Blood flow changes after trabeculectomy in and around the optic disc and the macula

Makoto Sasaki, Tomomi Higashide, Yoshimi Oshima, Satoshi Takeshima, Sachiko Udagawa, Kazuhisa Sugiyama

Department of Ophthalmology, Kanazawa University, Japan

Purpose:
To examine blood flow changes in the optic disc, peripapillary region and the macula after trabeculectomy (TLE).

Materials and Methods:
Thirty-two POAG eyes from 29 subjects that underwent trabeculectomy at Kanazawa University Hospital were enrolled. Mean blur rate in tissue in the optic disc (D-MT) and in a peripapillary region (PP-MT) and Mean blur rate of total area in the macula(M-MA) were measured using laser speckle flowgraphy (LSFG) before and 1, 3 and 6 months after TLE. PP-MT was measured in the circumpapillary region 75 pixels wide from the optic disc margin. The change of each blood flow parameter over time and the relationship between parameters were analyzed using the mixed-effects models.

Results:
The intraocular pressure decreased significantly at all time points after TLE(from 18.8 ± 0.72 to 10.5 ± 0.75, 9.2 ± 0.72, 8.6 ± 0.60 ; all $p<0.001$).Ocular perfusion pressure increased significantly at all time points after TLE (from 39.8 ± 1.6 to 52.6 ± 1.8, 52.5 ± 2.0, 54.1 ± 1.9 ; all $p<0.001$). D-MT decreased significantly at all time points after TLE (from 8.9 ± 0.38 to 8.4 ± 0.38, 8.3 ± 0.38, 8.4 ± 0.36; all $p<0.03$). PP-MT did not change significantly at all time points after TLE (from 6.2 ± 0.20 to 6.3 ± 0.20, 6.3 ± 0.20, 6.3 ± 0.18; all $P>0.05$). M-MA increased significantly at all points after TLE (from 9.7 ± 0.74 to 11.6 ± 0.73, 11.2 ± 0.68, 10.7 ± 0.61; all $p<0.01$). The change of PP-MT from the baseline was significantly correlated with that of D-MT (coef.= 0.59, $p=0.001$) and M-MA (coef.= 0.62, $p=0.002$). The change of M-MA from the baseline did not significantly correlate with that of D-MT.

Conclusions:
Although the blood flow change after TLE over time in the peripapillary region was different from that in the optic disc, the peripapillary change significantly correlated with that in the optic disc and in the macula.

Conflict of Interest: No, I don't. **Ethics Committee Approval:** Yes, I have obtained **Informed Consent:** Yes, I have obtained

P2-5

Correlation between optic disc vessel density and glaucoma severity : enhanced-depth imaging optical coherence tomography angiography study

Yuji Yoshikawa[1], Takuhei Shoji[1], Junji Kanno[1], Itaru Kimura[1], Masanori Hangai[2], Kei Shinoda[1]

[1]Department of Ophthalmology, Saitama Medical University Hospital, Japan, [2]HANGAI EYE INSTITUTE

Purpose: To evaluate correlation between optic disc vessel density (disc VD) measured using enhanced depth imaging (EDI) optical coherence tomography angiography (OCTA) and glaucoma severity.Subjects and method : 10 glaucomatous eyes of 8 patients and 11 non-glaucomatous eyes of 7 subjects underwent EDI-OCTA and conventional OCTA examinations with Spectral-Domain OCTA (RS3000 Advance, Nidek Co., Ltd) for optic nerve head (ONH) imaging. The disc VD measurements were compared between the two methods and between glaucomatous and non-glaucomatous eyes. Multiple regression analysis was used to determine factors that affected disc VD and to evaluate the correlation value between disc VD and mean deviation (MD) values.

Results: The disc VD was significantly lower in eyes with glaucoma than without glaucoma (p=0.029 for conventional and p=0.014 for EDI). The disc VD and MD value were significantly and positively correlated for both measurement methods (R2=0.27, p=0.020 for Conventional and R2=0.22, p=0.015 for EDI). Multiple regression analysis also showed a significant correlation between disc VD and MD values (B=0.30, p=0.018 for conventional and B=0.25, p=0.018 for EDI).

Conclusions: There was significant correlation between disc VD and glaucoma severity. MD value was only factor that affected disc VD. The correlation coefficient value was comparable between conventional and EDI measurements. The disc VD may be useful for monitoring glaucoma severity.

Conflict of Interest: No, I don't. **Ethics Committee Approval:** Yes, I have obtained **Informed Consent:** Yes, I have obtained

P2-6

Relationship between Optical Coherence Tomography Angiography (OCTA) macular vessel density and visual field loss in glaucoma

Yusuke Nakatani[1,2], Tomomi Higashide[1], Shinji Ohkubo[1,3], Kazuhisa Sugiyama[1]

[1]Department of Ophthalmology, Kanazawa University, Graduate School of Medical Sciences, Japan, [2]Himi Nakatani Eye Clinic, [3]Ohkubo Eye Clinic

Purpose: To evaluate the association between the macular vessel density (mVD) and Humphrey visual field (HVF) loss in primary open-angle glaucoma.

Materials and Methods: One hundred and six eyes from 77 glaucoma patients were studied (mean patient age: 69.7 ± 10.1 years; HFA30－2 mean deviation: -10.5 ± 7.3 dB). All eyes underwent 6 × 6 mm OCTA (Angioplex) scan, 6 × 6 mm SD-OCT (RS-3000) scan and 10－2 HVF. Macular VD was calculated at the macular superficial layer. Regional relationships between the mVD, ganglion cell complex (GCC), and 10－2 HVF were compared in 8 regions based on Early Treatment of Diabetic Retinopathy Study (ETDRS) sectors, excluding the fovea.

Results: Between the mVD and the GCC, a significant correlation was seen, except in the outer temporal and inner nasal regions. The association between the mean 10－2 HVF sensitivity (HFA10－2 total deviation) and the mean mVD was similar to the association between the mean 10－2 HVF and the GCC in both the linear and quadratic models (linear:R^2=0.29 and 0.34, quadratic: R^2=0.29 and 0.41, respectively). The regional relationship of the 10－2 HVF sensitivity to the mVD and the GCC was highest in the outer inferior region (R^2=0.32 and 0.45, quadratic model).In a comparison of best fit models of the relationship of the mVD and the GCC to 10－2 HVF, no significant difference was found between the linear and quadratic models in all sectors, whereas, three sectors showed large relationship in the mVD sectors with the quadratic model. In contrast, all sectors showed large relationship in the GCC sectors with the quadratic model. Multivariate regression analysis, adjusted for confounders, showed that each 1% decrease in the mVD was associated with a 1.49 dB loss in 10－2 HVF mean deviation.

Conclusions: For structure-function relationships by OCTA, the mVD was significantly associated with central visual field loss and showed comparable associations with GCC parameters in glaucoma. The linear model may be compatible in association between the mVD and central visual field loss.

Conflict of Interest: No, I don't. **Ethics Committee Approval:** Yes, I have obtained **Informed Consent:** Yes, I have obtained

P2-7

The association between glaucomatous visual field defect, foveal avascular zone area and vessel density using swept-source optical coherence tomography angiography

Yosuke Miyasaka, Yuji Yoshikawa, Takuhei Shoji, Junji Kanno, Hisashi Ibuki, Hirokazu Ishii, Kimitake Ozaki, Tadashi Akiyama, Itaru Kimura, Kei Shinoda

Department of Ophthalmology, Saitama Medical University Hospital, Japan

Purpose:
To investigate the association between glaucomatous visual field defect, foveal avascular zone (FAZ) area and vessel density using swept-source optical coherence tomography angiography (SS-OCTA).

Methods:
Twelve eyes from nine glaucoma patients and twelve eyes from twelve healthy control subjects were included in this study and went through comprehensive eye examinations, including visual acuity, axial length, intraocular pressure, spherical equivalent (SE) and mean deviation (MD) with Humphrey Visual Analyzer (HFA, Carl-Zeiss, CA). The all participants also underwent SS-OCTA (Triton®, Topcon, Japan) analysis and FAZ area and vessel density from OCTA scans centered on the disc and fovea were measured by image J software. To determine the factors that affected the MD value, univariate and multivariate analyses were conducted in this study.

Results:
There were statistically significant differences in age, best corrected visual acuity (BCVA) and MD value between glaucoma and healthy control group. Compared with normal healthy control subjects, the value of FAZ area was significantly higher and vessel density in disc area was significantly lower in glaucoma eyes; 0.40mm^2 (0.33 – 0.55) (median [quartile]) and 0.31mm^2 (0.23 – 0.40) (P = 0.04) for FAZ area, 49.7% (45.9 – 56.0) and 58.7 (57.0 - 60.4) ($p<0.01$) for vessel density in disc area. In contrast, vessel density in macula area was comparable between glaucoma and healthy eyes; 48.4% (45.5 – 51.3) and 50.4 (48.7 – 51.2) ($p=0.29$). Under the multivariate analysis, FAZ area was negatively correlated with MD (β =-22.9, $p=0.04$) and vessel density in disc area was positively correlated with MD (β =0.93, $p<0.01$).

Conclusion:
FAZ area and vessel density in disc area measured with SS-OCTA were significantly different from those in control and correlated with MD value using Humphry perimetry. These parameters might be useful to diagnose and estimate the severity of glaucoma.

Keywords:
glaucoma, optical coherence tomography angiography, vessel density, foveal avascular zone

Conflict of Interest: No, I don't. **Ethics Committee Approval:** Yes, I have obtained **Informed Consent:** Yes, I have obtained

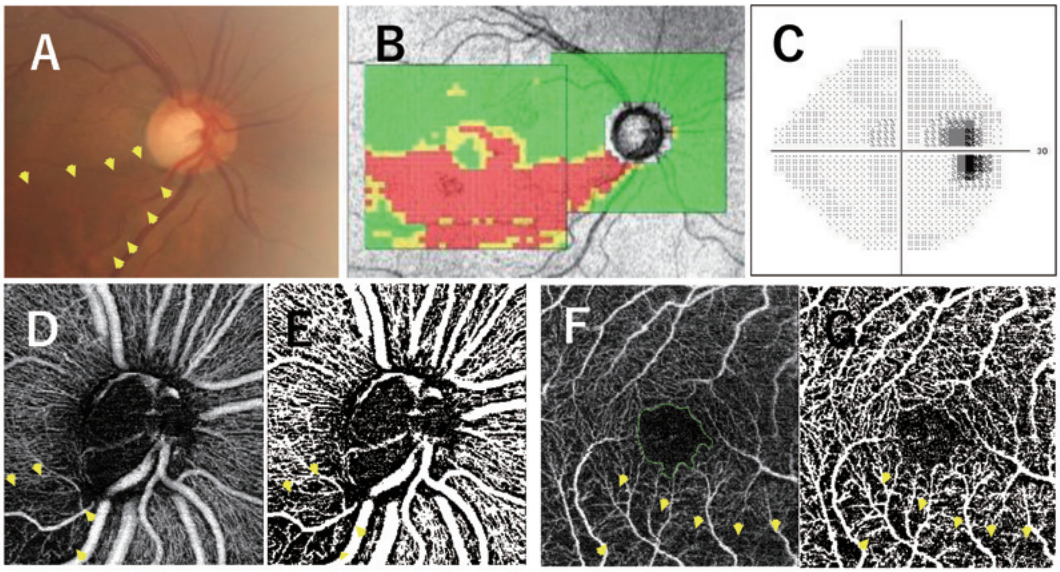

Figure 1 Glaucomatous optic neuropathy and nerve fiber layer defect (yellow arrow) were visible with fundus photograph. (A) OCT glaucoma analysis showed thinning of retinal nerve fiber layer (RNFL) in circumpapillary area and ganglion cell layer (GCL) in macular area, in accordance with visual field defect. (B, C)
SS-OCTA image (D, F) and these binarization image with Phansalkar method (E,G) showed vessel signal defects in RNFL and GCL thinning areas. (yellow arrow)

P2-8

The association between change of radial peripapillary capillaries and disc hemorrhage occurrence in normal tension glaucoma

Koji Nitta[1,2], Kazuhisa Sugiyama[2], Ryotaro Wajima[2], Gaku Tachibana[1,2], Yutaro Yamada[1,2]

[1]Department of Ophthalmology, Fukuiken Saiseikai Hospital, Japan, [2]University of Kanazawa

Purpose: In order to clarify the association between peripapillary vascular change and disc hemorrhage (DH) occurrence over time, we analyzed the density of radial peripapillary capillaries (RPC) and visual field parameters more than twice during follow-up periods in normal tension glaucoma (NTG).

Methods: Ninety-four eyes of 85 patients were subjected to analysis. We selected cases in 2015 initially having OCT angiography (OCTA) and took another OCTA again in 2017. Both OCTAs showed good quality images. In the period between the initial and final OCTA, we divided the fundus into superior or inferior sides and examined the sides with DH, sides with previous DH history and sides without DH. We investigated the relationship between the RPC, the circumpapillary retinal nerve fiber thickness (cpRNFLT), the ganglion cell complex (GCC), total deviation (TD) slope and the DH occurrence, and we evaluated the usefulness of OCTA in NTG.

Results: In that period, we detected DHs with 41 sides. The cpRNFLT of the sides with DH became significantly thinner between the three groups (DH sides; -3.32 ± 7.54 μ m, previous DH sides; 2.48 ± 8.35 μ m, non-DH sides; 3.07 ± 7.82 μ m, respectively. p=0.0003). The GCC of sides with DH became significantly thinner between the three groups (DH sides; -1.98 ± 2.77 μ m, previous DH sides; -0.54 ± 2.77 μ m, non-DH sides; -0.50 ± 2.70 μ m, respectively. p=0.0032). The vessel density of RPC in sides with DH decreased significantly between the three groups (DH sides; -4.54 ± 5.20%, previous DH sides; -1.09 ± 5.15%, non-DH sides; -1.05 ± 4.95%, respectively. p=0.0005). Otherwise, the TD slope of the visual fields of sides with previous DH history became significantly faster between the three groups (DH sides; -0.29 ± 0.49dB/y, previous DH sides; -0.62 ± 0.59dB/y, non-DH sides; -0.08 ± 0.39dB/y, respectively. p=0.0001).

Conclusion: The occurrence of DH may prompt the structural and vascular deterioration of NTG and the previous DH history may accelerate the functional progression of NTG.

Conflict of Interest: Yes, I have. **Ethics Committee Approval:** Yes, I have obtained **Informed Consent:** Not Applicable

P2-9

Deep-layer microvasculature dropout in glaucoma

Kimikazu Sakaguchi, Tomomi Higashide, Shinji Ohkubo, Sachiko Udagawa, Kazuhisa Sugiyama

Department of Ophthalmology, Kanazawa University, Japan

Purpose: To investigate the frequency and characteristics of deep-layer microvasculature dropout (MvD) in glaucomatous or normal eyes using Optical Coherence Tomography Angiography (OCTA).

Material and methods: One hundred and twenty nine eyes from 129 subjects (primary open angle glaucoma; POAG 94 eyes, glaucoma suspects; GS 17 eyes, and normal 18 eyes, male: female = 67: 62) were recruited. Patients with diseases other than glaucoma and diseases in optic pathways and/or subjects with past history of intraocular surgery were excluded. The vessel density map in the choroid layer of OCTA (AngioVue/RTVue-XR) was divided into 6 sectors based on the structure-function correspondence map according to Garway-Heath et al. Subsequently, the frequency and size of MvD were evaluated. To determine factors affecting MvD, multiple regression analysis was performed using the following parameters as independent variables; age, sex, axial length, signal strength index of OCTA, visual field sensitivity (average TD value), peripapillary chorioretinal atrophy (PPA), retinal nerve fiber layer (RNFL) vascular density, and circumpapillary RNFL thickness.

Results: MvD was observed in 56 eyes (60%) of POAG, but only 1 eye (6%) in GS, not in normal group. In sectoral analysis, MvD was the most frequently observed in the inferior temporal (42 eyes, 33%). MvD was the largest in temporal area (1.00 ± 0.12% in area ratio to the whole OCTA measurement area). In the multiple regression analysis, MvD was larger as the average TD value was lower in all 6 regions (β = -0.681 to -0.193, p <0.001 to p = 0.035). In the inferior temporal area, the larger the β and γ PPA, the larger MvD was (β = 0.257, 0.154; p <0.001, p = 0.032). In the temporal area, MvD was larger, when the larger the PPA (β = 0.288, p <0.001), the thinner the circumpapillary RNFL thickness (β = - 0.240, p = 0.006).

Conclusion: MvD is a specific structural change in glaucomatous eyes and showed significant correlation with visual sensitivity in all sectors.

Conflict of Interest: No, I don't. **Ethics Committee Approval:** Yes, I have obtained **Informed Consent:** Yes, I have obtained

P3-1

Visual field changes after vitrectomy for epiretinal membranes in glaucomatous eyes

Shunsuke Tsuchiya, Tomomi Higashide, Sachiko Udagawa, Kazuhisa Sugiyama

Department of Ophthalmology, Kanazawa University Graduate School of Medicine, Japan

This partially retrospective cohort study consists of consecutive cases with or without glaucoma who underwent vitrectomy with ILM peeling for ERM. Humphrey 10-2 VF tests were performed preoperatively and three times at about 3, 6, and 12 months postoperatively. Main outcome measures were; longitudinal changes in VF parameters and mean total deviation (TD) changes in 6 VF sectors (i.e. superior outer arcuate, superior inner arcuate, superior cecocentral, inferior outer arcuate, inferior inner arcuate, and inferior cecocentral) analyzed with mixed-effects models.

Results: Sixty-two eyes from 62 patients were enrolled (control, 33 eyes; glaucoma, 29 eyes). Baseline 10-2 MD values in the glaucoma and the control groups were -7.5 ± 0.9 dB and -1.9 ± 0.2 dB, respectively. In the glaucoma group, MD and pattern standard deviation significantly worsened postoperatively ($P<0.001$) while they did not in the control group. In both groups, best-corrected visual acuity was significantly improved ($P <0.001$). In the control group, none of 6 sectors showed significant changes after vitrectomy. Nevertheless, in the glaucoma group, the superior outer arcuate sector showed a significant decrease in the mean TD after surgery at all the follow-up visits ($P = 0.015$, 0.009, and 0.003 at 1st, 2nd and 3rd sessions, respectively). In addition, the inferior outer arcuate sector showed a significant TD decrease at the 1st and 3rd follow-up sessions ($P <0.001$, 0.129, and 0.042 at 1st, 2nd and 3rd sessions, respectively). The mean TD values in the other 4 sectors were stable during the follow-up periods in the glaucoma group.

Conclusions: VF parameters significantly deteriorated after surgery only in the glaucomatous eyes. In glaucoma patients, VF sector analysis revealed that sectors located in the outer temporal arcuate area showed significant worsening while VF sectors in the papillo-macular bundle area (superior and inferior cecocentral sectors) remained stable.

Conflict of Interest: No, I don't. **Ethics Committee Approval:** Yes, I have obtained **Informed Consent:** Yes, I have obtained

P3-2

Usefulness of Clock Chart Driving Edition for self-checking the binocular visual field

Marika Yamashita, Chota Matsumoto, Shigeki Hashimoto, Sachiko Okuyama, Hiroki Nomoto, Fumi Tanabe, Mariko Eura, Tomoyasu Kayazawa, Takuya Numata, Yoshikazu Shimomura

Department of Ophthalmology, Kindai University Faculty of Medicine, Japan

Purpose: We explored sensitivity and reproducibility of a simplified self-checking sheet for detecting the binocular visual field (VF) that is named CLOCK CHART Driving Edition (CLOCK CHART DE).Subjects and Methods: The CLOCK CHART DE has 4 targets arranged at the eccentricity 10° , 15° , 20° , and 25° . By rotating the CHART through a 360° turn, the subject comes to realize the VF defect by themselves. This study enrolled 67 cases of glaucoma (37 males, 30 females, mean age, 62.7 ± 11.5 yo) and sensitivity was calculated using CLOCK CHART DE and HFA SITA-Standard 30-2. Binocular VF was formed using IVF (Integrated VF). When 2 or more continuous scotomas less than 10 dB were detected within 30 ° , the subject was diagnosed with VF defects. Stages of glaucoma was classiffied (using both eyes) binocularly by counting the number of response points that are 10 dB or higher of the 76 points in IVF. In this study, 55 subjects (82%) showed 76 to 57 response points; 12 subjects (18%), 56 to 37 points; and no subjects showed lower than 37.To explore reproducibility of VF, 39 cases of the 67 were tested employing 2 methods to measure VF defects: 1) the self-check method in which the subjects themselves turned the sheet and 2) the supported method in which the examiner helped the patient in rotating the sheet. These 2 methods were performed 3 times for each method, totaling 6 times for each subject.

Results: Sensitivity of CLOCK CHART DE was 81% and that at the eccentricity 10° , 15° , 20° , and 25° was 73%, 68%, 69%, and 74%, respectively.Presence of reproducibility CLOCK CHART DE was confirmed when the same results were obtained from 3 measurements. Reproducibility of CLOCK CHART DE was 95% (self-check) and 90% (supported). For the superior hemifield, reproducibility was 95% (self-check) and 90% (supported). For the inferior hemifield, reproducibility was 85% (self-check) and 90% (supported).

Conclusions: CLOCK CHART DE showed less variability according to the eccentricity. It is also confirmed to have high reproducibility for both self-check and supported methods.

Conflict of Interest: Yes, I have. **Ethics Committee Approval:** Yes, I have obtained **Informed Consent:** Yes, I have obtained

P3-3

Perimetry for Children or Mentally Handicapped

Fritz Dannheim[1], Dagmar I. Verlohr[1,2], Harald Wohlgemuth[1,3]

[1]Ophthalmology Outpatient Unit Hittfeld, Germany, [2]Neurological Rehabilitation Clinic, 21226 Jesteburg, [3]Asklepios Clinic Barmbek, 22307 Hamburg

Purpose: Development and evaluation of a perimeter for patients with insufficient cooperation for standard automated perimetry (SAP).

Materials and Methods: Our handmade Manual Saccadic Perimeter (MSP) consists of a plate with a hole in the center through which the examiner watches the eye of the patient who is sitting in front of him. This method resembles visual acuity testing of children by preferential looking. He now can stimulate one of 8 LEDs, placed on the diagonals with an eccentricity of 45 and 35 or 22 and 16 degrees (distance to the patient 20 or 50 cm). The patient is asked to watch the examiner's retro illuminated eye in the central hole. After a signal he shall look immediately to the place where a bright object had flashed for 300ms. A fast correct saccade is recorded as perception, otherwise as defect. Screening may be carried out in 2 brightness levels, monocular or binocular, depending on the clinical question (diagnosis or degree of handicap). After each stimulus and reaction, the patient is asked to fixate the examiner's eye again until the next stimulation.

Results: The screening has been performed on 64 adult patients with limited cooperation for SAP, two third due to cerebral diseases with mental disorders or lesions of the central visual pathways, one third with peripheral lesions like ischemic optic atrophy, retinopathia pigmentosa or optic neuritis, and on a few children between 4 and 6 years of age. In the majority the results of the MSP was reliably better than a trial with SAP. About one half of patients had no relevant defects with MSP, the others had some constrictions fitting to their clinical condition. Some patients were not able to perform saccades, seldom caused by paralysis, more often due to mental problems. Most of them were able to show the correct direction of a surely perceived stimulus by hand or describe it, identically useful. In children a game design of the procedure made it even easier, with a laptop for the management and observation of the patient's reaction by a mirrored webcam image and a separate screen for the patient. We did not apply automated eye tracking, however, since this turned out as not flexible enough for limited cooperation.

Conclusions: The MSP turned out to be very helpful in problematic clinical cases when conventional perimetric methods failed or were not reliable. The advantage of this method lies mostly in the possibility to adapt the examination individually to the patient's cognitive and mobile state.DisclosureThere is no conflict of interest to be disclosed.

Conflict of Interest: No, I don't. **Ethics Committee Approval:** Not Applicable **Informed Consent:** Not Applicable

P3-4

Assessment of response reliability in visual field testing without using catch trials

Sachiko Okuyama[1], Chota Matsumoto[1], Hiroki Nomoto[1], Tairo Kimura[2], Keiji Yoshikawa[3], Shiro Mizoue[4], Mami Nanno[5], Shinji Kimura[6], Satoshi Inoue[6], Yoshikazu Shimomura[1]

[1]Department of Ophthalmology, Kindai University, Japan, [2]Ueno Eye Clinic, [3]Yoshikawa Eye Clinic, [4]Ehime University, [5]Kagurazaka Minamino Eye Clinic, [6]CREWT Medical Systems, Inc.

Purpose: Establish a method for assessment of response reliability in visual field (VF) testing without using false-positive (FP) and false-negative (FN) catch trials.

Materials and Methods: A total of 2598 VFs obtained with the head-mounted perimeter "imo" and the ambient interactive ZEST (AIZE) strategy from 2598 eyes of 1477 subjects were analyzed retrospectively. In order to clarify a range of reaction time (RT) in which the response is regarded as FP, we examined the RT distribution of all 332601 responses, the RT distribution of all 1861 responses for FP catch trials, and the relationship of the difference between stimulus intensity and measured VF sensitivity value (VA) to the range of RT. No-responses to the stimuli which were more than a certain intensity (A) than VA were regarded as FNs. While changing the number of A, the distribution of this FN ratio, the correlation of this FN ratio to the FN ratio obtained by catch trials, and the effect of excluding test points with low VA were examined.

Results: The average[SD, range] of mean deviation, FP and FN obtained by catch trials in our VFs were -5.5[6.8, -31.4 - 1.6]dB, 6.3[10.7, 0.0 - 100]% and 8.6[14.1, 0.0 - 100]% respectively. In all of the responses, the frequency of RT less than 300 msec (RT<300msec) was constantly low, and the ratio of RT<300msec was 2.4%. In all of the responses for FP catch trials, the RT frequency was not depend on RT, and the ratio of RT<300msec was 21.7%. The responses with RT<300msec could be regarded as FPs. The average of the ratio of RT<300msec for each VF was 2.5[SD: 3.4]% and the VFs with that ratio more than 10% were 3.7% in all VFs. Under excluding the test points with VA less than 10dB, the ratio of no-responses to 2dB brighter or more blight stimuli than VA averaged 3.1[SD: 3.5]% and it had a high correlation with the FN ratio obtained by catch trials. The VFs with that FN ratio more than 12% were 2.9% in all VFs.

Conclusions: The response reliability in the VF testing can be assessed without catch trials by using both the ratio of RTs<300msec and the ratio of no-responses to the stimuli, which are 2dB blighter or more blight than the VAs and are presented at the test points with VAs equal or greater than 10dB.

Conflict of Interest: Yes, I have. **Ethics Committee Approval:** Yes, I have obtained **Informed Consent:** Yes, I have obtained

P3-5

Influence of Head tilted angle on Blind Spot location in Visual Field Test

Fumi Tanabe, Chota Matsumoto, Sachiko Okuyama, Shigeki Hashimoto, Hiroki Nomoto, Tomoyasu Kayazawa, Takuya Numata, Marika Ishibashi, Yoshikazu Shimomura

Department of Ophthalmology, Kindai University Faculty of Medicine, Japan

Purpose: To investigate variation head tilt angle during the visual field testing, and whether this affects structure-function correlation in the assessment of glaucoma.

Methods: In Method 1, 44 subjects were enrolled, consisting of 30 normal eyes, 11 glaucomatous eyes and 3 eyes with ocular hypertension. (Average of SE; -3.2 ± 2.9 D, best corrected acuity better than log MAR 0.1.) In Method 2, 6 eyes of 6 normal subjects were assessed. Head tilt angle was recorded every 100 ms by a gyro sensor (IMU-Z Tiny Cube (ZMP®)). The positions of both pupils were measured by photography, first only with the subject positioned on the chinrest, and then during location of the blind spot (testing condition) using automated perimetry (Octopus 900). This testing protocol was repeated five times. Lastly, both pupils were aligned to horizontal using a built-in accelerometer (LUMIX DMC-TZ4, Panasonic) and head tilt angle was measured.

Results: The Fovea-disc angle and the Fixation-blind spot angle were significant correlation. ($p<0.01$, $R^2=0.65$). The average head tilt angle was between -3.6 and 3.9 degrees. The maximum intra-individual difference in head tilt angle was 5.8 degrees at rest. The average head tilt angle was between 4.2 and -3.6 degrees during testing. The maximum intra-individual difference in head tilt angle was 5.1 degrees. The variation of head tilt angle during testing was not significantly different from the resting condition ($P=0.11$) The intra-subject variation of head tilt angle during testing ranged from 0.25 degrees; to 0.52 degrees. This was smaller than the intra-individual variation of head tilt angle at rest. There was correlation between BS -fixation angle and head tilt angle. ($p<0.01$, $rS= -0.57$).

Discussion: The maximum intra-individual difference of head tilt angle was 6 degrees, and inter-individual difference of head tilt angle was 8 degrees. Head tilt could influence visual field testing as well as assessment of the temporal retinal nerve fiber raphe angle. Consideration should be given to these factors to better correlate structural and functional changes in glaucoma.

Conflict of Interest: Yes, I have. **Ethics Committee Approval:** Yes, I have obtained **Informed Consent:** Yes, I have obtained

P3-6

Contrast gain control in glaucoma under photopic and mesopic luminance conditions

Catarina A. R. Joao, Lorenzo Scanferla, Nomdo M. Jansonius

Ophthalmology, University Medical Center Groningen, Netherlands

Purpose: Previous questionnaire studies have suggested that visual performance in glaucoma is disproportionately affected under extreme (low, high, changing) luminance conditions. The aim of this study was to determine the influence of glaucoma on adaptation to rapidly changing background luminances (contrast gain control).

METHODS: Case-control study with 18 glaucoma patients and 21 controls, aged 50 to 75 years, with normal visual acuity. We measured foveal and peripheral contrast sensitivity (CS) using perimetry with a minimized testing grid (fovea and four peripheral test locations; eccentricity ± 9°, ± 9°) using a +4 -2 dB staircase procedure. Target stimuli (Goldmann size III; 50 ms; increment/decrement) were presented on a time-varying background whose luminance was sinusoidally modulated in time (modulation amplitude 60%) at different frequencies (0-30 Hz). As a reference, we also measured contrast sensitivity for temporally modulated targets (Goldmann size IV; 334 ms) on a static background (temporal modulation sensitivity [TMS]), using a +3.5 -1.5 dB staircase procedure, for the same frequency range and test locations. Experiments were performed under photopic and mesopic conditions (100 and 1 cd/m^2, respectively). In healthy subjects, peripheral thresholds were calculated using the average threshold of all peripheral test locations. In glaucoma patients, peripheral thresholds were calculated using threshold measurements averaged from intact regions of the visual field.

Results: LogCS dropped for background modulation frequencies between 10-20 Hz and increased at higher frequencies for healthy subjects. In glaucoma, the same effect was visible but with reduced CS. LogCS was lower for peripheral locations when compared to the fovea but with a similar frequency dependency in both populations. Decrements appeared to be more easily discriminated at both light levels in healthy subjects, but this difference was not so clear in glaucoma patients. LogCS was considerably reduced when the task was performed at 1 cd/m^2 and the lowest sensitivity was seen at approximately 2.5-5 Hz (compared to 10-20 Hz at 100 cd/m^2). TMS was lower in glaucoma patients than in controls across photopic and mesopic conditions. Glaucoma patients experienced complete loss of flicker sensitivity for the highest temporal frequencies tested under reduced light levels.

Conclusion: We demonstrated that loss of contrast gain control is directly related to loss of TMS for the fovea and periphery under photopic and mesopic Lighting. Even in intact or only mildly affected parts of the visual field, the processing of temporal information of glaucoma patients is considerably impaired when compared to that of healthy age-matched controls, especially under mesopic conditions.

Conflict of Interest: No, I don't. **Ethics Committee Approval:** Yes, I have obtained **Informed Consent:** Yes, I have obtained

P3-7

Dynamic color brightness adaptation abnormalities in early stages of glaucoma.

Muen Yang, Mitchell W. Dul, Romain Bachy, Qasim Zaidi

SUNY College of Optometry, United States

Purpose: Previous electrophysiology studies have shown that primate retinal ganglion cells (RGC) exhibit subtractive adaptation to prolonged stimuli (Zaidi et al. 2012). We were interested to know if early stages of glaucoma, a disease that affects RGC, causes color adaptation abnormalities. We measured adaptation to three cardinal color axes: blue-yellow (B/Y), red-green (R/G), and achromatic light-dark (L/D), that target konio, parvo, and magno RGC respectively.

METHODS: 12 glaucoma patients with MD better than -4 dB on a 24-2 HVF and 12 age matched controls were recruited. For one eye of each participant, we measured the speed and magnitude of adapting to 1/32 Hz color modulations along the three cardinal axes at central fixation, 8 degrees supra-temporal, supra-nasal, infra-temporal, and infra-nasal. Initially the perception followed the stimulus, but then accelerated to perceive gray before the stimulus physically reached this state. The stimulus' physical contrast at this point was called the "Nulled-Contrast:" a smaller value represented weaker and slower adaptation. Each subject was presented a total of 75 trials. To compare results with structure (OCT) and function (10-2 HVF) within the glaucoma group, we recruited 6 more subjects to have a total of 18 subjects with glaucoma.

RESULTS: For each location and color axis, the mean adaptation difference between glaucoma and controls were small and did not reach statistical significance. However, in 13/15 comparisons, adaptation was weaker and slower for the glaucoma group. The probability of this happening due to chance was low (0.37%, binomial cumulative distribution with p=0.5). To visualize individual data points, we plotted the Nulled-Contrast of every glaucoma subject against its age-matched control for each location and color axis. The majority of points (125/180) were above the unit diagonal, implying that, generally, glaucoma had weaker adaptation. The probability of no difference between glaucoma and controls was <0.0001% (binomial cumulative distribution with p=0.5), providing strong evidence against no difference. The correlation analysis within the glaucoma group (n=18) reached significance only between adaptation and 10-2 HVF for the B/Y (p=0.053) and L/D axis (p=0.038) of the infra-temporal quadrant. Correlations were closer to significance between adaptation and function (10-2 HVF) than adaptation and structure; this was expected because both adaptation and 10-2 HVF are functional tests.

Conclusions: Early glaucoma patients may have weaker neural adaptation than normal. However, due to the early stage of the disease and/or the sensitivity of our test, adaptation abnormalities may be too mild to be significantly different than controls. We plan to further explore adaptation testing by registering the nulled-contrast more precisely and optimizing the stimulus size.

Conflict of Interest: No, I don't. **Ethics Committee Approval:** Yes, I have obtained **Informed Consent:** Yes, I have obtained

P3-8

Estimating "True" Retinal Sensitivity from Time-series Visual Field Data Using Gaussian Process Regression

Eiji Murotani

Kahoku Eye Clinic, Japan

Purpose: A Gaussian process (GP) is an infinite-dimensional generalization of multivariate normal disbtribution. Realizations of random variables from a GP are functions. I propose a Bayesian method that models the trajectories of "true" sensitivity as arbitrary smooth functions using a GP prior.

Materials and Methods: The proposed model is illustrated in Figure 1. A GP is specified by a mean function and a covariance function. Exponentiated quadratic kernel was chosen for covariance function. Marginal standard deviation (α , measure of variability) and mean function (mean value of observed sensitivity, i.e., *const*) were set for each of 52 test locations. Accounting for spatial correlation, length scale (ρ , measure of smoothness) was set for each of 6 sectors (Garway-Heath et al., 2000). Informative priors were chosen for hyperparameters (α , ρ). Visual field data from Rotterdam Eye Study were analyzed (Humphrey Field Analyzer, program 24-2, Full Threshold algorithm, 15 examinations about a half year interval). Markov chain Monte Carlo method was implemented in probabilistic programming language Stan.

Results: A representative result is presented in Figure 2. At the location (*), median values and 90% credible intervals of "true" sensitivity at 1st, 5th, 10th, and 15th visit were 30.8 (28.9 ~ 32.7), 27.1 (25.6 ~ 28.6), 13.6 (10.1 ~ 16.5), and 8.22 (4.47 ~ 13.4) [dB], respectively.

Conclusions: For each observed sensitivity, the probability distribution of the "true" sensitivity was obtained by GP regression.

Figure 1. Squares represent known variables (measurement time, t; observed sensitivity, y) and circles represent unknown variables (latent variable, f; "true" sensitivity, x). Through sigmoid function (S), f is transformed to x in the range of 0 ~ 36 dB. Each y follows a mixture of Weibull distributions (WW; Zhu et al., 2014) and depends only on the corresponding x. On the other hand, each f depends on all the other fs (thick horizontal bar).

Figure 2. Observed sensitivity over time (dots) and 20 trajectories of "true" sensitivity (lines; selected at random from posterior distribution) are visualized (STUDY_ID: 33, left eye, nasal inferior quadrant).

Conflict of Interest: No, I don't. **Ethics Committee Approval:** Not Applicable **Informed Consent:** Not Applicable

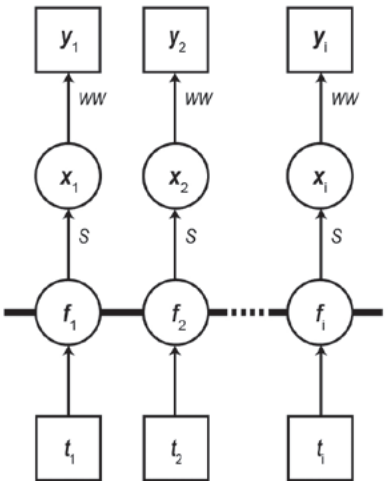

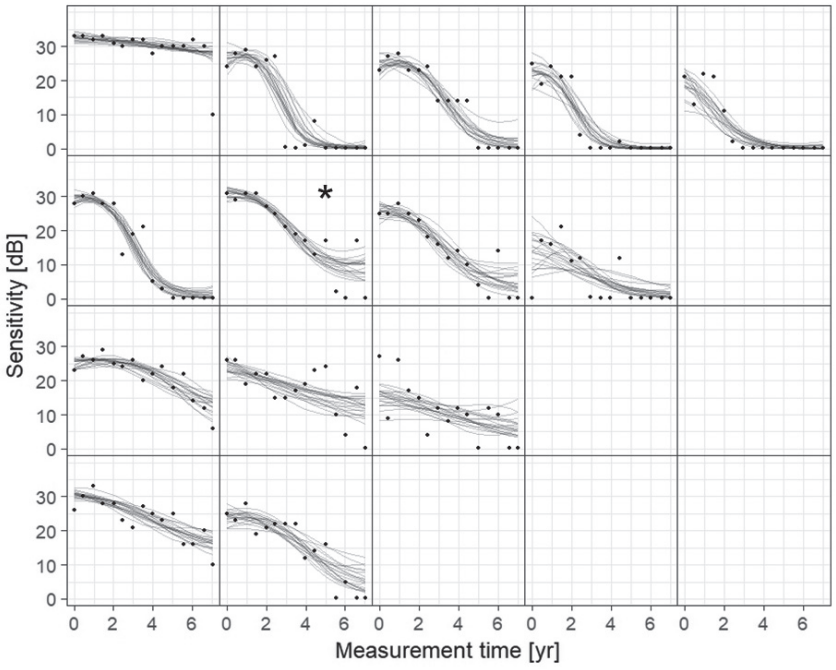

P4-1

Evaluation of pupil fields using a newly developed perimeter in glaucoma patients

Kazuko Totsuka[1], Ken Asakawa[2], Masayuki Kasahara[1], Kazuhiro Matsumura[1], Hitoshi Ishikawa[1,2], Nobuyuki Shoji[1]

[1]Department of Ophthalmology, Kitasato University, Japan, [2]Kitasato University, Department of Orthoptics and Visual Science

Purpose: To evaluate the objective pupil fields using a newly developed perimeter for detection of glaucomatous visual field loss.

Materials and Methods: Twenty-eight eyes of 23 glaucoma patients ranging in age from 45 to 69 years were examined. There were cases of normal-tension glaucoma in 10 patients and of primary open-angle glaucoma in 13 patients. The glaucomatous eyes were classified into 3 stages (early: 6 eyes, –3.75 ± 1.04 decibels (dB); moderate: 11 eyes, –9.68 ± 1.53 dB; and severe: 11 eyes, –17.85 ± 3.25 dB) by using the Hodapp-Anderson-Parrish grading scale. The newly developed head-mounted perimeter "imo®" (CREWT Medical Systems, Tokyo, Japan) was used to measure the percentage pupil constriction (PPC) as response to a stimulus at all 36 test points of the visual field. A stimulus size of 64 mm^2 (Goldmann target size V) with 0 dB light under 31.4 apostilbs background was presented. Visual field measurements were taken with a Humphrey Field analyzer using the 24-2 SITA standard program (Carl Zeiss Meditec, Dublin, CA, USA). The correlations (r) between PPC and visual field sensitivity, expressed as dB, were examined in correspondence to the test points. A pattern deviation of the pupil field was then calculated as a value representing the difference between an age-matched normal value at each test point for the degree of sensitivity of the entire visual field.

Results: Generally good correlations between PPC and dB were obtained: $r < 0.40$ (poor) early 1, moderate 3, severe 3 eyes; 0.41–0.60 (moderate) 4, 3, 5 eyes; 0.61–0.80 (good) 1, 2, 2 eyes; and > 0.81 (excellent) 0, 3, 1 eyes, respectively. There were no differences between the glaucoma types and the grading scale. Glaucomatous visual field losses were remarkably distinguished from the normal pupil fields by use of a pattern deviation.

Conclusions: Our results demonstrated that the difference of value between an age-matched normal PPC value and an abnormal value at each test point indicated a localized glaucomatous visual field loss.

Conflict of Interest: Yes, I have. **Ethics Committee Approval:** Yes, I have obtained **Informed Consent:** Yes, I have obtained

P4-2

Effect of non-measurement eyes on the result of measurement eyes by the monocular visual field tests under binocular open view

Hiroyasu Goukon[1,2], Fusako Fujimura[3], Masayuki Kasahara[1], Kazuhiro Matsumura[1], Nobuyuki Shoji[1,2]

[1]Department of Ophthalmology, Kitasato University, Japan, [2]Graduate School of Medical Science, Kitasato University, [3]Department of Orthoptic and Visual Science, Allied health Science, Kitasato University

Purpose: The head-mounted perimeter "imo" enables performing monocular visual field tests under binocular open view in almost same conditions as that in Humphrey Field Analyzer (HFA). However, it is believed that visual information of non-measurement eyes affects the measurement eyes' test due to the interaction between both eyes. Therefore, we compared the test results of HFA and "imo" by evaluating the presence or absence of visual field defect on non-measurement eyes in glaucoma patients.

Materials and Methods: Twenty eyes of 20 glaucoma patients who had complete visual field defect within central 30 degrees in non-measurement eyes (VF defect-positive group) and twenty eyes of 20 glaucoma patients who had less than -3.6 dB of mean deviation (MD) in both eyes, with no central visual field loss in non-measurement eyes (VF defect-negative group), were examined by SITA standard protocol of HFA 30-2 or 24-2 program. These eyes underwent monocular visual field tests under binocular open view by AIZE protocol of "imo" 30-2 or 24-2. We compared the global index obtained in both groups with HFA and "imo", respectively.

Results: The results of HFA and "imo" for VF defect-positive group were -9.8 dB and -8.9 dB (MD), 73.0% and 74.5% (VFI), and 9.3 dB and 8.9 dB (PSD), respectively. Statistically significant differences were not found in all factors (Wilcoxon signed-rank test; $p = 0.22$, $p = 0.13$, $p = 0.19$). The results of HFA and "imo" for VF defect-negative group were -9.5 dB and -8.1 dB (MD), 74.0% and 76.3% (VFI), and 10.4 dB and 9.4 dB (PSD), respectively, recognized significant differences in all factors (each, $p < 0.001$).

Conclusion: In glaucoma patients, it was suggested that the effect on measurement eyes from non-measurement eyes in monocular visual field tests under binocular open view.

Conflict of Interest: Yes, I have. **Ethics Committee Approval:** Yes, I have obtained **Informed Consent:** Yes, I have obtained

P4-3

The investigation of the difference of central visual field sensitivity between monocular and binocular measurement by head-mounted perimeter

Tomoyuki Kumagai, Itaru Kimura, Takuhei Shoji, Yuji Yoshikawa, Kei Shinoda

Department of Ophthalmology, Saitama Medical University, Japan

Purpose: A head-mounted perimeter imo® (CREWT Medical Systems, Inc., Tokyo, Japan) has been developed, and this device can perform a binocular random single eye test with dichoptic stimulation, besides the monocular eye test. We investigated the central visual field sensitivity obtained by binocular dichoptic stimulations using imo® and compared to the results with those obtained by conventional monocular stimulation in glaucoma patients.

Methods: Six glaucoma patients (5 males and 1 female, averaged age 64.8+/-12.0 years old) whose central visual field in one eye was disturbed by glaucomatous optic neuropathy were enrolled in this study. Foveal threshold and 4 values of sensitivity at central 4 points in 30-2 program were measured by monocular eye test, and binocular random single eye test with dichoptic stimulation. The averaged sensitivity (AS) of 5 points including foveal threshold was calculated and investigated.

Results: The mean of AS in monocular test was 23.1dB in the fellow eye, and 10.5dB in the affected eye. The mean of AS in binocular random single eye test was 24.3dB in the fellow eye, and 6.8dB in the affected eye. The AS value in binocular test was lower than that in monocular test in the affected eye in 5? cases. The difference of sensitivity between fellow eye and affected eye in binocular random single eye test with dichoptic stimulation tends to be greater than that in monocular eye test, though this result was not significantly different ($p=0.067$).

Conclusions: Central visual field sensitivity in eyes with disturbed central visual field tended to decrease when measured in binocular condition as compared to monocular condition in glaucoma patient.

Conflict of Interest: No, I don't. **Ethics Committee Approval:** Not Applicable **Informed Consent:** Yes, I have obtained

P4-4

Measurements of fixation eye movements during visual field test with head-mounted perimeter "imo".

Takuya Ishibashi[1], Chota Matsumoto[1], Hiroki Nomoto[1], Ikumi Umehara[1], Akemi Wakayama[1], Shinji Kimura[2], Yoshikazu Shimomura[1]

[1]Kindai University, Japan, [2]CREWT Medical Systems, Inc.

Purpose: While stable eye fixation during visual field (VF) test is one of important factors to obtain reliable results in clinical practice, fixation eye movements occur even though subjects are trying to control their gaze on the fixation target. The fixation eye movements during VF test in a clinical setting has not been well known. The Purpose of this study was to measure the fixation eye movements during VF test using head-mounted perimeter "imo".

methods: Subjects were seven healthy volunteers who underwent a customized VF test program for right eye with the imo 10 times, stimulus intensity: 20dB, stimulus size: Ⅰ Ⅰ Ⅰ , stimulus presentation duration was 200msec at 800msec intervals, test time: about 17sec, 10 test locations: (± 3,–3), (± 9,–3), (± 15,–3), (± 21,–3), (± 27,–3).Eye positions were monitored with a CMOS sensor camera (300fps, 640 × 508 pixels) built-in the imo perimeter (Matsumoto C, et al. PLos One. 2016). Fixation eye movements during stimulus presentation (200msec) and intervals (800msec) were calculated to measure changes of vertical and horizontal eye positions. Interval of before and after stimulus presentation was divided into 8 time windows (before-4 (b4), b3, b2, b1, after-1 (a1), a2, a3, a4: each the duration of 200msec. Timing of stimulus presentation was between b1 and a1).The bivariate contour ellipse area (BCEA) was used to evaluate the area of fixation eye movements.

results: Average BCEA of b4, b3, b2, b1, stimulus presentation, a1, a2, a3 and a4 were 0.089 (SD=0.258) deg2, 0.031(SD=0.051) deg2, 0.018(SD=0.012) deg2, 0.014(SD=0.011) deg2, 0.015(SD=0.014) deg2, 0.021(SD=0.041 deg2, 0.065(SD=0.233) deg2, 0.027(SD=0.044) deg2, 0.018(SD=0.012) deg2, separately, There were no significant difference in BCEAs between during presenting stimuli and interval periods. (conclusion)Fixation eye movements during VF test were measured with imo. BCEA of stimulus presentation period tended to be smaller compared to those value of interval periods, though there was no significant differences.

Conflict of Interest: Yes, I have. **Ethics Committee Approval:** Yes, I have obtained **Informed Consent:** Yes, I have obtained

P4-5

Influence of a Binocular Viewing Condition on Monocular Sensitivites Measured by imo® in Patients with Glaucoma

Akemi Wakayama, Yoriko Inoue, Hiroki Nomoto, Chota Matsumoto, Yoshikazu Shimomura

Department of Ophthalmology, Kindai University Faculty of Medicine, Japan

Purpose: We have previously shown that binocular interaction is activated under both eyes open and affects not only binocular sensitivity but also monocular sensitivity in visually normal adults. Here we investigated whether monocular sensitivities measured with both eyes open in patients with glaucoma were affected by the sensitivity difference between the two eyes corresponding under a binocular viewing condition.

Materials and Methods: Subjects were 16 eyes of 16 patients with glaucoma (2 males and 14 females; mean age, 54.9 ± 10.7 years). Using imo®, monocular sensitives were measured with the non-tested eye occluded (occlusion condition) and with both eyes open (binocular condition). Of both eyes, the eye with a less severe visual field defect (i.e. with a greater MD value) was used as the target eye. This study used a 30–2 or 24plus test pattern, a stimulus duration of 200 msec, and the Ambient Interactive ZEST (AIZE) thresholding algorithm. To compare the monocular sensitivities under occlusion and binocular conditions, the result for each test point under binocular condition was classified into one of the four groups: 1) both eyes had normal sensitivities, 2) the target eye had normal sensitivity and the fellow eye had abnormal sensitivity, 3) the target eye had abnormal sensitivity and the fellow eye had normal sensitivity, and 4) both eyes had abnormal sensitivities. The classification was defined as abnormal with 5% or less in pattern deviation. Sensitivities under occlusion and binocular conditions were compared for all 4 groups.

Results: In group 1 and 2, the monocular sensitivities under binocular condition were higher than those under occlusion condition ($p<0.01$ for both groups). On the contrary, the monocular sensitivities under binocular condition were lower than those under occlusion condition in group 3 ($p<0.05$) and 4 ($p<0.01$).

Conclusions: In patients with glaucoma, the difference between the monocular sensitivities under occlusion and binocular conditions indicated that monocular sensitivities under binocular condition were affected by the relationship between the sensitives of the two eyes corresponding under a binocular viewing condition.

Conflict of Interest: Yes, I have. **Ethics Committee Approval:** Yes, I have obtained **Informed Consent:** Yes, I have obtained

P4-6

SMARTPHONE-BASED PERIMETRY FOR FAST AND LOW-COST VISUAL FIELD ACQUISITION

Jan Stapelfeldt, Serife S. Kucur, Raphael Sznitman

ARTORG Center, University of Bern, Switzerland

Purpose: Perimetry quantifies the visual function of the patient within their field of vision which is well used for diagnostics of eye diseases such as Glaucoma. A perimetry test is performed using a bowl-shaped machine called Perimeter in a separate room in the presence of specialist(s). The preparation of the environment as well as performing the test is cumbersome and costly which makes perimetry not easily accessible everywhere in the world. Accordingly, we present a new low-cost and fast smartphone-based perimeter for cheaper and quick visual field acquisition.

Materials & Methods: We propose a novel low-cost smartphone-based perimetry for faster and cheaper visual field (VF) acquisition. Accordingly, we created a perimetry application that runs a Tendency Oriented Perimetry (TOP) on Samsung S8 G9500 5.8" Phone integrated with Google DayDream virtual reality (VR) headset. The perimetry test environment is simulated by projecting the VF coordinates on the screen plane. The stimulus size is set to the standard Goldman size III. The stimulus intensities are described in decibel (dB) scale and adjusted based on maximum light intensity of the smartphone. The barrel distortions and chromatic aberrations due to the VR goggle lenses were corrected in order to provide intensity homogeneity within the screen plane. The patient feedback is enabled via a remote Bluetooth controller. We implemented TOP strategy in order to obtain VFs of fast but poor quality acquisition. We therefore incorporated a deep learning-based post-processing step into the perimetry application to increase the accuracy of the VF measurement. All the software implementations were done using Android Studio 3.0.1.

Results: We compared our perimetry application with Normal Strategy (NS) of Octopus 900 Perimeter. We have tested our method and NS with 5 healthy subjects and have observed that our proposition leads to comparable VF measurements with the ones acquired with NS of Octopus perimeter. We also compared the experiences that the subjects have gone through with two systems. Accordingly, the proposed system is said to be more comfortable for perimetry tests as it provides more physical flexibility and takes less time to perform the test.

Conclusion: In this study, we proposed a cheap and fast perimetry system that runs TOP strategy and a post-processing step on a mobile phone. We have run preliminary trials with the new system on healthy subjects and compared it to a standard clinical system, i.e. NS in a Octopus Perimeter. The results show that the proposed system is faster and cheaper VF measurement with comparable quality to a standard clinical setting. Such results bring new possibilities for perimetry for use in developing and rural regions of the world.

Conflict of Interest: No, I don't. **Ethics Committee Approval:** Yes, I have obtained **Informed Consent:** Yes, I have obtained

Sponsored Seminar

Afternoon Seminar 1

Thursday, May 10 15:45 ~ 16:45
Room 1 (Concert Hall)

TOPCON

YOUR VISION. OUR FOCUS.

An Update on the detection and management of Glaucoma with swept source OCT Triton

23rd International Visual Field & Imaging Symposium

Afternoon Seminar 1

(AS1)(IPS)

- **Thursday, May 10**
- **15:45 - 16:45**
- **Room 1**

(Ishikawa Ongakudo Concert Hall)

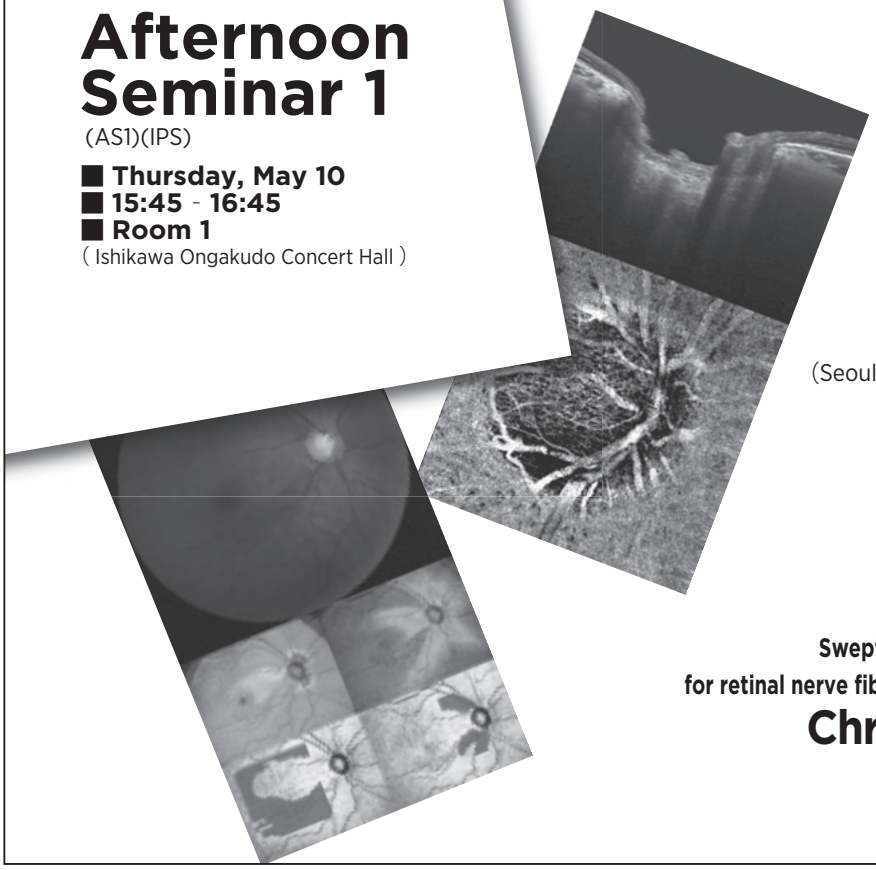

Moderator

Linda Zangwill, Ph.D.

(Hamilton Glaucoma Center UCSD)

Clinical Application of Deep Optic Nerve Head and Peripapillary Imaging

Tae Woo Kim, MD

(Seoul National University Bundang Hospital)

Swept-source optical coherence tomography for retinal nerve fiber layer optical texture analysis (ROTA)

Christopher Leung, MD

(The Chinese University of Hong Kong)

Sponsor : TOPCON CORPORATION

Luncheon Seminar 1

Thursday, May 10 12:20 ~ 13:20
Room 1 (Concert Hall)

New Era in Perimetry


Aiko Iwase

Chair：Aiko Iwase, M.D., Ph.D.

（Director, Tajimi Iwase Eye Clinic）

Vice-President of International Perimetric Society (Imaging Perimetric Society, IPS)
Clinical Professor, Department of Ophthalmology, Kanazawa University 2015 –

Message from the Chairman

It has been more than 30 years since the first Humphrey Field Analyzer（HFA）was launched as an Automated Static Perimeter in the world, which is since then positioned as the global gold standard perimeter which almost stands for a visual field testing today. The device has been evolved through some generations by having several testing algorithms. The most familiar one was the SITA on the HFA II（the second generation）introduced in 1996 and has been utilized commonly in the world until now. As of today the most modern modality is the HFA3 which was introduced in 2015. Because of its novelty of the HFA3, it is expected to be more capable for new features on visual field testing in the future. The first new feature which is already available now is the SITA Faster. At this symposium, we have Professor Heijl, who has developed the Strategy with HFA including SITA, will talk about the SITA Faster as the additional testing algorithm to the HFA3. Since Professor Heijl is always standing in the first line of Perimetry with Zeiss we may be able to expect to hear something new beyond the SITA Faster then.

Information from Zeiss : Gary Lee, PhD

（Carl Zeiss Meditec, Inc. Clinical Affair）

“HFA central testing and the new 24-2C”


Anders Harald Robert Heijl

Speaker：Anders Harald Robert Heijl, M.D., Ph.D.

（Senior Professor and Consultant ,the Department of Ophthalmology, Skåne University Hospital in Malmö, University of Lund）

Professor at the Department of Ophthalmology, Malmö University Hospital, later re-named Skåne University Hospital in Malmö, University of Lund 1990 – 2012
President of the International Perimetric Society 1988 – 1996,
President of the Glaucoma Research Society 2003 – 2008,
President of the Swedish Glaucoma Society 2010 – 2016

“A new SITA test – SITA Faster”

The SITA tests SITA Standard and SITA Fast were released in 1996 after almost 10 years of development. The tests were very advanced for that time, used maximum likelihood calculations of pointwise threshold values in real time, and required computational power that was uncommon at that time. These two tests saved 50% test time as compared to the earlier Full Threshold and Fastpac tests, and were rapidly adopted by the ophthalmic community.

We have now further developed the SITA concept, tested and released a new SITA test alled SITA Faster. SITA Faster is a further development of SITA Fast, and saves about 30% test time as compared to SITA Fast and about 50% as compared to SITA Standard.

This presentation will summarize the development of SITA Faster and report results from several clinical test series – the most recent involving 5 centers: in Tajimi Japan, Hong-Kong, China, Tampere Finland, Malmö Sweden and Berkeley USA.

Sponsor：Carl Zeiss Meditec Co., Ltd.

Luncheon Seminar 2

Friday, May 11 12:00 ~ 13:00
Room 1 (Concert Hall)

OCT-Based Phenotyping of Eyes in Glaucoma Diagnostics

Chairman

Dr. Makoto Araie

Director of Kanto Central Hospital of The Mutual Aid Association of Public School Teachers, Japan

Speaker

Dr. Balwantray C. Chauhan

Dalhousie University, Canada

The Importance of Aging Effects in the Assessment of Structural Changes in Glaucoma

Speaker

Dr. Tomomi Higashide

Kanazawa University, Japan

Detailed structural characteristics of the optic disc revealed by the Spectralis OCT

Sponsor : Heidelberg Engineering GmbH

Luncheon Seminar 3

Saturday, May 12 12:00 ~ 13:00
Room 1 (Concert Hall)

Anterior Segment OCT and Glaucoma

Chair

Prof. Kazuhisa Sugiyama
Department of Ophthalmology,
Kanazawa University

Presenter

Prof. Aung Tin
Singapore National Eye Centre

Organizer: Kazuhisa Sugiyama, MD, PhD

Anterior segment optical coherence tomography (AS-OCT) systems can demonstrate detailed images of anterior segment structures at resolutions exceeding that of ultrasound biomicroscopy (UBM). AS-OCT allows visualization of the iridocorneal angle and, thus, can contribute to the diagnosis and management of glaucoma. AS-OCT systems are advantageous, being noncontact procedures and providing finer resolution than UBM, especially in spectral-domain systems, owing to high speed and noninvasive character, which allows it to be performed in the immediate postoperative period. AS-OCT permits an objective, quantitative description of angle anatomy using a variety of standard biometric parameters for the screening and management of glaucoma.

Professor Aung is a clinician scientist, with clinical practice focusing on glaucoma and research interests in angle closure glaucoma and glaucoma genetics. He will present useful information regarding clinical application of anterior segment optical coherence tomography (AS-OCT) for assessment in glaucoma patients.

Sponsored by Senju Pharmaceutical Co., Ltd. / Otsuka Pharmaceutical Co., Ltd.

Sponsor : Senju Pharmaceutical Co., Ltd. / Otsuka Pharmaceutical Co., Ltd.

Morning Seminar 1

Thursday, May 10 8:00 ~ 9:00
Room 1 (Concert Hall)

23rd
International Visual Field
& Imaging Symposium

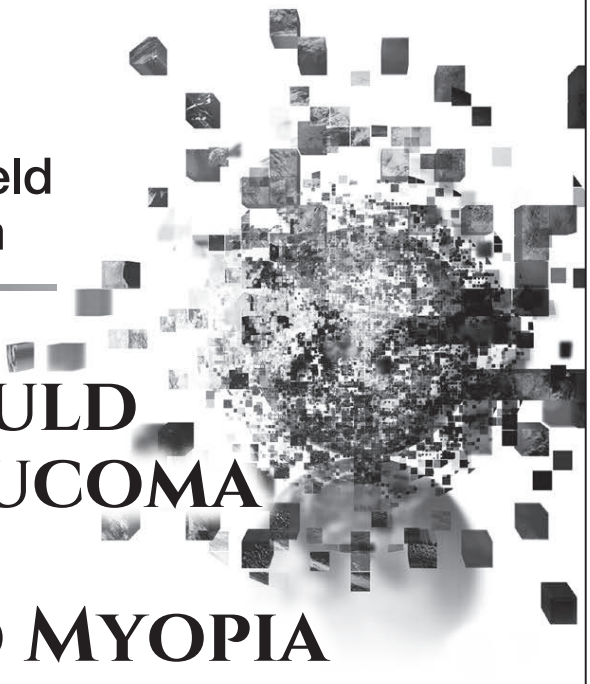

How we should manage glaucoma patients : Elderly and Myopia

Chairman **Tetsuya Yamamoto**
Professor and Chairman, Dept. of Ophthalmology,
Gifu University Graduate School of Medicine, Japan

Management of the Perimetry in Elderly Glaucoma Patients

Speaker **Megumi Honjo**
Assistant Professor, Dept. of Ophthalmology, Tokyo University, Japan

Managing Patients with Myopia and Glaucoma -How AI Can Help

Speaker **Robert T. Chang**
Assistant Professor of Ophthalmology,
Stanford University School of Medicine, USA

Sponsor：Alcon Pharma K. K. / Novartis Pharma K. K.

Morning Seminar 2

Friday, May 11 8:00 ~ 9:00
Room 1 (Concert Hall)

Santen A Clear Vision For Life®

Early detection and early treatment of PPG

—Improvement of diagnostic skill and points of therapeutic intervention of PPG with using OCT—

Chair

Prof. Kazuhisa Sugiyama
Kanazawa University

Chair

Prof. Goji Tomita
Toho University
Ohashi Medical Center

Lecturer 1

Prof. Ki Ho Park Seoul National University

Utilization of OCT —Structural change detection of PPG—

When detecting the change in structure by OCT, a simple method is comparing the baseline OCT data with the current one. However it should be kept in mind whether the detected change is within the variability of the measurements by the instrument or not. If the change is within the variability of the measurements, the chance of real progression is very low. Retinal nerve fiber layer (RNFL) thickness is most widely used parameter for detection of progression. Macular inner retinal thickness including ganglion cell-inner plexiform layer (GCIPL) thickness may provide additional information detecting progression.
Recently, after introduction of Guided Progression Analysis (GPA) for both RNFL and GCIPL it became more convenient and more reliable to detect progression. Further, a wide-field scanning covering both parapapillary and macular area became available and will provide easier overview detecting the region of progression and analyzing the sequence of structural change especially in PPG.

Lecturer 2

Prof. Toru Nakazawa Tohoku University

Utilization of glaucoma inspection instrument
—Diagnosis of PPG / Judgment of therapeutic intervention—

Due to the progress and development of inspection instrument including OCT and LSFG, opportunities to diagnose PPG are increased, and discussions are being made on at which stage treatment should be started and treatment policy.
In this lecture, we will discuss the point of PPG diagnosis and therapeutic intervention whether PPG should be treated or not, and what should be considered when starting treatment, based on latest evidence through a prospective pathology study of PPG in Tohoku University.

Case Examination

Sponsor : Santen Pharmaceutical Co., Ltd.

Morning Seminar 3

Saturday, May 12 8:20 ~ 9:20
Room 1 (Concert Hall)

How should we evaluate the data provided by "imo"?

Head-mounted perimeter "imo"

Chairman

Chota Matsumoto, M.D, Ph.D.
Department of Ophthalmology
Kindai University Faculty of Medicine

Speaker 1

"What is imo?"

Hiromasa Sawamura, M.D, Ph.D.
Department of Ophthalmology The University of Tokyo

Speaker 2

"Binocular visual field test with imo in clinical use."

Hiroki Nomoto, M.D, Ph.D.
Department of Ophthalmology Kindai University Faculty of Medicine

CREWT

Sponsor : CREWT Medical Systems, Inc.